NAVAL POSTGRADUATE SCHOOL
Monterey, California

THESIS

THERMAL IMAGES OF SKY AND SEA-SURFACE
BACKGROUND INFRARED RADIATION

by

Panagiotis Psihogios

December 1988

Thesis Advisor: A. W. Cooper

Approved for public release; distribution is unlimited

REPORT DOCUMENTATION PAGE

1a REPORT SECURITY CLASSIFICATION UNCLASSIFIED		1b RESTRICTIVE MARKINGS			
2a SECURITY CLASSIFICATION AUTHORITY		3 DISTRIBUTION AVAILABILITY OF REPORT Approved for public release; distribution is unlimited			
2b DECLASSIFICATION DOWNGRADING SCHEDULE					
4 PERFORMING ORGANIZATION REPORT NUMBER(S)		5 MONITORING ORGANIZATION REPORT NUMBER(S)			
6a NAME OF PERFORMING ORGANIZATION Naval Postgraduate School	6b OFFICE SYMBOL (If applicable) 61	7a NAME OF MONITORING ORGANIZATION Naval Postgraduate School			
6c ADDRESS (City, State, and ZIP Code) Monterey, California 93943-5000		7b ADDRESS (City, State, and ZIP Code) Monterey, California 93943-5000			
8a NAME OF FUNDING SPONSORING ORGANIZATION	8b OFFICE SYMBOL (If applicable)	9 PROCUREMENT INSTRUMENT IDENTIFICATION NUMBER			
8c ADDRESS (City, State, and ZIP Code)		10 SOURCE OF FUNDING NUMBERS			

PROGRAM ELEMENT NO	PROJECT NO	TASK NO	WORK UNIT ACCESSION NO

11 TITLE (include Security Classification)

THERMAL IMAGES OF SKY AND SEA-SURFACE BACKGROUND INFRARED RADIATION

12 PERSONAL AUTHOR(S)
Psihogios, Panagiotis E.

13a TYPE OF REPORT Master's Thesis	13b TIME COVERED FROM _____ TO _____	14 DATE OF REPORT (Year, Month, Day) 1988 December 15	15 PAGE COUNT 157

16 SUPPLEMENTARY NOTATION
This work was supported by the Naval Academic Center for Infrared Technology under Naval Postgraduate School direct funding

17 COSATI CODES			18 SUBJECT TERMS (Continue on reverse if necessary and identify by block number)
FIELD	GROUP	SUB-GROUP	Thermal Radiation, Emissivity, Blackbody Radiators, Background Radiance, Computer Code LOWTRAN 6, AGA, Thermovision 780 System, Schwartz-Hon Model

19 ABSTRACT (Continue on reverse if necessary and identify by block number)
Thermal Images of the sky and the sea surface background radiance were analyzed using the AGA Thermovision 780 system. Calculated sky radiance was compared with that predicted by the computer code LOWTRAN 6. The Schwartz-Hon computer model for the emissivity of the sea surface was validated using the results from AGA measurements and LOWTRAN 6. The factors which affect the radiance measurements were determined, and the degree of influence they exert was estimated. The radiance emitted from an overcast sky was found to be higher than that emitted from a clear sky. The wind speed reduces significantly the infrared sky radiance. Emissivity of the sea surface depends upon the wave roughness, remaining almost constant with the viewing angle. The whole result showed that LOWTRAN 6 provides a good prediction of the atmospheric radiance with deviation from measurement generally within 10% with cases to 15%, for the elevation angle

20 DISTRIBUTION/AVAILABILITY OF ABSTRACT ☐ UNCLASSIFIED UNLIMITED ☐ SAME AS RPT ☐ DTIC USERS	21 ABSTRACT SECURITY CLASSIFICATION UNCLASSIFIED	
22a NAME OF RESPONSIBLE INDIVIDUAL A. W. Cooper	22b TELEPHONE (Include Area Code) (408) 646-2452	22c OFFICE SYMBOL 61Cr

Block 19 cont'd.

range from 0 to 19 degrees and that the Schwartz-Hon model agrees well with observation showing deviation varying up to 14% in the elevation angle range from 5 to 10 degrees.

Accession For

A-1

Approved for public release; distribution is unlimited.
Thermal Images of Sky and Sea-Surface
Background Infrared Radiation

by

Panagiotis Psihogios
Major, Hellenic Army
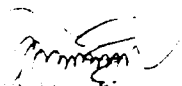B.S., Hellenic Army Cadet School, 1973

Submitted in partial fulfillment of the
requirements for the degree of

MASTER OF SCIENCE IN ENGINEERING SCIENCE

from the

NAVAL POSTGRADUATE SCHOOL
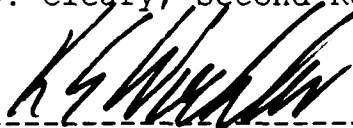December 1988

Author: _____
Panagiotis Psihogios

Approved by: _____
A. W. Cooper, Thesis Advisor

_____
D. D. Cleary, Second Reader

_____
K. E. Woehler, Chairman,
Department of Physics

_____
G. E. Schacher
Dean of Science and Engineering

iii

ABSTRACT

Thermal images of the sky and the sea surface background radiance were analyzed using the AGA Thermovision 780 system. Calculated sky radiance was compared with that predicted by the computer code LOWTRAN 6. The Schwartz-Hon computer model for the emissivity of the sea surface was validated using the results from AGA measurements and LOWTRAN 6. The factors which affect the radiance measurements were determined, and the degree of influence they exert was estimated. The radiance emitted from an overcast sky was found to be higher than that emitted from a clear sky. The wind speed reduces significantly the infrared sky radiance. Emissivity of the sea surface depends upon the wave roughness, remaining almost constant with the viewing angle. The results showed that LOWTRAN 6 provides a good prediction of the atmospheric radiance with deviation from measurement generally within 10% with cases to 15%, for the elevation angle range from 0 to 19 degrees and that the Schwartz-Hon model agrees well with observation showing deviation varying up to 14% in the elevation angle range from 5 to 10 degrees.

TABLE OF CONTENTS

ACKNOWLEDGMENT

I. INTRODUCTION

All objects absorb and emit radiant energy, due to thermal vibration-rotation of their own electrons and molecules. They may also reflect energy emitted from other heat sources. This energy, known as thermal energy, is a spectral function of temperature. Most objects of interest have terrestrial temperatures, and the exchanged thermal energy is radiated mainly in the infrared region of the electromagnetic spectrum [Ref1:p18]. Compared to visible light (sun), the infrared radiation can be observed day and night.

An entirely new technology, concerning the detection and tracking of the thermal image of targets, has been developed during the past few decades. The main technique of such detection is based upon the temperature differences between target and surroundings. The infrared radiation from the target is affected by the atmosphere and is also mixed with the so called background noise (land/sea/sky radiation). Thus the function of a modern thermal imaging search is to estimate, as well as possible, the level of atmospheric or background interference and to produce techniques and models which will optimize the performance of detection systems.

This thesis examines the interaction of the sea surface with thermal radiation from the sky. The intent is to validate the apparent sky radiance predicted by the propagation/radiance code LOWTRAN 6, relative to that measured with the AGA Thermovision 780 detection system. The most interesting area is that of low altitude (2° to 5° above the sky horizon). A further investigation of sky radiance coming from higher altitudes follows. The other important apparent background radiance comes from the sea surface. It is composed of the radiance emitted by the sea surface and the sky radiance reflected by it. In this case both the AGA system and the LOWTRAN 6 code are used to validate the Schwartz-Hon (SH) modelling of the sea surface emissivity and the sky radiance incident (or reflected) on the sea.

The present work consists of the following seven chapters and two appendices. In the first of these, (chapter two), the basic radiometric quantities and the necessary radiation's equations are given. Chapter three contains the description of the marine and sky background radiance. The atmospheric propagation of the infrared radiation is examined in chapter four, where the atmospheric propagation code LOWTRAN 6 and Schwartz-Hon model are also reviewed. The fifth chapter describes the AGA sensor system used in this work. Chapter six contains the signature measurements derived from data taken on November 4, 1987 and on July 14, 15, and 25, 1988 at

the same location under different weather conditions. The analysis of the measurements and the validation of the modelling codes are presented in chapter seven. Conclusions from this work and recommendations for further work are discussed in the last chapter. Appendix A contains all the Figures and Appendix B all the Tables referenced in the text.

II. THERMAL RADIATION

A. THE INFRARED SPECTRUM

A thermal radiator emits energy due to its temperature. This energy is spectrally distributed, and for typical environmental temperatures the emission is concetrated in the infrared spectral band. This is bounded by the visible region at short wavelengths (0.75 µm), and at the long wavelengths by the millimetrwave band (1000 µm). For practical purposes the following subdivision is used; near infrared 0.75 to 3 µm, middle infrared 3 to 6 µm, far infrared 6 to 15 µm, and extreme infrared 15 to 1000 µm, [Ref. 2:p. 11.3].

B. RADIATION QUANTITIES - LAWS

It is necessary to describe some quantities and equations involved with the thermal radiation of objects. These are taken from Pinson [Ref. 3:p. 13-19].

1. Radiant Energy

The radiant energy Q (in joules) is the basic physical quantity of radiation and has a multiple dependence on time, wavelength, spatial coordinates, and source (material properties, surface, relative orientation, and temperature of the source).

2. Radiant Flux

The radiant flux or radiant power P (in Watts) is the partial derivative with respect to time of radiant energy.

$$P = dQ/dt \qquad (2.1)$$

3. Radiant Intensity

Radiant intensity I (in W/sr) is defined as the radiant flux per unit solid angle radiated in a given direction from a point source.

$$I = dP/d\Omega \qquad (2.2)$$

4. Radiant Exitance (Emittance) - Irradiance

Radiant exitance or radiant emittance M (in W/m^2) is the radiant flux per unit area emitted by the surface. If it is incident upon a surface, is called irradiance E.

$$M , E = dP/dA \qquad (2.3)$$

5. Radiance

Radiance L (W/m^2-sr) is the radiant flux in a given direc ion per unit area and solid angle.

$$L = dI/dA \qquad (2.4)$$

5

6. Lambertian Surfaces

A Lambertian or diffuse surface is a planar surface from which the radiant intensity I (W/sr) varies by the cosine of the angle θ defined by the viewing direction and the surface normal n.

$$I_\theta = I_n \cos\theta \qquad (2.5)$$

It can be shown that the radiance from a Lambertian surface is independent of the angle θ. For instance the brightness of an emitting planar surface does not change with the viewing angle. For a Lambertian surface radiating into a hemisphere it can be shown also that [Ref. 3:p.16]:

$$L = I_n/dA = P/\pi dA = M/\pi \qquad (2.6)$$

7. Absorptance

Absorptance α is defined as the ratio of a radiant quantity absorbed by an object to that incident upon it.

8. Reflectance

Reflectance r is defined as the ratio of reflected to incident radiant quantity.

9. Transmittance

Transmittance t is the ratio of a transmitted radiant quantity to the incident radiant quantity.

6

10. Emissivity

Emissivity ϵ is the ratio of the emitted radiant quantity to that emitted from a blackbody source at the same temperature (and wavelength).

All the radiant quantities defined above are usually spectral functions (denoted in the text by the subscript λ). Then, the dimensioned quantities are expressed per unit of wavelength (μm).

11. Photon Energy

Energy is transferred quantitatively by discrete energy quanta called photons. Each photon has energy Q_λ depending on its wavelength λ, given by

$$Q_\lambda = hc/\lambda \qquad (2.7)$$

where   h = Planck's constant = $(6.6261)10^{-34}$ (J s)
         c = speed of light   = $(2.9979)10^{8}$ (m/s)

12. Kirchhoff's Law

In the general case the energy incident (Q_i) on a material is absorbed (Q_α), transmitted (Q_t), and reflected (Q_r). The principle of conservation of energy states that

$$Q_i = Q_\alpha + Q_t + Q_r \qquad (2.8)$$

Under equilibrium conditions materials have constant internal

7

energy, so the energy absorbed must be balanced by energy emitted (Q_ϵ). This is Kirchhoff's law, expressed by

$$Q_\alpha = Q_\epsilon \quad \text{(at equilibrium)} \tag{2.9}$$

Using the previous definitions eq. (2.8) and (2.9) are written

$$\alpha + t + r = 1 \quad , \quad \alpha = \epsilon \tag{2.10}$$

C. RADIATION SOURCES

1. Blackbody Radiators

A blackbody radiator is "a hypothetical radiator with emissivity=absorptance=1, reflectance=transmittance=0, that emits isotropic random radiant energy over a continuous distribution of wavelengths from zero to infinity. The radiant exitance as a function of temperature and wavelength is given by the experimentally verified Planck Distribution Law" [Ref. 3:p. 24].

3. The Planck Distribution Law

This law gives the spectral radiant emittance M_λ into a 2π steradian solid angle (hemisphere), for a blackbody radiation source by the equation

$$M_\lambda(T) = (C/\lambda^5)[1/(e^{D/\lambda T}-1) \quad (W/m^2-\mu m) \tag{2.11}$$

8

where C and D are the Planck radiation constants

$$C = 2\pi c^2 h = (3.7417)10^4 \quad (W\text{-}\mu m^4/cm^2)$$

$$D = hc/k = (1.4388)10^4 \quad (\mu m\text{-}K)$$

$$k = \text{Boltzmann's constant} = (1.38054)10^{-34} \quad (J/°K)$$

Blackbody radiation curves are shown in Fig. 2.1 [Ref. 3:p. 26]. Combining eq. (2.8) and (2.11) Planck's law is expressed in photon flux units

$$M_\lambda(T) = (2\pi c/\lambda^4)[1/e^{D/\lambda T}-1] \quad (\text{photons/s-m}^2\text{-}\mu m) \quad (2.12)$$

The radiant emittance M over a certain wavelength region $[\lambda_1, \lambda_2]$ is given by the integration of the spectral radiant emittance over this region

$$M(T) = \int_{\lambda_1}^{\lambda_2} M_\lambda(\lambda, T)\, d\lambda \quad (W/m^2) \quad (2.13)$$

For small differences in temperature, as occur between sea surface and sky horizon, the integrated thermal derivative of the Planck Distribution Law, is of great importance, [Ref.1:p.22]

$$dM/dT = \int_{\lambda_1}^{\lambda_2} [dM_\lambda(\lambda, T)/dT]\, d\lambda \quad (W/m^2\text{-}°K) \quad (2.14)$$

Typical values of the spectral integral of the thermal derivative are given in Table 2.1 taken from [Ref.1:p.28].

3. The Stefan - Boltzmann Law

This law is derived from Planck's Distribution Law by integration over all wavelengths:

$$M = \int_0^{\infty} M_{\lambda} d\lambda = \sigma T^4 \quad (W/m^2) \qquad (2.15)$$

where σ = Stefan-Boltzmann constant = $(5.6686)10^{-8}$ $(W/m^2 K^4)$

4. Real Radiators

Real radiators are distinguished in terms of the emissivity as blackbodies with $\epsilon = 1$, graybodies with ϵ = constant < 1, and selective radiators with ϵ varying with the wavelength [Ref. 2:p. 11.6].

Emissivity, absorptivity, and reflectivity, are basically surface effects, although they require a thin surface layer of material. Emissivity in metals is low and increases with the temperature, while in metal oxides it has values about ten times higher. Non-metals have higher values of emissivity, which increases as the temperature decreases. Selective absorbers are also selective emitters but the dominant emission may not occur at the same wavelength as the dominant absorption [Ref. 4:p. 3/08].

The radiance L (assuming a Lambertian surface) of a radiator with emissivity ϵ, and radiant emittance M is given by

$$L = \epsilon [M/\pi] \qquad (2.16)$$

10

III. BACKGROUND RADIANCE

A. GENERAL

The term "background", with respect to some optical target, refers to the surroundings which emit random electromagnetic radiation in the same spectral region as the target. Background sources are considered to be the earth surface (land, sea), the several atmospheric constituents (clouds, gases, particles), the sky, and the sun. The thermal background radiation is exhibited through the emissivity/reflectivity of surfaces, the refractivity of objects and the scattering of the atmosphere. All these properties are strongly affected by the environmental conditions and the nature of the materials.

In the following paragraphs, the interesting background radiances of sea and sky are reviewed, and several factors which determine the limits of such radiances, are examined.

B. SEA SURFACE THERMAL RADIANCE

1. Introduction

The equation for the balance of the sea surface infrared radiance L_s, can be derived from Fig. 3.1 in the form

$$L_s = (1-r_s)L_w + r_sL_i \qquad (3.1)$$

11

where L_w is the thermal radiance emitted from the water to the sea surface, L_i is the thermal radiance incident from the sky and the sun to the sea surface, and r_s is the reflectivity of the sea surface.

The sea surface radiance depends mainly on the following factors [Ref. 5:p. 3/105]:

1. Optical properties of water.

2. Wave-slope distribution.

3. Sea surface temperature distribution.

4. Properties of the sea bottom materials.

2. Optical properties of water

Optical properties of water vary with the wavelength of the infrared radiation and with the thickness of the water layers. For radiation at wavelengths longer than 3 μm, water is almost opaque, (transmissivity negligible). In the infrared range, the sky radiation is not scattered in subsurface layers. Surface contamination layers do not affect seriously the thermal radiation, except in case of capillary waves and alteration of heat exchange during evaporation. Thus, the water surface layer of 0.01 cm thickness, determines the water thermal radiance. The transmittance of sea water and that of distilled water in thin layers are almost the same in the range of 2 to 15 μm. Reflected incident radiation includes radiation direct from the sun and sky thermal radiation. The first dominates in the 0.35-3.0 μm

12

region (solar range), but contributes a very small amount in the region of 8-14 μm. Thus the only reflected thermal radiation accounted for is that from the sky. Fig. 3.2 shows the transmittance and reflectance for a free sea-water surface versus the angle of incidence. [Ref. 5:p. 3-105,106].

3. **Wave Slope Distribution**

The wave slope distribution affects the reflectance of a roughened sea-surface. Fig 3.3 shows the reflectance of solar radiation from a flat sea surface, (σ=0) and from a sea surface roughened by a Beaufort 4 wind, (11 to 16 knots, white caps, σ=0.2) [Ref. 5:p. 3-108]. The reflectance for a roughened sea is about 20% near the horizon, while that of a flat sea is higher than 31% reaching 100% at 90°.

4. *Sea-Surface Temperature Distribution*

The temperature of the upper surface layer of the sea (0.01 cm) regulates the sea thermal radiation. Temperature in turn depends on the heat capacity, which is low, of the surface layer, the net incoming heat from the air and from below, and the radiation exchange. If any surface contamination layer exists, the sub-surface heat flow is reduced and thus the upper layer appears to be colder in contaminated areas. Another factor which causes the upper surface layer to be colder than the water below is the evaporization conditions. In this case it has been found that the upper 0.01 cm is as much as 0.6°C colder than the

13

water a few centimeters below. Fig. 3.4 shows the sharp temperature gradient of the upper layer. [Ref. 5:p. 3-109].

5. Bottom Material Properties

Water is essentially opaque to infrared radiation at wavelengths longer than 3 μm, as stated in section III.B.2. Thus the properties of the bottom materials are of no concern in this wavelength band.

C. SKY RADIANCE

1. Introduction

Sky radiation in the infrared region comes from the scattering of the solar radiation and the thermal emission of the atmospheric constituents. The scattered solar radiation is present the day time and is not transmitted beyond the 3 μm region. The atmospheric thermal emission is present day and night and dominates beyond the 4 μm wavelength. A representation of the sky radiation is shown in Fig. 3.5. The upper dashed blackbody curve is approximately the spectral radiance of the sun. This radiance is scattered in the atmosphere (lower dashed curve), and also gives rise to the thermal emission of the sky (300 K curve). However the sky does not scatter as much as the sunlit cloud but only that which is given by the solid curve to the left, (clear sky). Thus, the background radiance of the sky is described by these two solid curves. [Ref. 5:p. 3-71].

14

2. Spectral Radiance of Clear Sky

Spectral radiance of clear sky in the thermal region depends on the elevation angle, the absorption of the atmospheric constituents, the air mass character (humidity), and the ambient temperature. The information on the effectiveness of these factors comes from measurements which are presented in Fig. 3.6, 3.7, 3.8, taken from Wolf and Zissis [Ref. 5:p. 3-72, 3-74].

The elevation angle determines the atmospheric path and thus the emissivity. Figures 3.6 and 3.7 show the elevation angle dependence of the spectral radiance. It seems that near the horizon, the sky behaves as a blackbody source. In the regions of 6.3 μm (water vapor absorption band) and 15 μm (carbon dioxide absorption band) the emissivity still remains high, ($\epsilon \approx 1$), even at 90°. Between these two wavelengths the atmospheric absorptivity (=emissivity) is low and the sky can no longer be considered blackbody. The peak at 9.6 μm is due to ozone. The zenith measurement in Fig. 3.6 is taken from a high, dry location, and Fig.3.7 is taken at a humid, sea-level location, so a comparison can be made between the bottom curves. It shows that the humid environment increases the sky absorptivity (=emissivity).

The temperature of the atmosphere affects the emissivity in the thermal range. Fig. 3.8 shows the variation of the sky spectral radiance with the ambient temperature.

15

The total thermal irradiance for a clear sky, E_{sk}, is given [Ref. 5:p. 3-76] by the empirical relation of Idso-Jackson, based on the ground-level meteorological absolute air temperature T_A:

$$E_{sk} = \sigma T_A^4 \{1-0.261 \exp[(-7.77)10^{-4}(273-T_A)^2]\} \qquad (3.2)$$

3. Spectral Radiance of an Overcast Sky

At lower altitudes, clouds consist of water droplets of radii from 1 μm to 10 μm at concentrations above 300 cm^{-3}, at temperatures close to that of surface. Water has been found to be a good absorber, (Fig. 3.2). Thus at low altitudes infrared radiation incident on a water droplet is highly absorbed and partially reflected and transmitted. Furthermore because of the multiple scattering in all neighbouring droplets in the cloud, the transmittance of the cloud turns out to be negligible, and thus the emissivity approaches unity. [Ref. 7:p. 31].

An approximate relation for the overcast sky radiance, taken from the Infrared Handbook gives

$$L_V(\theta) = L_V(\text{horizon})(1+A\cos\theta) \qquad (3.2)$$

where A is 2.0 and θ is the angle from zenith [Ref. 5:p. 3-74]. This equation combined with the aspect angle for good

16

emissivity of an overcast sky at low altitude as in the former paragraph, indicates to a first approximation that an overcast sky can be considered as a blackbody radiator at all altitudes. As a verification of this conclusion, Fig. 3.9, [Ref. 5:p. 3-74], can be used; this shows the spectral radiance of overcast skies in winter and summer. The peak is about 800 μW cm^{-2} sr^{-1} μm^{-1}, a typical value for a blackbody emitter.

4. Spectral Radiance of Clouds

Generally the scattering of thermal radiation in a cloudy medium is neglected. The reflectivity (albedo) of a cloud is assumed to be zero, and only the cloud emission and transmission are considered. If the content of water droplets (or ice crystals) exceeds 0.5 g/cm^2, then the clouds do not transmit radiation and their emissivity approaches unity. However, this is a simplification and several factors have to be considered. For instance, real clouds are spatially inhomogeneous, and they may have different transparency in different areas. Clouds of some types are almost never optically dense, but have considerable transmissivity. [Ref. 8:p. 221].

Another fact frequently disregarded is that the scattering by the low- and medium-altitude clouds (water clouds) is largely different from that by the high-altitude clouds, which consist basically of ice crystals (ice clouds)

17

These clouds are better scatterers than droplet clouds, since the crystals are larger. Finally, radiation fluxes penetrating through a cloud show changes in intensity and create radiation sinks and heat sources. The latter is not described in the black body approximation. Fig 3.10 shows the spectral emissivity of cloud layers versus wavelength and thickness dz. Fig 3.11 shows the integral emissivity, transmissivity and reflectivity changes versus thickness dz. [Ref.6:p.303], [Ref.7:p.224,225].

Thick clouds are taken as good absorbers. From Fig. 3.11, it seems that for thickness greater than 60 m the transmissivity goes to 0 and emissivity goes to one, while the absorptivity goes to a limit.

The emission from clouds in the infrared region is in the range from 8 to 13 μm and depends on the temperature of the clouds. The atmosphere has two strong emission bands at 6.3 and 15.0 μm, so a cloud may not be visible in these regions and the radiation is the resultant of emission from both the cloud and from the atmosphere. Fig. 3.12 taken from [Ref. 5:p. 3-73] is characteristic of this matter. A cloud of temperature -10° C is in an atmosphere at 10° C. The radiation curve of the cloud follows the blackbody curve for -10° C in the middle but at the edges 6.3 μm and 15.0 μm, the radiation of the atmospheric path below the cloud is added, and the cloud curve follows the blackbody curve of 10° C.

18

The spectral radiance of thin cirrus clouds is shown in Fig. 3.13 [Ref. 5:p. 3-74]. Here the emission has been raised compared with those of clear sky condition, (Fig. 3.6, 3.7). The ozone radiation peak is also reduced since it comes from a region higher than the clouds which serve as a filter on it.

D. THE SCHWARTZ-HON (SH) MODEL

The Schwartz-Hon (SH) model describes the effect of the sea surface roughness upon the emissivity. Basic assumptions of the model are the following [Ref. 9]:

a. The entire surface emits at a constant temperature.

b. The emissivity is a function of the surface roughness only.

c. The surface is composed of many contiguous flat elements.

d. For a given flat horizontal element of the surface, water has an emissivity which is a function of view angle with respect to the surface normal, (Fig. 3.14).

e. The radiance of the surface depends on the slope and orientation of each element of the fluid surface.

The emissivity of the surface is the spatial average of the emissivities of all the elements. The correspondence between wind speed and elevation variance of the wave results from the direct relation between sea surface roughness and wind speed. Thus the view angle (zenith) θ_v, and the wind

19

speed are the input parameters. The surface average emissivity is computed from the model. The water emissivity of a flat sea surface and of a sea surface roughened by various wind speeds in nadir angles $0°$ to $90°$ are shown in Fig. 3.15. The model also computes a zenith angle

$$\theta_r = (180°-\theta_v)-2\alpha = \theta_i-2\alpha \qquad (3.3)$$

where α is the slope angle of the wave, (Fig. 3.14), for the incident sky radiance L_i, associated with the average emissivity of the surface for a constant wave slope. The model does not account physically for self-shadowing on the surface, but includes it only computationally. [Ref. 9].

For a non zero slope for views looking straight down, ϵ_s is less than unity. As the angle θ_v from the zenith is increased towards the normal, ϵ_s increases until it reaches its maximum value and then decreases to a positive minimum value when the viewing vector is near grazing. The grazing analysis must not be taken seriously because at that view angle, self-shadowing becomes dominant. [Ref. 9].

IV. ATMOSPHERIC PROPAGATION

A. ATMOSPHERIC REFRACTION

The propagation of the thermal radiation through an atmospheric slant path is affected strongly by the absorptivity and the scattering ability of the molecular constituents of the atmosphere and the particles suspended in it. Both these factors are parts of the atmospheric complex refractive index. This is different from that of free space, because of the interaction of the wave electric field with the atmospheric molecules. Using an electron oscillator model, it is described by the complex formula of Sellmeier

$$\tilde{n}^2 = 1 + \{ e^2/m\epsilon_0 \Sigma_j [Nf_j / (\Omega_j^2 - \Omega^2 + i\tau_j \Omega)] \} \qquad (4.1)$$

where the summation Σ includes all the atomic and molecular absorption transitions, f_j is the "oscillator strength" of the jth oscillator, Ω_j is the natural radian frequency and τ_j is the damping coefficient of the same transition, N is the molecular number density, and e and m are the electron charge and mass. This complex refraction index is resolved in to a real part $n(\Omega)$ representing the wave dispersion, and an imaginary extinction coefficient $-\mu(\Omega)$ representing the wave absorption at the resonant frequency. [Ref. 4:p. 12-1,12-2].

A formula for the atmospheric refractive index n, used in waves propagation estimations, is

$$(n-1)10^6 = (77.6p/T)(1+0.0075/\lambda^2) - (17.04-0.185/\lambda^2)p_w/t_w \quad (4.2)$$

where the scaled refraction index $N=(n-1)10^6$ is called refractivity, p and p_w are the barometric and the partial water vapor pressures in mbar, T is the absolute temperature in K, t_w is the temperature of water vapor in °C, and λ is the wavelength in μm of the absorption frequencies of the constituent molecules. For dry air $p_w=0$. The above formula is good at wavelengths remote from major absorptions, and in the visible and infrared ranges the dependence upon the wavelength is small. [Ref. 4:p. 12.3].

The water vapor has a negligible effect on the refractive index in the visual range, so the second term of Eq. (4.2) is omitted. The pressures p and p_w decrease rapidly and the temperature T decreases slowly with height. A typical value of the index n near the earth surface is 1.0003, and in a standard atmosphere it decreases at the rate of $(4)10^{-8}$/m of altitude. [Ref. 10:p. 448].

The Lorenz Law gives the refraction index of the air as a function of density d, and includes the wavelength dependence in the Gladstone-Dale constant K_{GD}

$$(n^2-1)/(n^2+2) = (K_{GD}) d \quad (4.3)$$

22

B. ATMOSPHERIC EXTINCTION

Thermal radiation is attenuated through the atmospheric path by two mechanisms, selective absorption-emission and non-forward scattering, caused by the several atmospheric gases, (water vapor, carbon dioxide, ozone), and small particles such as rain, snow, smoke, fog, or haze, suspended in the atmosphere [Ref. 1:p. 30]. Absorption in the atmospheric gases determines the so-called atmospheric windows. Absorption-emission and scattering by particles are referred to jointly as "extinction". [Ref. 6:p. 20-26].

Both kinds of attenuation depend on the wavelength, and are described by the imaginary part of the atmospheric refraction index, the extinction coefficient $-\mu(\lambda)$. This is the sum of the absorption coefficient μ_α and the scattering coefficient μ_s of both molecular and aerosol components of the atmosphere

$$\mu = \mu_\alpha + \mu_s = [k_m + k_\alpha] + [\sigma_m + \sigma_\alpha] \qquad (4.4)$$

where k_m is the molecular absorption coefficient, k_α is the aerosol absorption coefficient, σ_m is the molecular scattering coefficient, and σ_α is the aerosol scattering coefficient. Scattering by both molecules and aerosols is of greater importance in the visible range, while absorption from both constituents dominates in the far infrared region

23

(8-14 μm).[Ref. 4:p.12-7]. The atmospheric gases in order of importance are the water vapor, (with absorbing bands centered at 2.7, 3.2, 6.3 μm), carbon dioxide (2.7, 4.3, 15 μm), ozone (4.8, 9.6, 14.2 μm), nitrous oxide (4.7, 7.8 μm), carbon monoxide (4.8 μm), and methane (3.2, 7.8 μm). The absorptions of carbon dioxide at 2.7, and 15 μm, and that of water vapor at 6.3 μm define the two atmospheric windows of the IR radiation [3.5-5 μm] and [8-14 μm]. Scattering particles are listed in Table 4.1.

C. LOWTRAN 6 CODE

1. Atmospheric Propagation Codes

Atmospheric propagation codes are used to predict the attenuation of the atmospheric path, in which the infrared detection systems are operating. To do this, it is necessary to consider all the absorption and scattering sources along the path for several frequencies, to define the composition, density, temperature, pressure, etc. for all species, and to consider the internal energy transitions of absorbing molecules. This complex problem has been faced by computer modeling codes which can be classified into Line-by-Line direct integration methods, and Band Models. The former are more precise, but very tedious. Of the latter, the Aggregate method and the LOWTRAN method are the more important. The

24

Aggregate method is more accurate, but the LOWTRAN is faster and has been used widely. [Ref. 4:p. 13-1].

2. LOWTRAN 6 General Description

LOWTRAN is a low resolution FORTRAN computer code, used for broad band prediction for thermal sensor systems. LOWTRAN 6, the latest version of this code, was used in the present work. It calculates the atmospheric transmittance and the thermal radiance over a band ranging from 350 to 40000 cm^{-1} (or 0.25 to 28.5 μm), with 20 cm^{-1} increments, in steps of 5 cm^{-1}. It relates empirical precomputed attenuation data with meteorological and other environmental input parameters. The output transmittance is an averaged value of all the transmittances due to water vapor line absorption, water vapor continuum absorption, uniformly mixed gases line absorption, nitrogen continuum absorption, aerosol absorption, aerosol scattering and molecular scattering [Ref.6:p. 36]. The program calculates the refraction and earth curvature along the atmospheric slant paths. It utilizes an atmosphere of 33 layers, at 1 km spacing up to 25 km, 5 km spacing from 25 to 50 km, and 70 to 100 km altitude. [Ref. 4:p. 13-9].

3. LOWTRAN 6 Input Data

The data input to LOWTRAN 6 consists of four cards or screens that ask for input parameter data. The first card

25

provides a selection of seven atmospheric models, the type of the atmospheric path, the execution mode, and the profiles of temperature/pressure, water vapor and ozone. This card also asks for the temperature and the reflectivity (=surface albedo=1-emissivity) of the opaque radiating surface at the start of the path. The second card requires selection of the extinction type and default range from nine boundary layer aerosol models. If radiosonde data are used, the program requests entry of the weather data for the atmospheric layers The third card defines the geometrical path, and the radius of earth. In the fourth card the desired spectral range for atmospheric transmittance or radiance and the frequency increment to average the data must be input. A detailed description of the functions of these cards and the required data is given in [Ref. 11].

V. THERMOGRAPHIC VIEWING SYSTEM

A. INTRODUCTION

Thermography is the technique of producing images from the invisible thermal radiation of the objects. The AGA Thermovision 780 system is designed for both thermal imaging and image analysis. The functions of the system are real time infrared scanning, thermal image display and measurements and digital recording, storing, and processing of thermal images. The main components corresponding to these above functions are, a real time scanner, a black and white monitor chassis display with measurement capability, a color monitor display, and a microcomputer with digital processing abilities. Thermal energy radiated from an infrared source is converted to electronic video signals in the scanner. The electronic signals are amplified and produce a thermal image on the black and white monitor display. The same signal can also be fed to the color monitor for a real time color image. Finally video and data signals are transmitted to the microcomputer where the thermal image is displayed in color and can be recorded, stored on a data disk and processed for temperature evaluation using color codes. The system is described in the following sections of this chapter. The information is taken from the Operating Manuals for AGA Thermovision 780 [Ref. 2],

27

and for the DISCO 3.0 Processing Software [Ref. 12]. Technical data for the AGA Thermovision 780 sensor are shown in Table 5.1.

B. AGA THERMOVISION 780 SYSTEM

1. The Infrared Scanner

The infrared scanner is a dual channel scanner consisting of a standard shortwave (SW) scanner, which covers the 3 to 5.6 μm spectral band, and the longwave (LW) one, which covers the 8 to 14 μm spectral band, (Fig. 5.1). [Ref. 2:p. 3.1]. Each unit consists of the following parts:

a. Electro-optical scanning mechanism.

b. Infrared detector.

c. Liquid nitrogen Dewar.

d. Control electronics and preamplifier.

A simplified block diagram is shown in Fig. 5.2. The electromagnetic energy emitted from a target is focused by infrared lenses into a vertical prism rotated at 180 rpm, and its optical output is passed through a horizontal prism which rotates at 18000 rpm. The rotation of both prisms is controlled by slotted discs which are electronically connected to the horizontal and vertical triggering circuits to provide horizontal and vertical trigger pulses to the monitor. The vertical and horizontal motors are synchronized so that four fields of 100 horizontal scanning lines each

28

produce one interlaced frame. There are 70 active lines per field, or 280 per frame. The scanning rate is 25 fields per second. [Ref. 2:p. 3.1].

The output from the horizontal prism passes through selectable filter (if desired) and aperture unit, and finally it is focused onto a single point detector, which is located in the wall of a Dewar chamber. The electronic output signal from the detector is proportional to the incident radiation. This signal is preamplified within the scanner and the video signal is connected to the Black/White monitor chassis. [Ref. 2:p. 3.2].

The aperture discs mentioned above are eight in number and range from f/1.8 to f/20. This range gives the ability to measure temperatures from -20° C to +800° C without the use of filters. The smaller the aperture selected the higher the temperatures which can be imaged since increase in signal is interpreted as increase in temperature. The apertures also offer a 20% overlap between temperature ranges. The detector is cooled with liquid nitrogen which maintains the chamber at a temperature of -196°C. The scanner unit can be fitted with any one of five different lenses with fields of view varying from 3.5° to 40°. The LW unit used in this work has available a 3.5° and a 7° lens. The arrangement of the electro-optical components in the scanner is shown in Fig. 5.3. [Ref. 2:p. 3.2, 3.5].

2. Black/White Monitor Chassis

As mentioned above the video output signal from the scanner unit is applied to the black/white chassis, (Fig. 5.1), where it is amplified and fed to the display screen. Outputs from this monitor chassis are used for the color monitor display and for the microcomputer processing [Ref. 2:p. 4.1].

3. Digital Image Processor

This set consists of an interconnecting link unit and a microcomputer. The first digitizes the image, holds the image data during the time these data are transferred from the Thermovision to the computer, and controls the data transferring speed. The IF 800 microcomputer is a CP/M based dual-floppy system which runs the AGEMA proprietary DISCO 3.0 software. [Ref. 7:p. 42].

The DISCO 3.0 software consists of three main programs (DISCO, IMAGE PROCESSING, UTILITY). Each of these contains subprograms (Fig. 5.4). The DISCO / F1 RECORD IMAGE subprogram is used to record thermal images and display them on the computer screen. The same subprogram is used to enter the parameters of the scanner, and of the atmospheric path. The DISCO / F2 EVALUATE IMAGE subprogram is used to evaluate the temperature profiles of the image, using 3 to 36 different color combinations. Each color corresponds to a particular temperature range. The standard table of the

system has 8 colors. The subprogram is also used for displaying histograms and single isotherms, magnifying the image, transferring a new image on to the display from the set of stored images, printing data such as temperature profiles, and integrating the spot temperature meter and horizontal and vertical profiles. [Ref. 12:p. 8, 22].

The last function labeled by "PROF/SP" ("PROFILE" + "SPOTMET") was used extensively in the present work. When the button "PROF/SP" is pressed a small, cross-hair like, cursor is shown in the image. The coordinates of its position are shown below and to the right of the screen. This cursor is moved by the arrow keys. The following text (in yellow) comes up:

F8 : SPOT (Off)

F9 : HOR P(Off), F10 : VER P(Off)

When the button F8 is pressed the "Off" text shifts into "On" with yellow background, and the spot temperature function is activated. If the cursor is moving horizontally and vertically the temperature is shown below the color scale (e.g. "SPOT" = 27.7 °C). The cursor can be moved by single steps corresponding to picture elements (lines). The picture is divided in 128 vertical and 64 horizontal pixels (lines). Thus, when a 3.5°lens is used the vertical movement of the cursor corresponds to a 3.5°/64 = 0.0546875° of zenith angle per line or 0.109375° if a 7° lens is used. [Ref. 12:p. 27].

31

C. THERMAL MEASUREMENT TECHNIQUES

1. Introduction

The power received by the detector is recorded instrumentally as "Thermal Value" (THV), in terms of the arbitrary "Isotherm Unit" (IU). The relation between Thermal Value and received photon flux is linear (proportional), but the relation between thermal value and object temperature is non-linear. The latter relationship is the calibration function which can be given as a graphical curve or a hand held calculator program. This represents the basic means for translating measured thermal value into object temperature. The calibration function assumes a perfect blackbody radiator and no atmospheric effects. The calibration curves are accurately described by the equation

$$I = A/[Ce^{B/T}-1] \qquad (5.1)$$

where I is the thermal value in isotherm units (IU) for the absolute temperature T in °K, and A,B,C are calibration constants that depend on the aperture, filter, scanner etc. These constants may be determined by an empirical procedure and stored for future use. Default values are provided for the equipment.

Equation (5.1) is used by the DISCO microcomputer program to calculate the temperature of the target for a

32

known thermal value after the calibration constants A, B, and C, for the LW shown in Table 5.2 had been inserted. Calibration curves in LW for all the aperture sizes are shown in Fig. 5.5 through 5.8. [Ref. 2:p. 10.1, 10.6].

The two basic methods of thermal measuring are:

a. Direct measurement. This utilizes the instruments built-in clamping and temperature compensation system that permits temperature measurement without the use of an external temperature reference.

b. Relative measurement. An external reference thermal source with known temperature and emissivity is used.
The first method is easier but not absolutely accurate. The second method is generally recommended if a suitable and accurate reference is available. [Ref. 2:p. 10.2].

2. Direct Measurement

A short description of the monitor chassis front panel controls and indicators, shown in Fig. 5.9, is given below. [Ref. 2:p. 4.3].

a. THERMAL RANGE (item 9): This switch selects the thermal span of interest with the nine position calibration, between 2 and 1000 isotherm units.

b. THERMAL LEVEL (item 10): This control sets the thermal value of the isotherm scale zero point. Full scale equals 1000 isotherm units.

c. PICTURE MODE "NORMAL"(item 12b): It selects the normal

33

image display, in which the cooler objects appear as black and the hotter as white.

d. ISOTHERM LEVEL 1 (item 13): This control turns on the isotherm function and identifies the discrete thermal levels on the target. The isotherm function is indicated by saturated white areas, which represent areas of common temperature. A marker on the vertical isotherm scale indicates the relative position of the selected level.

e. ISOTHERM SCALE (item 16): This is a scale calibrated from -0.5 to +0.5. A reading of the isotherm marker multiplied by the thermal range gives the relative thermal value in isotherm units.

The step by step measurement procedure is:

a. Picture mode NORMAL.

b. Adjust the THERMAL RANGE and THERMAL LEVEl controls to obtain a good thermal picture. Note the setting "L" of the THERMAL LEVEL control knob.

c. Adjust the ISOTHERM LEVEL 1 control to brighten up the point of interest on the object of view. A marker on the vertical scale indicates the relative position of the selected level. The reading of the isotherm marker multiplied by the thermal range gives the relative thermal value "i" in isotherm units, as shown in Fig. 5.10.

d. Add the values "L" and "i" to get the measured thermal value I_O in isotherm units.

e. For a black body radiator, and without atmospheric attenuation, the calibration curves can be used to give directly the object temperature. [Ref. 2:p.10.2].

3. Relative Measurements

In this type of measurement, the thermal difference between the object and a reference surface is measured. The THERMAL LEVEL and the THERMAL RANGE controls must be set at the same values for both the surfaces. [Ref. 2:p. 10.2] describes in detail the method. The temperature of the object can be calculated from the temperature of the reference. The ideal reference has a temperature close to that of the object and the same emissivity, and is situated near to the object. The AGA Temperature Reference Model 1010 is recommended whenever applicable. It has a temperature range from +100 °C down to +40 °C in steps of 5°C and from +40 °C to +16 °C in steps of 2 °C. It has emissivity approximately 0.97, diameter 100mm, accuracy -/+0.2 °C in calm air, and influence of ambient temperature 0.01 °C / °C in calm air. The ambient temperature must be at least 2 °C below the required control temperature. When the desired temperature is set, the Model 1010 reference will radiate as a blackbody at that temperature. [Ref. 2:p. 8.1].

4. Complex Thermal Measurements

The AGA Thermovision 780 system gives the object temperature correctly if that object is a perfect radiator

and if no external factors influence the measurements. Thus the true object temperature must be derived by taking into account these factors, which include the emissivity of the target, the background surrounding the target, the target opacity, the target size, and the atmospheric effects. All these have been discussed in the previus chapters, except the target size, which should not be less than 2.5x2.5mm as seen on the black/white monitor chassis display screen. [Ref. 2:p. 10.3].

An exact measurement formula is discussed below. The thermal radiation that reaches the detector is the sum of the target-emitted thermal radiation, the radiation reflected by the target and the radiation emitted from the atmosphere as shown in Fig. 5.11. An opaque object at temperature T_o and with emissivity ϵ_o emits photon flux $\epsilon_o S_o$, where S_o is the photon flux of a blackbody at the same temperature. If the atmospheric transmittance is t, then the object radiation reaching the detector is $\epsilon_o t S_o$. Assuming also that the surrounding surfaces are at the same ambient temperature T_a and the ambient emissivity ϵ_a approaches unity, the radiation reflected by the object is $r_o S_a$, where S_a is the blackbody photon flux of the surroundings ($\epsilon_a = 1$), at temperature T_a, and where $r_o = 1 - \epsilon_o$ is the reflectance of the opaque object. This reflected radiation reaches the detector as $t(1-\epsilon_o)S_a$. The atmospheric radiation is $(1-t)S_{atm}$ where S_{atm} is the

photon flux due to the atmospheric emission and scattering. Hence the total photon flux reaching the detector is

$$S_o' = \epsilon_o t S_o + t(1-\epsilon_o)S_a + (1-t)S_{atm} \qquad (5.2)$$

This photon flux relation can be converted into a thermal units relation since, as was mentioned before, the thermal value (IU) measured by the AGA Thermovision 780 is proportional to the photon flux reaching the detector. Therefore, we can write the relation I=CxS where I is the thermal value, C the proportionality constant, and S the photon flux. Substituting S=I/C Equation 5.2 becomes

$$I_o' = t\epsilon_o I_o + t(1-\epsilon_o)I_a + (1-t)I_{atm} \qquad (5.3)$$

This equation can be solved for I_o to find the exact temperature through the calibration curves or can be solved ϵ_o if the exact temperature of the object is known and I_o estimated from the calibration curves. This formula can be used in both direct and relative measurements.[Ref. 2:p.10.4].

5. Thermal Measurements with Color Monitor

First it must be said that color thermograpy is not more valid than the gray-tone. The great advantage of color thermography is that it offers a thermally quantitative

37

display which can not be obtained in any other way. The gray-tone thermal image is a continuous display of temperatures variations, while the color display consists of a number of "sliced levels" of the total energy (temperature distribution) being displayed. The selection of color or B+W display should be made on the basis of the information desired.

The input signals to the Color Monitor in the AGA Thermovision 780, are the vertical and horizontal trigger pulses and the video signal, which is sliced into ten levels each of which is assigned a color. The temperature range of each color is displayed in the picture by a color-temperature scale. The same color indicates different temperature ranges for different settings of the THERMAL RANGE and THERMAL LEVEL controls. Conversely the absence of a color from the image display indicates the lack of the corresponding temperature from the input data, assuming a standard level control. Also the same color appearing in different places in a display, represents the same energy, temperature range of the image. A simplified Color Monitor block diagram is shown in Fig. 5.12. [Ref. 2:p. 10.9].

The Color Monitor system has also two variable sensitivities. If the areas of interest are at the ends of a large temperature range, the color isotherm widths and levels can be adjusted so that a number of narrow levels appear at

one end of the temperature range while the remaining levels appear at the opposite end. The center, very wide interval may be blanked out for ease of viewing (Fig. 5.13a). The other kind of variable sensitivity is used in the intermediate range. The Color Monitor can be adjusted such that the ten color levels cover only the temperature range desired (Fig. 5.13b). [Ref. 2:p. 10.9].

In the normal color image, the color isotherm levels are arranged in a linear fashion such that each color represents an equal number of isotherm units. These units are converted to temperature by means of the calibration curves. Temperature is a very non-linear function of thermal value in isotherm units. Thus, in the normal scale, each color represents a different range of temperatures depending upon where on the calibration curve it falls. The system has the ability to invert this linear-non linear correspondence, if it is desired. In this case, each color represents an equal number of temperature degrees, but not of isothermal units. [Ref. 2:p. 10.9].

A zero or non-level, is indicated by black, and the top color level (usually white), indicates a level greater than the threshold. These levels do not represent discrete temperature values. [Ref. 2:p. 10.9].

VI. SIGNATURE MEASUREMENTS

A. INTRODUCTION

The present work is an evaluation of the AGA thermal images taken at Moss Landing Marine Laboratories in November 4, 1987 by the NPGS/NACIT staff [Ref. 14], and in July 14, 15, 25, 1988 by Ridgeway and Psihogios [Ref. 15]. The objective of the evaluation is to relate the background sky thermal radiance to the elevation angle, to compare the radiance computed using LOWTRAN 6 to that measured with the AGA system, and then to validate the Schwartz-Hon model.

B. PROCESSING PROCEDURE

From November 4th data, two sets were selected, with the more appropriate weather information and elevation angle completeness. A problem implied from the study of the pictures and the notebook information, was to define the horizon angle. This could be done by correlating the physical horizon of the observer, with the estimated horizon of the thermal image taken by the AGA. In this work the following procedure was observed:

1. Look at the thermal image of the picture in the transition area between sea surface and sky.

2. Move the cursor of the computer display in this area, line by line and take the spot temperatures.

3. Look for spot temperature discontinuity and correspond this with the change of colors in the thermal picture in the direction from the sea surface to the sky.

4. The lower limit of the temperature change represents the sea, or the last optical ray which touches the earth surface before it goes to the sky. The upper limit represents the sky, or the physical horizon, and this is taken as the 0° elevation angle.

5. If there are three distinct temperature values (two sequential temperature "jumps"), then the lower value is attributed to the sea surface and the upper two to the sky. This can be justified by the fact that the region just above the sea surface is the area of evaporization of the water in which the dominant element is the wet air rather than the sea water. In this region the temperature is between the sea and sky temperature.

C. TABULAR DATA PRESENTATION

There are 29 tables of data, in Appendix B. Each table contains weather data for the location where the AGA device was and for the sea surface. Next they contain the AGA data in five columns. The first is the subdivision of the image into 64 horizontal lines or pixels, (pixels=picture elements), in the direction from the top of the picture to the bottom, in increments of two lines. The cursor in the

41

computer display is located always at the top of each pixel, so that the center of the picture is taken at the 33rd line. The second column is the zenith angle. Here the increment was accounted at 0.109375° per two lines, where the 3.5° lens is used and at 0.21875° per two lines, where the 7° lens is used. The MathCAD software [Ref. 16], was used to compute the zenith angle steps with a precision of three decimal digits. The third column contains the spot temperatures given by the AGA computer. The next column contains the corresponding radiance, computed with the MathCAD software, with a six decimal digits precision and for a 0.97 emissivity. Equation (2.16) was used in this computation.

The AGA spot temperature is given with one decimal digit precision. The six decimal digits precision was selected for the radiance because the values computed have always the two first decimal digits zero, while the differences in values start with the fourth or fifth decimal digit.

The weather data for the sea were taken from the R. V. POINT SUR for the first date and from the Monterey Bay bouy for the second date.

The first set of data (Tables 6.1 to 6.11) is from November 4th, with an angle increment 3.5°, and a range from 0° to 35°. These data were collected between 09:24 and 09:31 hours. According to the NACIT notebook the sun came out at 09:44 hours, so, for these data, the sky is taken as overcast. The horizon is estimated at 89.945° zenith angle.

42

The second set (Tables 6.12 to 6.17) is also from November 4th, with the 7° lens of the AGA used, for an elevation range from 0.0° to 35°. Here the sky was mostly blue, but at some limiting altitude and above the temperature is very low compared with that for low elevation angles. These low temperatures can be attributed to the existence of ice particles (section III.C.4). The horizon was estimated at 89.890° zenith angle.

The data from July 1988 are in Tables 6.18 to 6.29. The 3.5° lens was used. On July 14 and 15, with fair sky, the horizon was estimated at 89.97°, and 90.02° respectively. On July 25, with an overcast sky, the horizon was estimated at 90.07°.

The fact that the zenith angle of the apparent horizon varies from day to day is due to the variation of the refractive index with atmospheric parameters explained in section IV.A.

The emissivity recorded for all the images taken is 0.97. The most probable reason is that the same value is set at the AGA Temperature Reference Model 1010 which is used in order to estimate the validity of the spot temperatures with the AGA (section V.C.3).

Some comments can be discussed here about the results of the Tables:

43

a. The maximum and minimum values of the radiance on 4NOV87 are 4.345 mW/cm^2-sr at 89.563° and 1.659 mW/cm^2-sr at 51°. On JUL88 these values are 4.381 mW/cm^2-sr at 87.236° and 3.324 mW/cm^2-sr at 79.25° respectively.

b. The temperature gradient is not smooth, but varies with the altitude, due to weather conditions. From the results of both 4NOV87 and JUL88 measurements it seems that at low altitudes (zenith angle larger than about 70°) the temperature gradient, locally and totally, is smaller than in higher altitudes.

c. Fig. 3.9 allows us to make a comparison of the radiance values measured for overcast sky. For the winter curve the average spectral radiance is 0.540 mW/cm^2-sr-μm and for the summer curve 0.760 mW/cm^2-sr-μm approximately. Thus in the atmospheric window 8 μm to 14 μm the radiance values are 3.240 mW/cm^2-sr for the winter curve and 4.560 mW/cm^2-sr for the summer curve. From the Tables, the maximum and minimum radiance values 4.345 mW/cm^2-sr and 1.989 mW/cm^2-sr for 4NOV87 give an approximate mean value 3.167 mW/cm^2-sr which is close to the value for the winter curve. From the measurements of 25JUL88 the maximum 4.410 mW/cm^2-sr and minimum 4.251 mW/cm^2-sr radiance values give an approximate mean value 4.330 mW/cm^2-sr which is also close to the value for the summer curve.

44

D. VALIDITY OF AGA MEASUREMENTS

1. Historical Information

Some questions may arise concerning the validity of the temperature measurements. The AGA Thermovision 780 system used in both experiments was calibrated some two years ago, by Fudali [Ref 17]. However, an error of three to four isotherm units was found between direct and computer readings in the recent work. This error was minimized for all the work described here by adjusting the THERMAL LEVEL control to read four units higher, using the THERMAL LEVEL ADJ control in the Black/White monitor chassis [Ref. 7:p. 102]. A recent calibration experiment done on 05 August 1988, by Ridgeway [Ref. 17], showed that the calibration remains almost constant and thus the AGA measurements can be input directly into the LOWTRAN 6 program. What will be attempted here is a verification of the appropriateness of the critical parameters of aperture, thermal range, and thermal level, used in the experiments.

2. Laboratory Measurements of AGA Parameters

It is known that the measurements of November 4, 1987 were performed with an f/1.8 aperture and a thermal range 20. It is also known that, with the same aperture, the ratio thermal range / thermal level was 5/43 for July 14, 5/40 and 5/42 for July 15, and 5/44 for July 25 1988. In both dates the air and sea surface temperatures were varying around 15

°C. Thus the effort was directed to check the spot temperature of a known blackbody source emitting under circumstances as close as possible to those of the measurements. The most ideal blackbody reference source available was the AGA Temperature Reference Model 1010 already mentioned in section V.C.3. The lowest blackbody temperature obtained was 20 °C, at least two degrees above the ambient temperatures. The input parameters used, together with the spot temperatures acquired are shown in Table 6.30. Eight measurements were taken in order to get a more representative knowledge of the AGA measurement capability. The technique used was that of the direct method described in section V.C.2. The isotherm marker was always in the zero position. Each time the thermal range was preset, while the thermal level control alone was used to obtain a satisfactory (saturated) image.

Two important results came out from this multiple laboratory experiment. The first is that the spot temperature scale built into the system depends significantly on the thermal span (range), which is set by the operator before taking the spot temperature. The thermal value (thermal power), emitted by the object, is the summation of the thermal level with the product of the thermal range times the indication of the isotherm marker. In this laboratory measurement the isotherm marker is preset at the zero

46

position, so that the thermal value measured by the AGA is the thermal level alone, which remains almost constant in the measurements. However, the measured spot temperatures do not remain closely grouped, as appropriate to the thermal values, but show significant variation with thermal range setting. This first observation shows that the temperature measurement scale built into the AGA depends on the expansion of the thermal range. So given that the system measures temperatures between -20 °C and +800 °C, (section V.B.2), independently of the range used, it suggests that a certain thermal level which in the thermal span of two isotherm units is, say, in the center of the span, will be below the center of a larger span, say 100, and will correspond to a spot temperature lower than the first. The set of colors follows the expansion or contraction of the thermal ranges, and this explains the change of image colors with the change of the thermal range. This effect needs further investigation.

The second result is associated with the validity of the thermal ranges used in field AGA measurements. As Table 6.30 shows, the average error for thermal range 2 is 4.25 %, for range 5 0.71 %, for range 10 0.68 %, and for range 20 -4.0 %. This shows that the parameters used in November 87 and July 88 are acceptable to give accurate spot temperatures. Furthermore, Table 6.30 shows that the most preferable thermal ranges for typical environmental

temperatures are the ranges 5 and 10. This Table also shows that the higher thermal ranges become more representative at higher temperatures (e.g in 100 °C), while the lower ones still retain the same accuracy.

This laboratory investigation was not extended to the validity of the higher thermal ranges for very low and very high temperatures, since the Reference Model 1010 is not useful in these cases.

VII. DATA ANALYSIS

A. INTRODUCTION

In this chapter, the thermal radiance values obtained through the AGA spot temperature measurements, are compared with the values given by the LOWTRAN 6 program. A model with radiosonde data is used in this program. For the 4th of November radiosonde data are plentiful but collected four and half hours later than the time of the measurements at a distance 31 nmi distant from the AGA location. Radiosonde data were not available in July 1988. For this case a new model, based on the updated weather data from the Monterey Bay Buoy, from MLML, and the default values of the model was developed. The values of radiance computed with the use of the LOWTRAN 6 program are compared with those measured with the AGA system and the observed deviations are analysed. Using the same method the validation of the Schwartz-Hon model is described next. The effects of wind speed and sky, (fair/overcast), on the thermal radiance are discussed. Values measured with the AGA are used as references for two reasons. First, these are real-time values, while LOWTRAN 6 is fed with non real-time or non plentiful radiosonde data. Second, successive calibrations of the AGA system ensure operation with satisfactory accuracy (section VI.D).

49

B. RADIOSONDE DATA

The radiosonde data for the November 87 measurements, (containing 199 values of time, altitude, pressure, temperature, dew point temperature, relative humidity, and wind speed), are taken from data provided by the NPS Environmental Physics Group. The launch time is 23:02 hours Greenwich or 15:02 hours local time; thus, there is a 04:39 hours difference from the real time weather data of November 4. The station latitude is 36.20.00 North and the longitude 122.01.20 West, while the location of the AGA system at MLML is at latitude 36.48.02 North and 121.47.17 West. This implies that the closest radiosonde data are from a distance about 31 nmi South-Southwest from the location of the experiment, (each minute of latitude on the map is equivalent to one nmi distance on the earth). As will be shown in the following analysis, these approximations of time and distance will not distort seriously the results. Radiosonde data of 4 November 1987 were used to create the atmospheric layers required to input in the LOWTRAN 6 program (Table 7.1).

It was mentioned before that radiosonde data were not available in July 88. However, for reasons of uniform use of data, and validation of the results, a new atmospheric model was developed using 4 levels with data derived from the Monterey Bay Buoy, Moss Landing Marine Laboratory and the LOWTRAN default values (Table 7.2). lt consists of 4

atmospheric levels, at 0.0, 0.014, 0.019, and 16 km of altitude. At 0.0 km pressure, air temperature and dew point are taken from Monterey Bay bouy data (location 36.48 North / 122.24 West). At 0.014 km, pressure, air temperature, and relative humidity are taken from the MLML Station data. At 0.0 km the relative humidity is chosen to be one unit higher than that at 0.014 km, while at 0.014 km the dew point is chosen one decimal unit lower than that at 0.0 km. At 0.024 km, pressure and dew point are chosen one decimal unit and relative humidity one unit lower than those at 0.019 km, while the same temperature is used for the three altitudes. Finally at the 16 km altitude level, LOWTRAN default values for pressure, temperature, and relative humidity are used.

C. APPLICATION OF LOWTRAN 6

LOWTRAN 6 was used to compute sky thermal radiance with the input data shown in Table 7.3. The same program was also used to compute the Schwartz-Hon radiance of the sea surface. Because of the choice of the atmospheric model (radiosonde data), a certain number of atmospheric layers had to be entered. For November 87, data from 23 atmospheric layers, each approximately 0.5 km were entered. These data are shown in Table 7.1. The four atmospheric layers created for the days of July 1988 are contained in Table 7.2.

In the computations for November 87, the range for the AGA radiance was chosen as 16 km. This value is based on the right triangle "center of the earth - horizon on the earth surface (right angle) - AGA detector at 0.014km", where the radius of the earth is taken as four thirds of the actual radius, (6378.388 km), in order to account for the refraction of the atmosphere. Thus, at each zenith angle at the range of 16 km, a certain altitude was computed. From the radiosonde data for this altitude the relative air temperature was estimated by linear interpolation. This temperature was used as the temperature of the boundary atmospheric layer at the target, in place of the default value of 0.0 °K.

But the parameter which most affects the radiance, is the wind speed, which varies gradually from 5.3 m/sec at 230 m, to 25.6 m/sec at 11,156 m. The author's opinion is that the value of the wind speed to be entered for a certain slant path should take into account the variations of wind along the entire path. Thus it would be better to consider a function of the wind speed, as a function of altitude averaged along the path since the slope variation is not constant. However for simplicity of computation and because of irregularity of data, wind speed is assumed constant up to 230 m at 5.3 m/s. The wind speed used for each slant pathwas then computed as the average of values from zero to this

altitude. The curves of single and average wind speed are shown in the plot of Fig 7.1.

For July 88, the default value of -56.5°C was chosen as the temperature of the boundary atmospheric layer, due to lack of radiosonde information. The wind speed used was that of the location of the AGA sensor, the only value available. As was said before the radiance, in LOWTRAN 6, is affected basically by the wind speed.

The sky radiance given by LOWTRAN 6 is compared with that measured by the AGA system. The results are shown in Tables 7.4 through 7.15, and the corresponding plots in Fig. 7.2 through 7.13. The first four Tables are for November 87 and contain also the computed values for altitude, boundary temperature and averaged wind speed. The last column gives the percentage error of the LOWTRAN 6 radiance relative to that of the AGA. Tables 7.4, 7.5 and Figures 7.2, 7.3, compare the sky radiance near the horizon, in increments of 0.438°, for an overcast and fair sky respectively. Tables 7.6, 7.7 and Figures 7.4, 7.5 refer to sky radiance from the horizon to about 55°. Here the angle increment is about 1°. The next Tables and Figures refer to the four measurements of July 88. The sky is fair, except for July 25, when the sky was overcast. The increment of zenith angle for the July measurements is 0.21875°. All the Figures include the plots for AGA and LOWTRAN radiance and the percentage deviation

53

between these two radiances. The MathCad software [Ref. 16] was used in plotting the curves.

D. VALIDATION OF SCHWARTZ-HON MODEL

The procedure for the validation of the Schwartz-Hon model was the following.

1. Define the incidence angle θ_i of the sky radiance on the sea surface, by subtracting the zenith angle θ_v from 180° (Fig. 3.14).

2. Define following the Schwartz-Hon model the emissivity ϵ_s of the sea surface and the zenith angle of the incident ray $\theta_r = \theta_i - 2\alpha$, (Eq. 3.3), where α is the slope angle of the wave surface. Computations were performed using the program PC-TRAN / EMISSIVITY for the Schwartz-Hon model. The other input data besides the angle θ_i, was the wind speed. For July 1988, the input wind speed was the average of values at the sea surface and the AGA location.

3. Compute the sky radiance at angle θ_r, $L_i(\theta_r)$, by applying the Planck Law at the spot temperatures measured with the AGA.

4. Compute the radiance $L_w(SST)$ emitted by the sea surface, for the sea surface temperature (SST) taken from the meteorological data, by applying the Planck Law.

5. Estimate the total radiance L_s emitted by the sea surface, using Eq. 3.1.

54

6. Define an effective blackbody temperature T_{bb} given by

$$T_{bb} = [L_s-L_w]\pi/[dM/dT] + (SST) \qquad (8.1)$$

suitable to be treated as input temperature in LOWTRAN 6, assuming the sea surface to be a blackbody source (section III.B). The above equation is derived as follows. For small differences between sea surface effective temperature $T_s=T_{bb}$ and the measured sea surface temperature $SST=T_w$, the integrated thermal derivative, defined by Eq. 2.14, is written as $dM/dT = M_s-M_w/T_s-T_w$, and thus $T_s = [M_s-M_w]/[dM/dT]+T_w$, or using Eq. 2.16, $T_s = \pi[L_s-L_w]/[dM/dT]+T_w$, at the neighborhood of T_{bb}.

7. Temperature T_{bb} is necessary, in order to compute by the LOWTRAN 6 program, the sea surface radiance L_{SH} of the Schwartz-Hon model, considering the sea surface as a black body source. In order to obtain a more realistic value of the thermal radiance along the slant path, the wind speed used was the average value of wind speeds at the detector location and the sea surface.

8. Compare the radiance L_{SH} with that measured with the AGA system.

Tables 7.16 through 7.20, and Figures 7.14 through Figures 7.18 contain the above validation of Schwartz-Hon model for Novenber 4, 87 and for July 14, 15, 25, 1988.

55

E. ANALYSIS OF RESULTS

1. LOWTRAN 6/AGA Thermal Radiance versus Zenith Angle

A look at the plots for the sky radiance (Fig. 7.2 through 7.13) yields some useful results:

a. Thermal radiance of the sky decreases with the altitude above the horizon, with a reducing rate. It was expected since the real sky temperature is known to decrease.

b. The LOWTRAN 6 curves exhibit a bending downwards as they approach the horizon from higher altitudes, while the AGA radiance curves usually do not. This shows clearly in the first LOWTRAN values (near the horizon) of radiance in the Tables 7.6, 7.10, 7.12 (inability of prediction), 7.14. The case of Table 7.12 particularly proves that a problem there is with the LOWTRAN 6 computations near grazing (at least for horizon at 90° zenith angle).

c. In the plots from NOV87 the error is usually larger at the lowest elevation angles, then goes to a minimum. The opposite occurs in the plots from JUL88. It can be attributed to the fact that in NOV87 the wind speed profile was unknown below 230 m, while in JUL88, the wind speed was best known in the first 15 m above the sea surface.

d. The curves for radiance calculated with the AGA and with LOWTRAN 6 follow parallel directions in most cases. This means that the model used in LOWTRAN 6 works correctly. The gap between the two curves is consistent for both dates

56

NOV87, and JUL88. More specifically the points of the AGA curve are always above the corresponding points of the LOWTRAN 6 curve, (except in Fig. 7.4 and Fig. 7.5). Certain assumptions could be discussed here. In Fig. 7.4 the AGA curve simply does not exceed that of LOWTRAN, while in Fig.7.5 the AGA curve is lower beyond the zenith angle of 85°. This latter inversion in Fig.7.5 can be attributed to the probable existence of ice crystals, lying in higher altitudes and not predicted by LOWTRAN 6. It is known (section III.C.4) that ice clouds are better scatterers than common clouds; thus the sky emissivity is reduced, leading to the lower values of AGA radiance in this plot. The constant exceeding of the AGA curve in the remaining plots can be attributed to either or both of the following reasons; error in LOWTRAN 6 radiance or error in AGA radiance. The former could arise from the fact that on the first date the radiosonde data were plentiful but not at the time or location of the measurement, while for the latter date the radiosonde data were of poor quality. On the contrary probable error in AGA radiance might be anticipated from the fact that the AGA values are consistently higher than the LOWTRAN values under a variety of atmospheric conditions. This could arise from an overestimate of an input parameter in the Thermovision, such as emissivity, thermal range, or thermal level. Emissivity, certainly is not as high as

assumed (0.97). For a clear sky the spectral radiance is decreasing in elevation angles between 0° and 90° (section III.C.2, Figures 3.6, 3.7); this means the emissivity, which is proportional to spectral radiance of a non-blackbody source, (section II.B.10), is decreasing too. Emissivity is reducing also with the thinness of the cloud layer. Figures 3.10, 3.11 show that for cloud thickness below 100 m the emissivity is decreasing. Expressions for quantitative influence of high emissivity can not be derived from these Figures (3.6, 3.7, 3.10, 3.11) because other parameters are unknown (e.g. temperature). The problem with the thermal range/level was discussed in the previous chapter. The author's opinion is that both the errors exist, and for that reason, real-time checks of AGA parameters have to keep up with real-time weather knowledge.

These were some theoretical justifications of the source of the expected error. This qualitative exploitation provides the direction for better work in the future. The quantitative analysis will show how great was the error in the present work and the measurements taken.

From the Tables and plots some arithmetical errors come up. In 4NOV87 in the range ≈90.000° to 86.500° of zenith angle, the mean deviation of the LOWTRAN from the AGA radiance is -5.266% for overcast sky, (Table 7.4) and -5.119% for fair sky (Table 7.5). The same date for a zenith range

≈90° to 55° the deviation is 12.86% for overcast sky (Table 7.6) and 41.963% for fair sky (with ice particles) (Table 7.7). For 14JUL88 (fair sky), the mean error was -5.567% in the range ≈90.000° to 87.345° (Table 7.8), -9.713% in the range 83.461° to 80.361° (Table 7.9), on 15JUL88 A (fair) it was -8.949% in the range 90.020° to 87.012° (Table 7.10), -8.836% in the range 82.351° to 79.250° (Table 7.11), on 15JUL88 B (fair) -3.012% in the range 90.000° to 87.211° (Table 7.12), and -4.716% in the range 85.531° to 82.250° (Table 7.13), and on 25JUL88 (overcast) -15.583% in the range 90.070° to 86.679° (Table 7.14) and -29.279% in the range 81.530° to 78.250° (Table 7.15). It is obvious that the prediction of the sky radiance is more accurate at zenith angles greater than 85°.

Assuming that all the factors which contribute to the error can be arranged so as to minimize this at the level of 2% to 3%, then it can be said that the LOWTRAN 6 prediction model works efficiently and can be used with success. Attention is required for computations only at the horizon angle range (less than one degree). On the other hand the measurements with the AGA Thermovision 780 system must be taken with a sky emissivity which will be decreased with the elevation angle, the thinness of clouds, and the temperature. The main problem will be to define such a decreasing emissivity. Real-time radiosonde data should be a

prerequisite in this case. Alternatively the problem can be faced by using statistical results for the emissivity or the radiance.

2. Parameters Affecting the Radiance

Because of the multiplicity of the measurements, it is possible to study the influence of the weather conditions (fair/overcast sky), and the wind speed upon the radiance calculated through the AGA system.

a. Fig. 7.19 shows that the overcast sky in NOV87 emits a slightly greater amount of radiance than the fair sky. In the plot of Fig. 7.20 it seems clearer, that with a wind speed 4.9 m/s the overcast sky of 25JUL88 emits more radiance than the fair sky of 15JUL88 with a wind speed 4.02 m/s, although, as shown below, the radiance decreases with the windspeed.

b. Fig. 7.21 and Fig. 7.22 will be used to show that the radiance decreases rapidly with increase in the wind speed. In Fig. 7.21 the decrease seems to be very linear, with a slope -1 W/cm^2_sr per m/s for overcast/fair sky, and in Fig. 7.22 the linearity is approximated by a slope -0.79 W/cm^2-sr per m/s for overcast/fair sky.

c. Fig. 7.23 shows the dependence of the radiance versus the zenith angle with parameter the wind speed. The data are for the same day 15JUL88/fair sky with one or two hours difference.

3. Validation of SCHWARTZ-HON Model

a. The comparison plots for the SH model are shown in Fig. 7.14 through 7.18. The radiance of the sea surface computed by the SH model with LOWTRAN 6 is always higher than that measured directly by the AGA. The two curves are almost parallel, independent of the viewing angle and day, but the gap varies from day to day. The most probable reason for this appears to be the variation of the wind speed which narrows or widens the gap. Thus with better knowledge of the wind speed profile, the SH model would be expected to perform very well.

b. The radiance of the sea surface seems about constant at all the viewing angles, (slope approximately zero) (Fig. 7.14 through 7.18, θ_v greater than 85°). Thus, this radiance depends basically upon the emissivity of the sea surface. Emissivity (=1-reflectivity) as a surface function, should be dependent upon the wave roughness which, in turn, depends obviously upon the wind speed. Conversely for a given wind velocity (same speed, same direction) over a sea surface area, the waves show uniform elevation variance, with the same roughness which implies the same emissivity and constant sea surface radiance. All these simply justify that the basic concepts of the SH model are correct. Fig. 3.20 shows indeed that the emissivity suggested in the SH model remains constant for zenith angles greater than 55°.

c. Fig. 7.24 gives the radiance versus the zenith angle with the wind speed as a parameter. The result mentioned above that the sea surface radiance depends basically upon the emissivity, implies that the plots represent also the emissivity as a function of the wind speed, a result which is similar to that of SH model shown in Fig. 3.20. and also similar to Fig.3.5.

d. Fig. 7.24 shows also that the radiance with overcast sky is higher than with a fair sky. This combined with the similar result of paragraph (VII.E.2.a), implies that probably an overcast sky is better emitter than a fair sky. However the predictive capability for overcast is less than for clear sky.

e. Fig. 7.24 (b) shows that for the same sky (fair), radiance is reduced with the speed significantly.

f. The deviation of the radiance in the SH computed with LOWTRAN for NOV87 relative to that measured with AGA is 13.494% (overcast sky), 10.077% (fair sky), for 14JUL88 4/653% (fair sky), for 15JUL88 3.247% (fair sky), and for 25JUL88 -0.984% (Tables 7.17 through 7.20). Here the deviation is much smaller than in the case of sky radiance, and shows that the SH model works successfully, over distances mostly shorter than five km.

VIII. CONCLUSIONS AND RECOMMENDATIONS

A. CONCLUSIONS

Thermal images of the sky and the sea surface previously taken, were analysed, and the calculated infrared radiance was compared with the radiance computed by computer codes.

Sky radiance computed by using the LOWTRAN 6 code was found to be lower than the radiance measured with the AGA Thermovision 780 system. The mean deviation of the radiance computed with LOWTRAN relatively to that measured with the AGA was found to be of the order of -5.0% on 4NOV87, -5.5% on 14JUL88, -9.0%, and -3.0% on 15JUL88, for zenith angles between horizon (≈90°) and about 85° with a fair sky. The mean deviation for angles between 85°-79° was found to be of the order of -10.0% for 14JUL88, -9.0%, and -5% for 15JUL88, with the same sky. One measurement for the range 90°-55° gave a mean deviation about 42% on 4NOV87. For overcast days the mean deviation was found to be greater than that on fair days; on 4NOV87 about -5.3% in the zenith range 90°-85° and 13% in the range 90°-55°, on 25JUL88 about -15.6% in the range 90°-85° and -29.3% in the range 81°-78°. These relative deviations show that the measurements are more accurate in the zenith range 5° above the horizon.

The averaged deviation of the sea surface radiance predicted in the SH model with LOWTRAN was 10.077% on 4NOV87, 4.653% on 14JUL88, and 3.247% on 15JUL88 with fair skies. For overcast skies it was found to be 13.494% on 4NOV87 and -0.984% on 25JUL88 for overcast skies. Here the deviations were in general smaller, probably due to the shorter viewing distances (less than five km).

On overcast days the the background thermal radiance of sea/sky is higher than it is in fair skies. Radiance depends significantly upon the wind speed decreasing approximately linearly with this. Also the radiance decreases with the elevation. Emissivity of the sea surface is related to the wave roughness and the wind speed, while the sea radiance does not differ much with the viewing angle.

Computer codes (LOWTRAN 6, SCHWARTZ-HON), work satisfactorily. LOWTRAN has a weakness at grazing angles. A better knowledge of atmospheric conditions is required. The Thermovision system provides detailed thermal images with accurate temperature differences, but needs care with input parameters to give precise and accurate absolute values.

B. RECOMMENDATIONS

Thermal imaging is simple in concept, but the process of obtaining distinct thermography of an object is very complicated. It depends upon atmospheric effects, which can

64

not be controlled but only predicted. To allow precise analysis, better knowledge of atmospheric conditions and a larger statistical body of thermographic measurements are required.

The problems which appeared in this paper included the differences in radiance of a clear and an overcast sky, the rate of change in radiance with the wind speed, the change of the radiance with the zenith angle, the effect of ice particles at higher altitude, the weakness of LOWTRAN code to describe precisely the horizon radiance, the distortion of the radiance value keeping parameters as the emissivity constant along an extended angle range, the radiance of the sea surface as a function of the viewing angle and the wind speed, and the influence of a clear/overcast sky upon the sea surface radiance. Answers to these questions can be given only with more measurements, directed each time to a specific purpose, and with as detailed measurements of environmental parameters as possible.
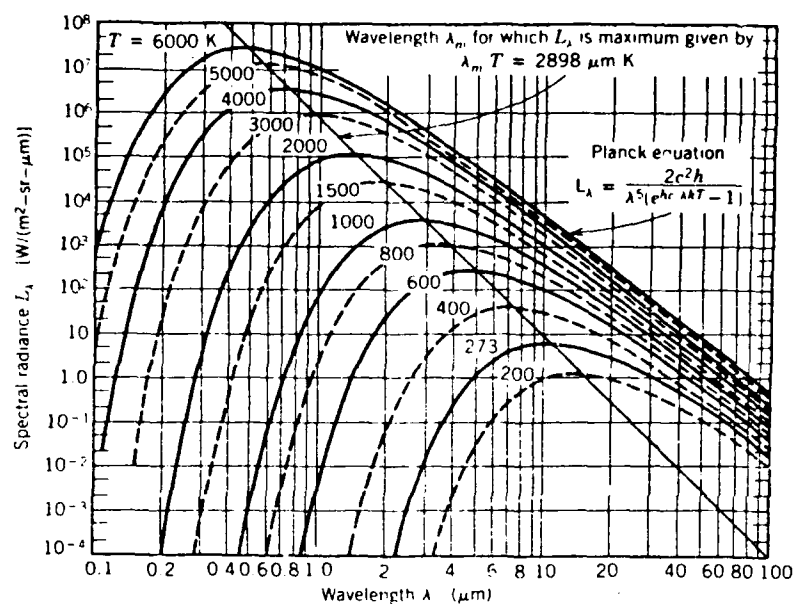
Figure 2.1 Blackbody radiation curves [Ref. 3:p. 26]

$$L_s = L_w(1-R) + L_i \cdot R$$
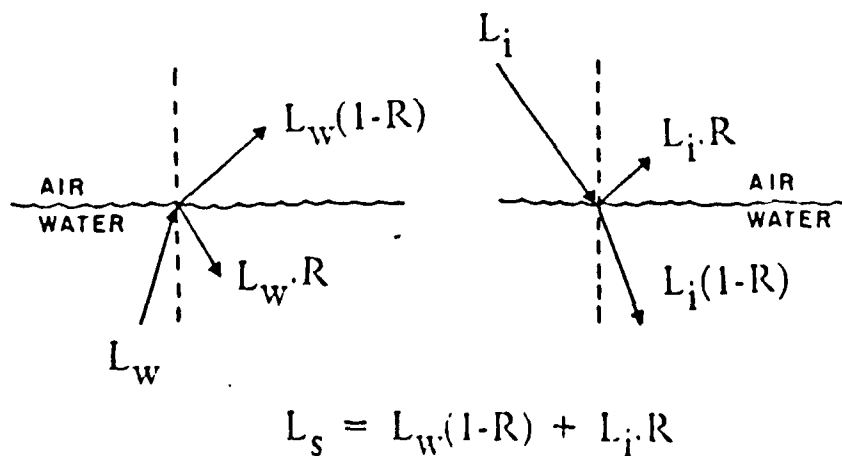
Figure 3.1 Sea surface infrared radiance [Ref. 7:p. 20]

66
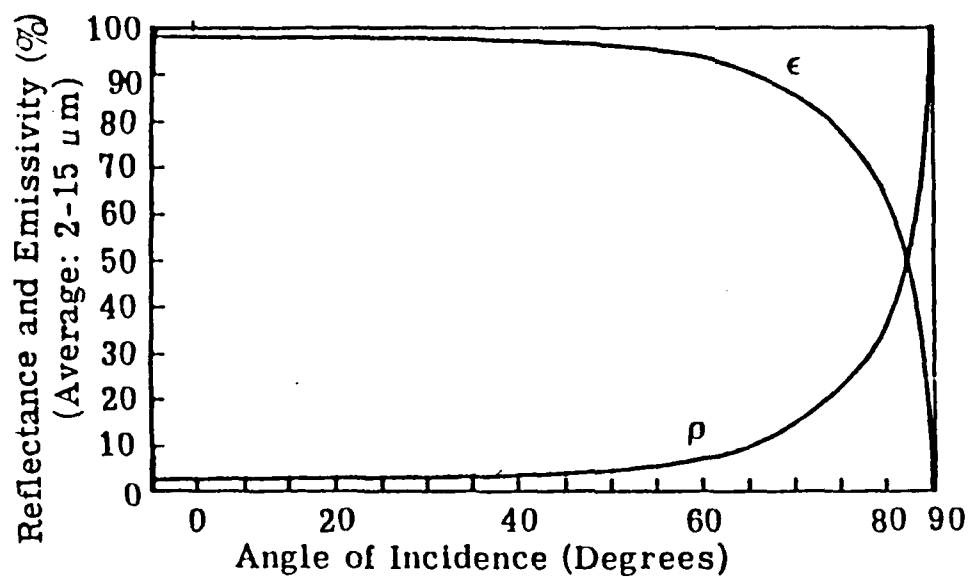
Figure 3.2   Reflectance and emissivity of water
(2 to 15 μm average) [Ref. 5:p. 3-106)
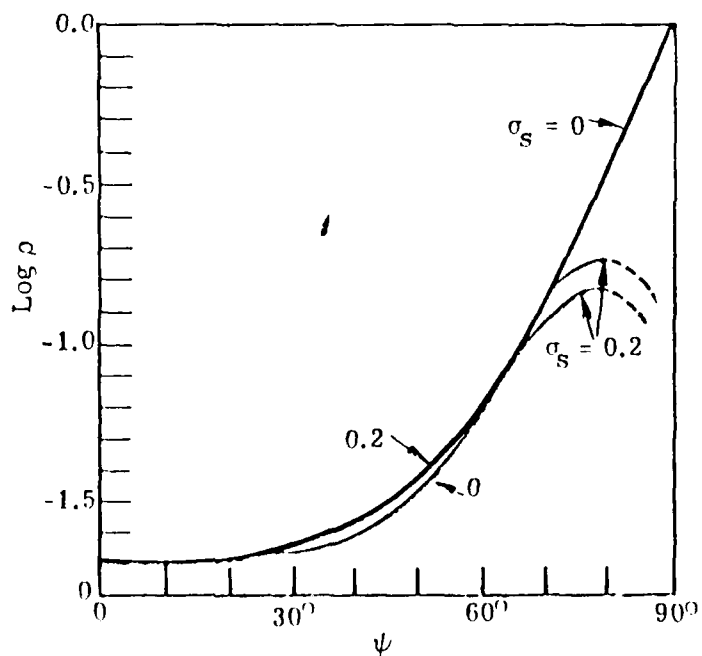
Figure 3.3   Reflectance from a flat (σ=0) and a
roughened sea surface (σ=0.2) [Ref. 5:p. 3-108]
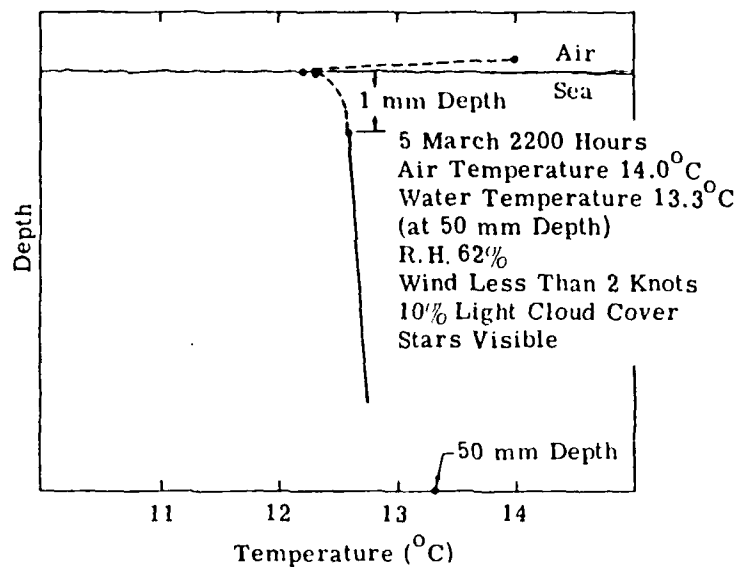
Figure 3.4   Thermal structure of sea boundary layer
[Ref. 5:p. 3-109]
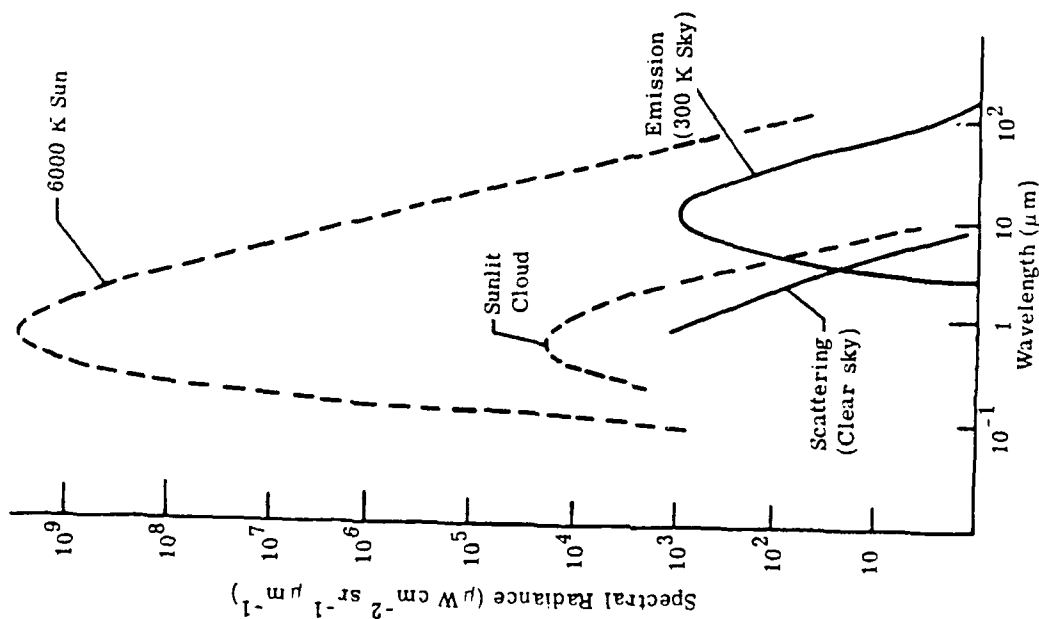
Figure 3.5   Spectral radiance of the sky [Ref. 5:p. 3-71]
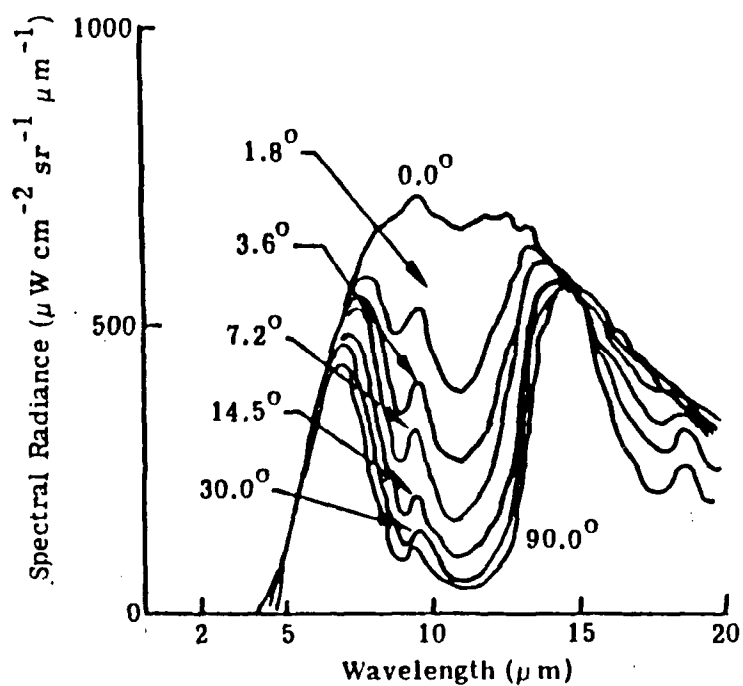
Figure 3.6   Spectral radiance of clear night-time
sky at a dry location [Ref. 5:p. 3-72]
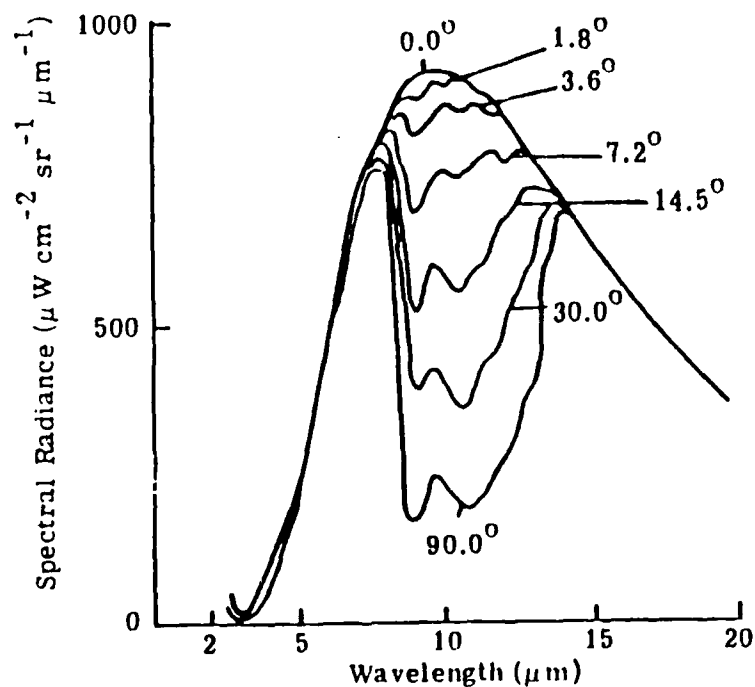
Figure 3.7   Spectral radiance of a clear night-time
sky at a humid location [Ref. 5:p. 3-72]
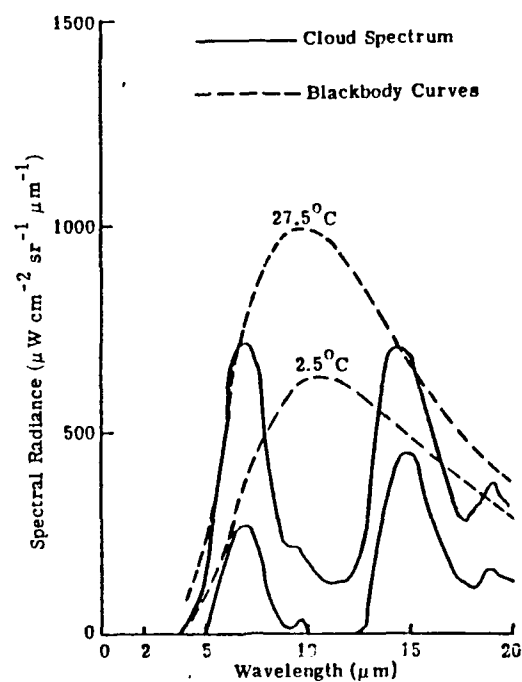
Figure 3.8   Variation of zenith sky with ambient
temperature [Ref. 5:p. 3-74]
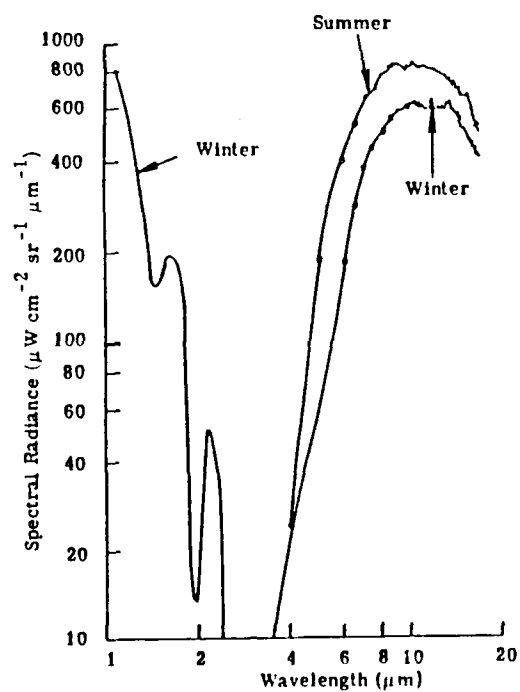
Figure 3.9   Spectral radiance of overcast skies
[Ref. 5:p. 3-74]

70
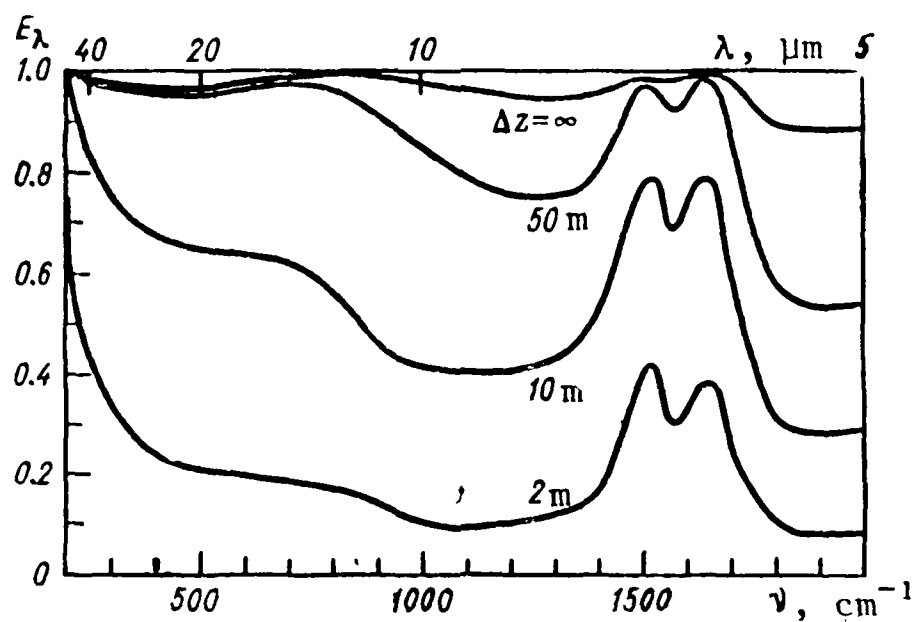
Figure 3.10   Spectral emissivity of cloud layers
for varius thickness [Ref. 8:p. 224]
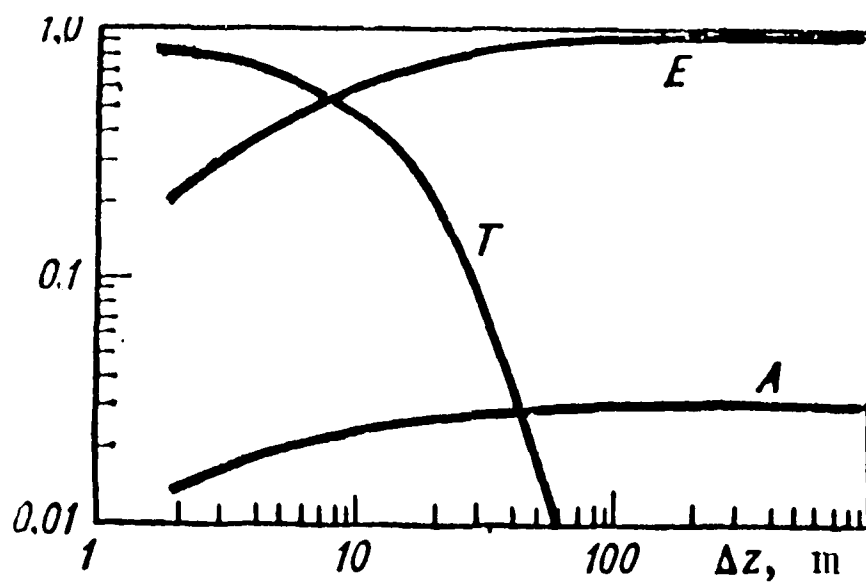
Figure 3.11   Integral emissivity, transmissivity and
reflectivity versus cloud thickness [Ref. 8:p. 225]

Cloud Spectrum

— — — — **Blackbody Curves**

Elevation Angle = 14.5°

+10°C

-10°C

1000

500

0

Spectral Radiance (μW cm^{-2} sr^{-1} μm^{-1})

0 2 5 10 15 20

Wavelength (μm)
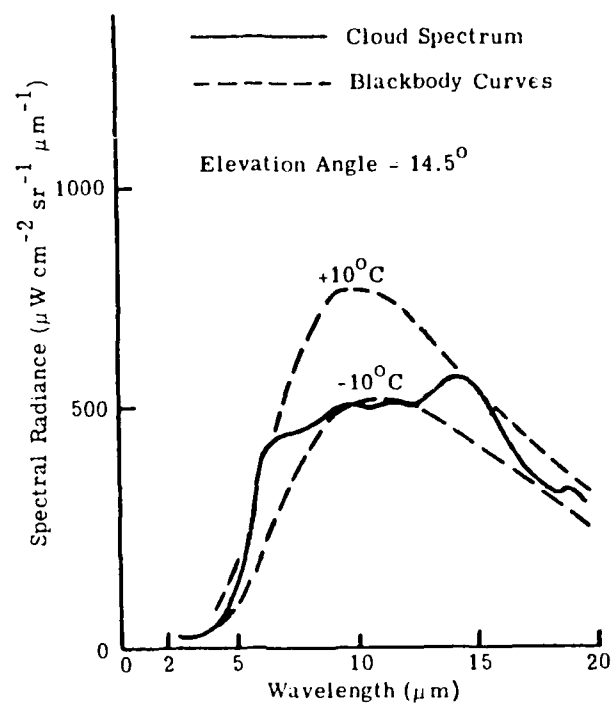
Figure 3.12 Spectral radiance of the underside of
a cumulus cloud [Ref. 5:p. 3-73]

1.8°
0.0°
3.6°
7.2°
14.5°
30.0°
90.0°

1000

500

0

Spectral Radiance (μW cm^{-2} sr^{-1} μm^{-1})

2 5 10 15 20

Wavelength (μm)
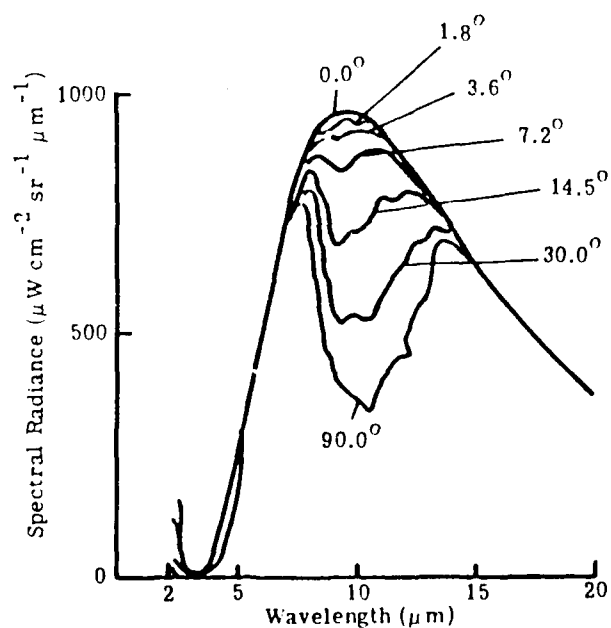
Figure 3.13 Spectral radiance of sky covered
with cirrus clouds [Ref. 5:p. 3-74]

θ_V=zenith angle at observer height h_0 α=wave tilt
θ_I=zenith angle of reflected ray N_F=normal to the wave
θ_R=zenith angle of incident ray N_T=normal to earth

Figure 3.14   Geometry of sea surface for the
Schwartz-Hon model [Ref. 9]
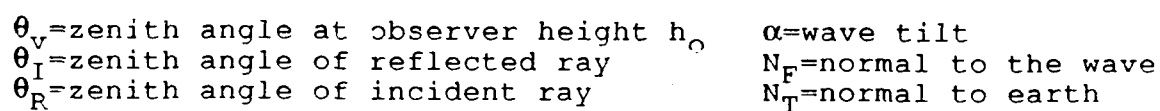
Figure 3.15   Sea surface emissivity vs. nadir
angle in Schwartz-Hon model [Ref. 9]
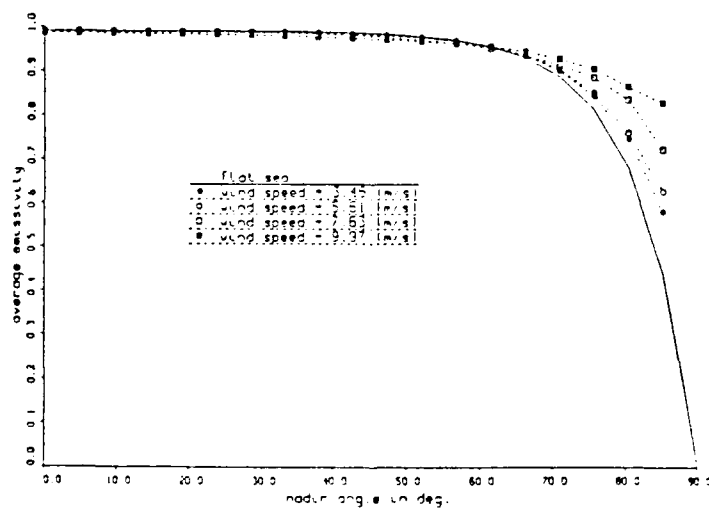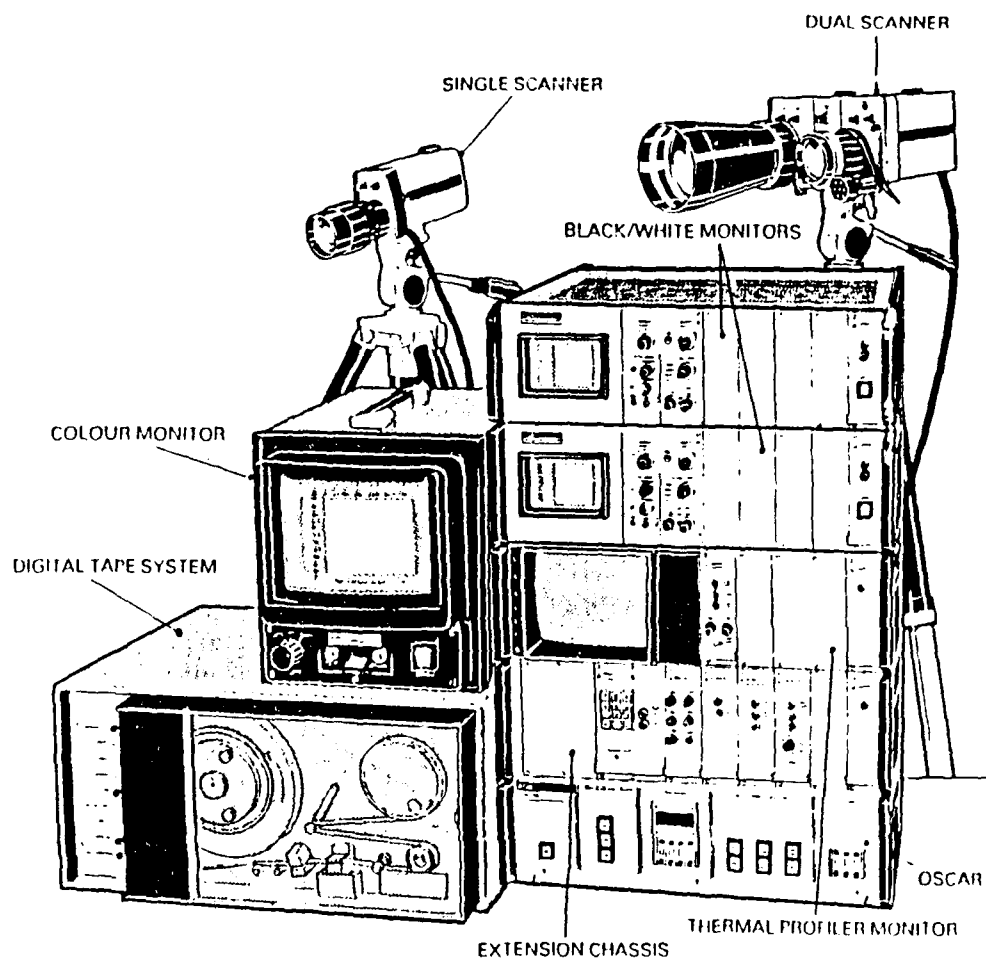
Figure 5.1   Major units of AGA Thermovision 780 System
[Ref. 2]
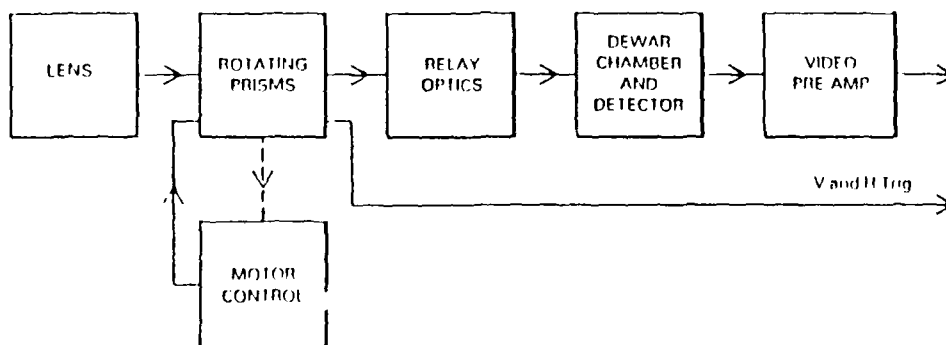
Figure 5.2   Simplified block diagram of AGA scanner
[Ref. 2:p. 3-1]

74
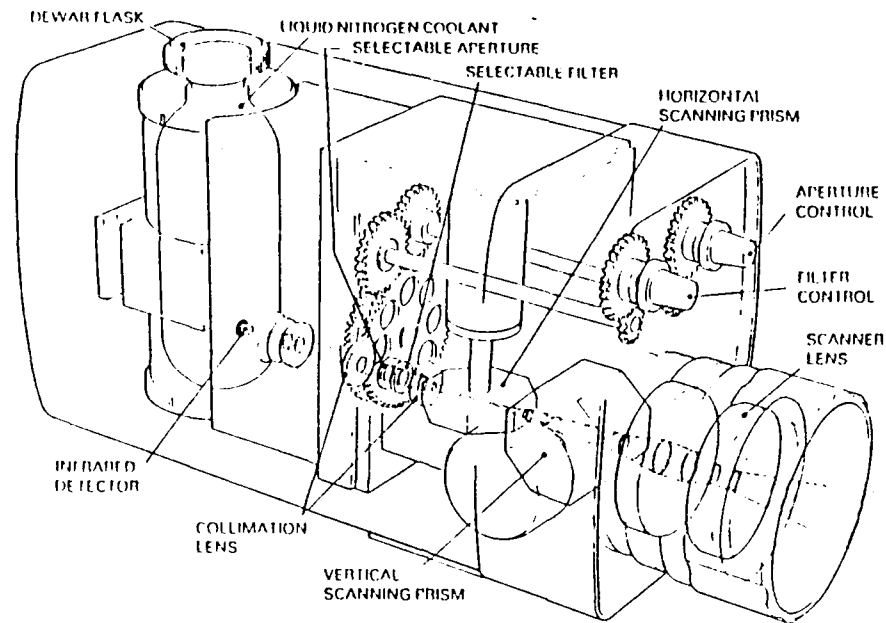
Figure 5.3 Arrangement of electro-optical components
in the AGA scanner [Ref. 2:p. 3-2]
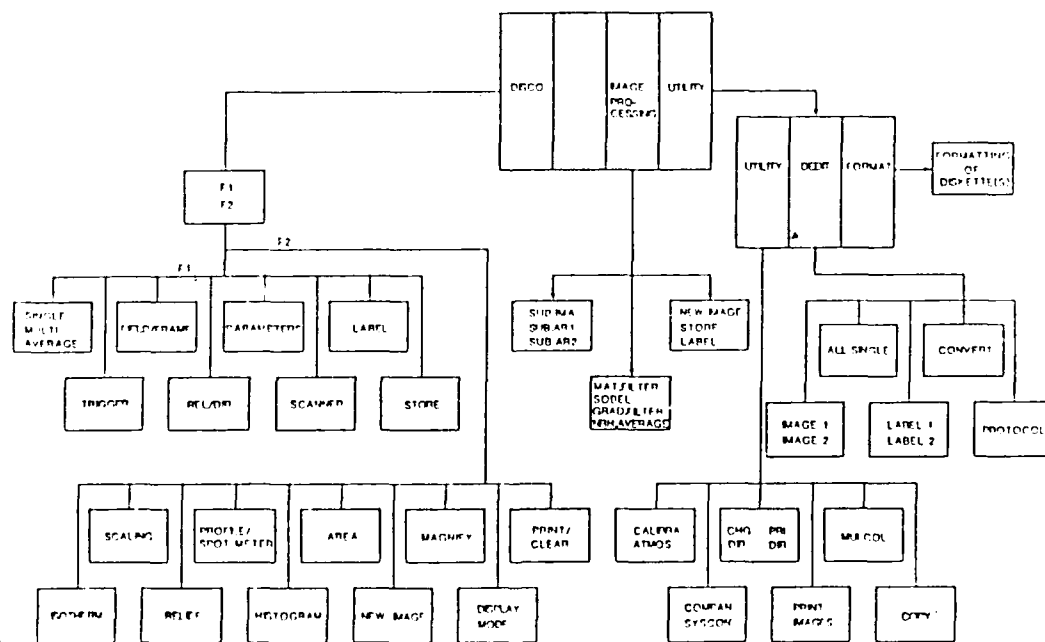
Figure 5.4 Block diagram of DISCO 3.0 software [Ref. 12]

75
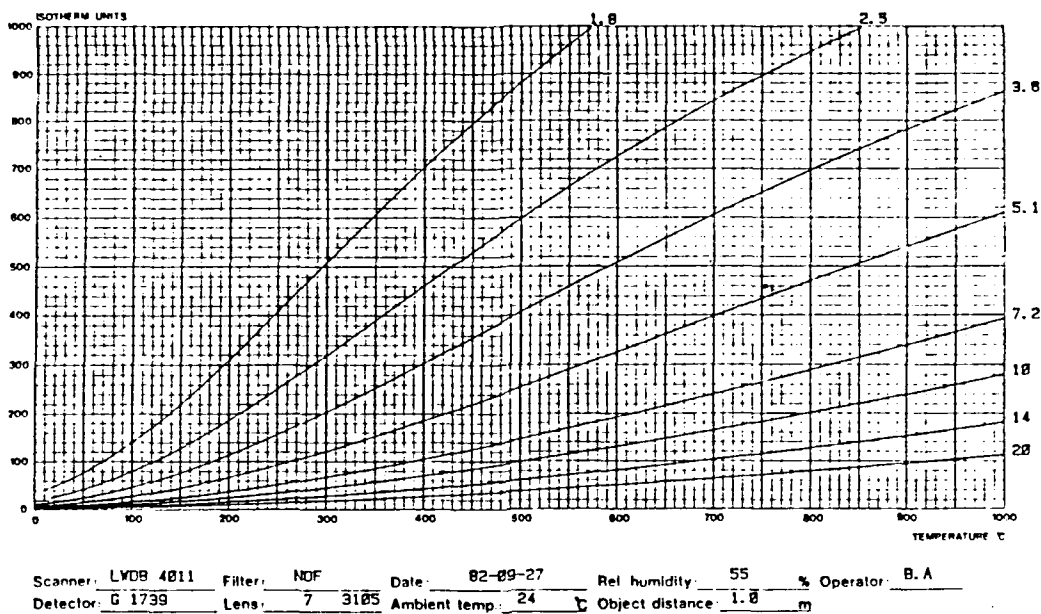
Figure 5.5   LW calibration curves from 0 °C to 1000 °C
[Ref. 2]
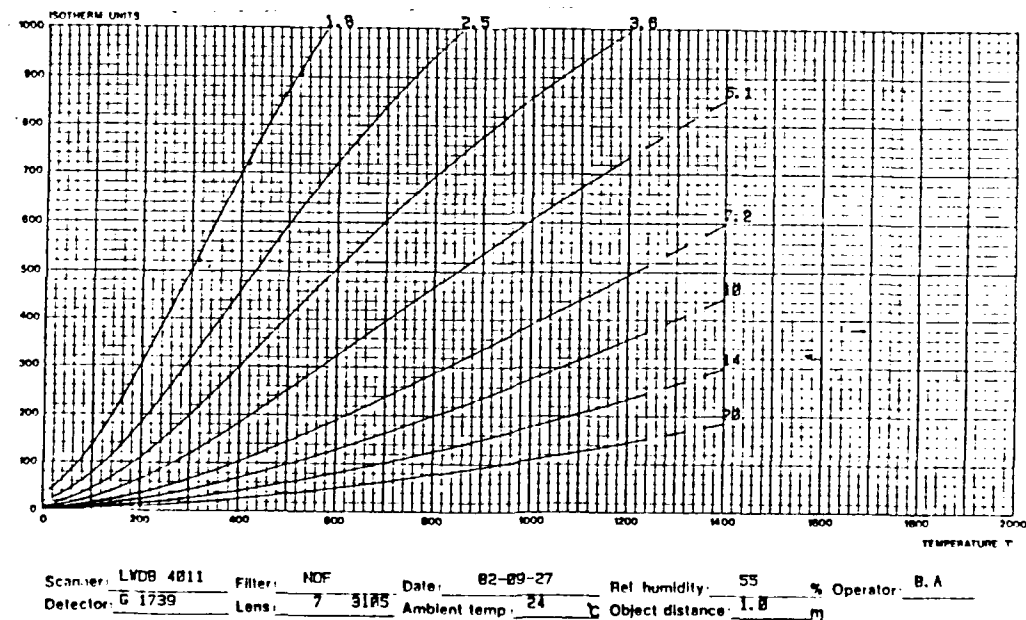
Figure 5.6   LW calibration curves from 0 °C to 2000 °C
[Ref. 2]
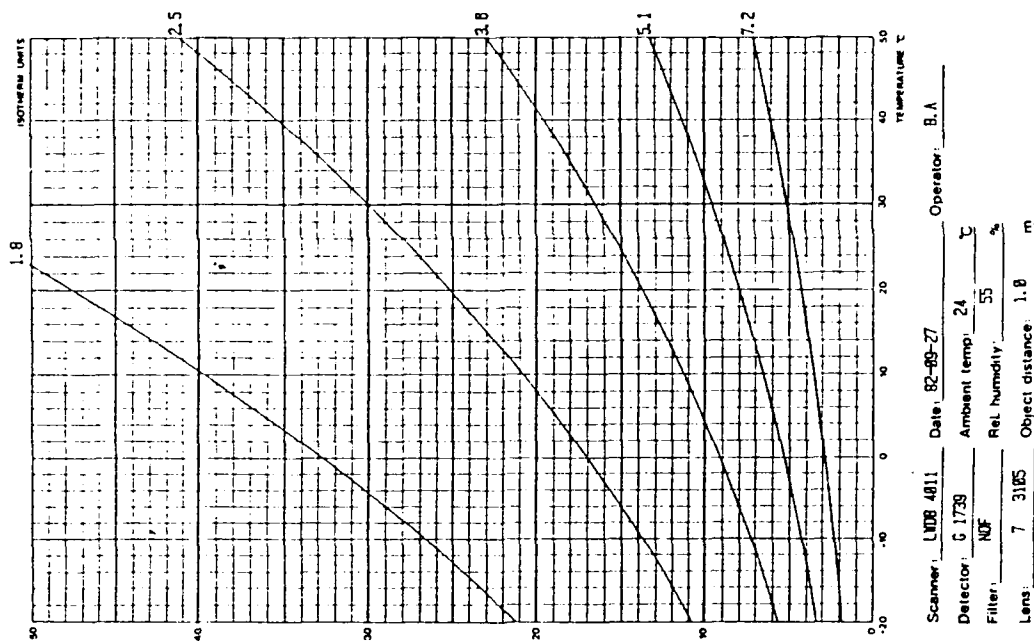
Figure 5.7 LW calibration curves from -20 °C to 50 °C
[Ref. 2]
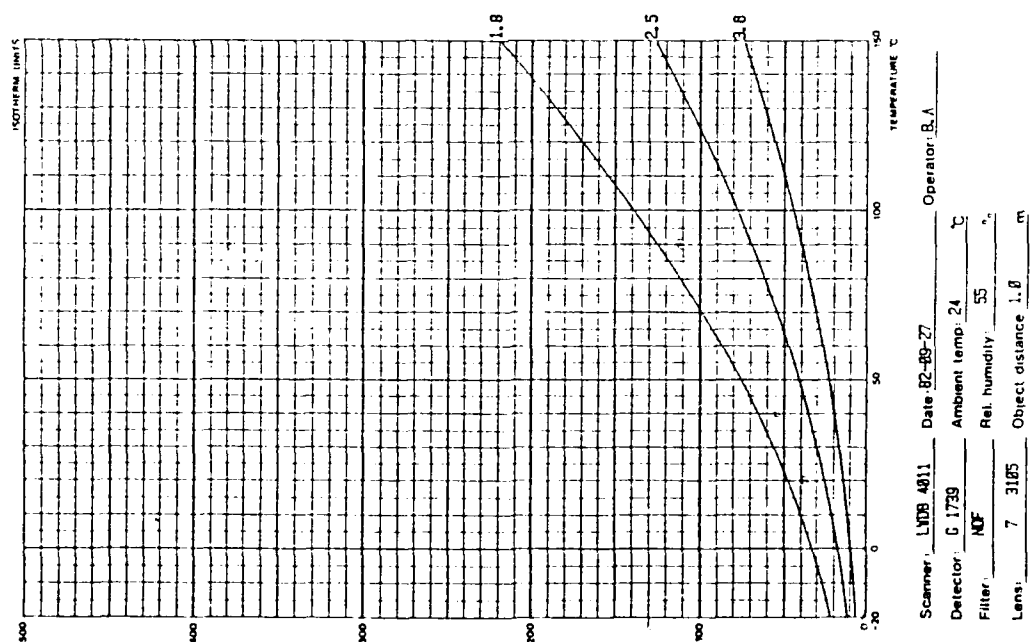
Figure 5.8 LW calibration curves from -20 °C to 150 °C
[Ref. 2]

1	POWER	8.	CONTRAST	
2	LED	8a.	CONTRAST PRESET	
3	FOCUS	9	THERMAL RANGE	
4	LINE/BATT	10	THERMAL LEVEL	
5	POWER LED	11	THERMAL LEVEL ADJ.	
6	PHOTO	12	PICTURE MODE	
7	BRIGHTNESS	13	ISOTHERM LEVEL 1	
7a	BRIGHTNESS PRESET	14	ISOTHERM LEVEL 2	
		15.	ISOTHERM WIDTH	
		16.	ISOTHERM SCALE	
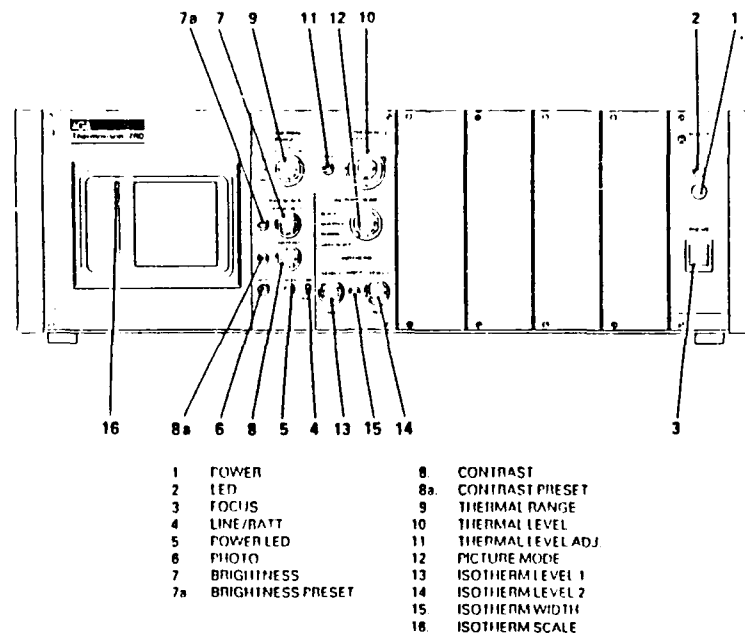
Figure 5.9 Black/White monitor chassis controls
and indicators [Ref. 2:p. 4-2]

NOTE:

THERMAL LEVEL = L
RELATIVE THERMAL VALUE = I
MEASURED THERMAL VALUE = I_o = L + I
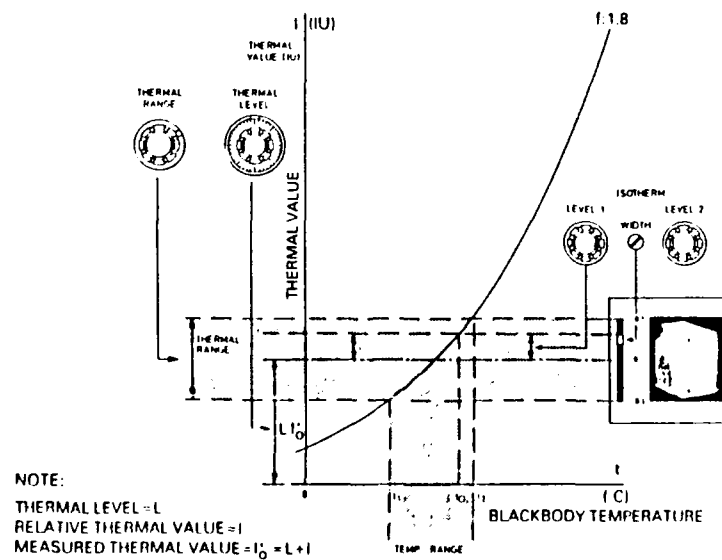
Figure 5.10 Direct measurement method [Ref. 2:p. 10-1]
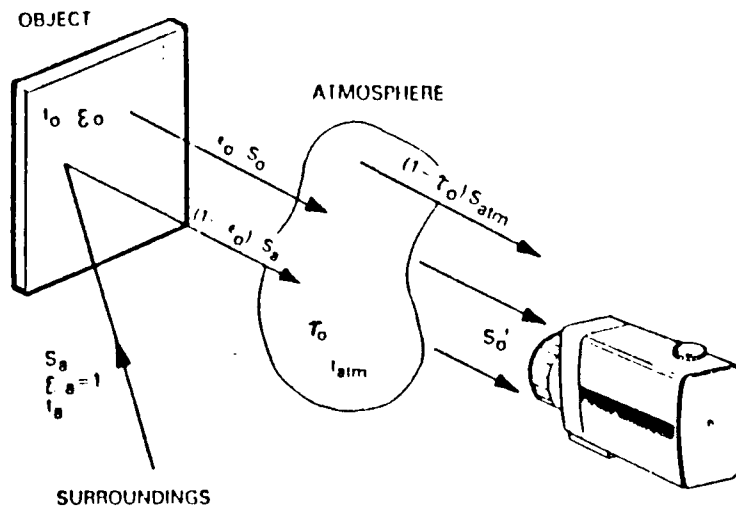
Figure 5.11   Radiation conditions in complex
measurements [Ref. 2:p. 10-4]
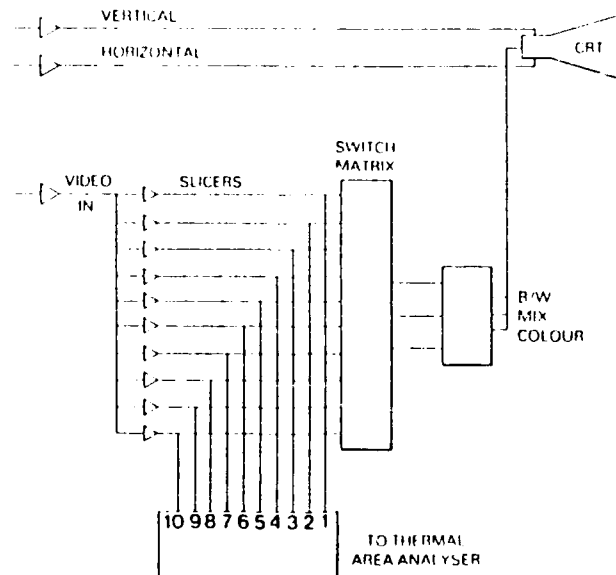
Figure 5.12   Simplified block diagram of Color
Monitor [Ref. 2:p. 10-8]
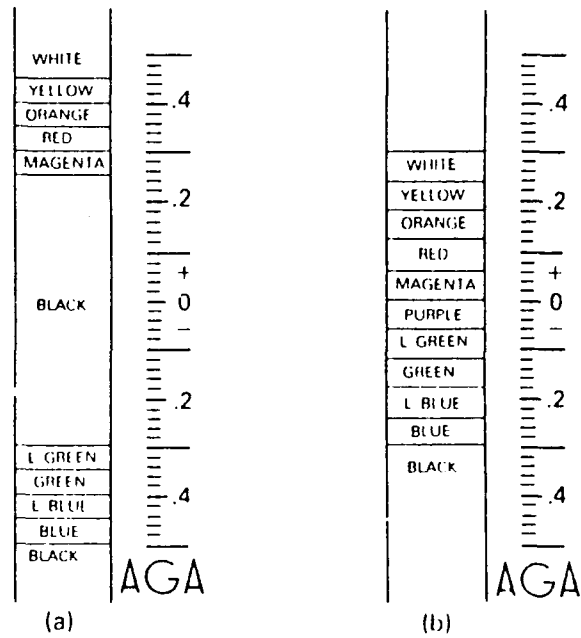
Figure 5.13   Color isotherm scales in different modes
[Ref. 2:p. 10-9]
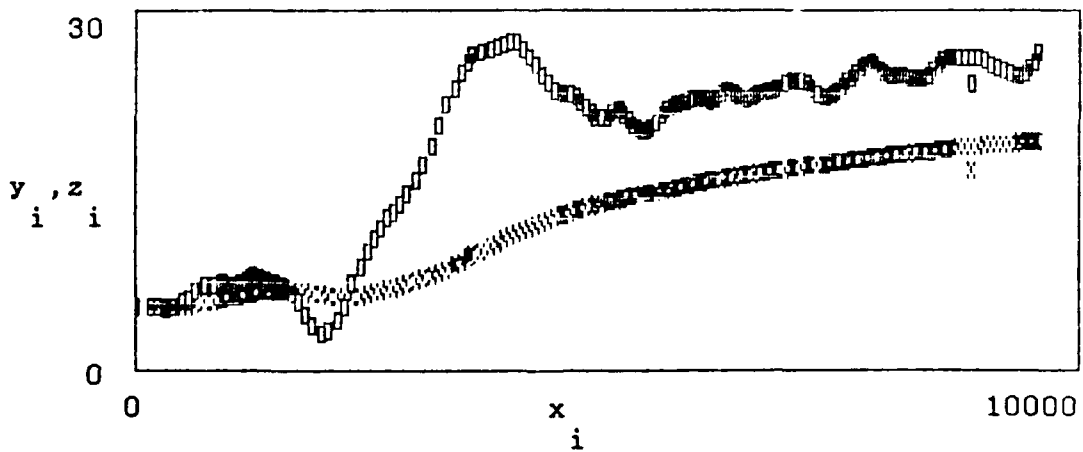
Figure 7.1   Normal y_i and average z_i wind speed (m/s)
versus altitude x_i (m) (4NOV87)
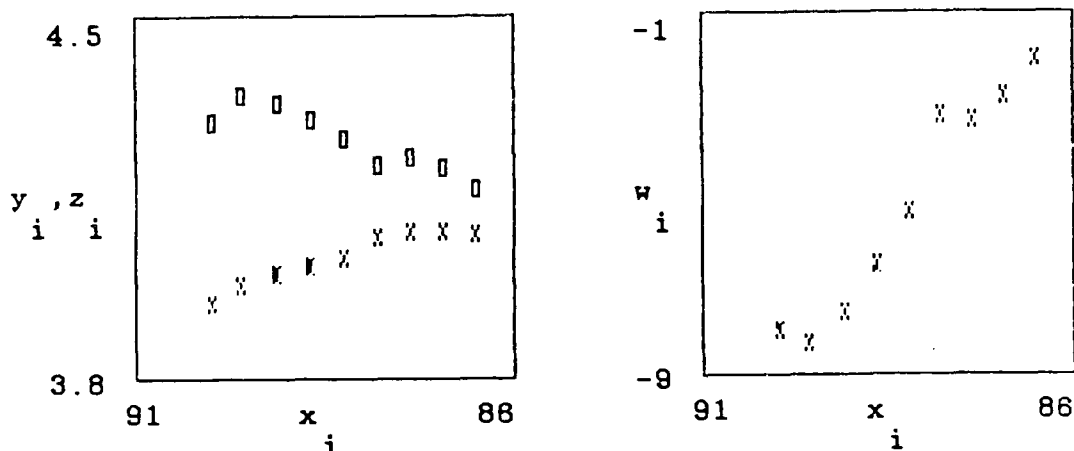
Figure 7.2   Overcast sky radiance vs zenith angle (4NOV 87)
        x_i=zenith angle (°)
        y_i=AGA radiance (mW/cm^2-sr) (rectangle points)
        z_i=LOWTRAN 6 radiance (mW/cm^2-sr) (x points)
        w_i=error=(z_i/y_i-1)%
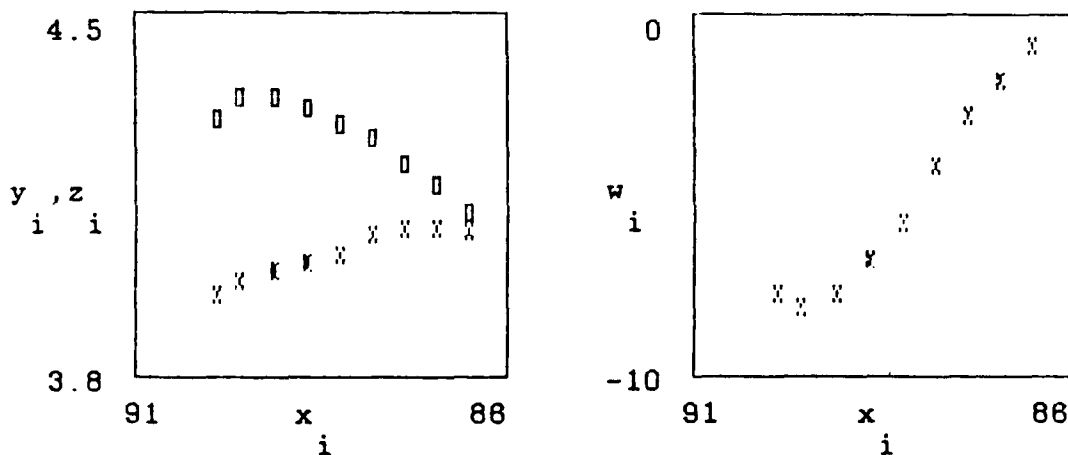
Figure 7.3   Fair sky radiance vs zenith angle (4NOV 87)
        x_i=zenith angle (°)
        y_i=AGA radiance (mW/cm^2-sr) (rectangle points)
        z_i=LOWTRAN 6 radiance (mW/cm^2-sr) (x points)
        w_i=error=(z_i/y_i-1)%

81
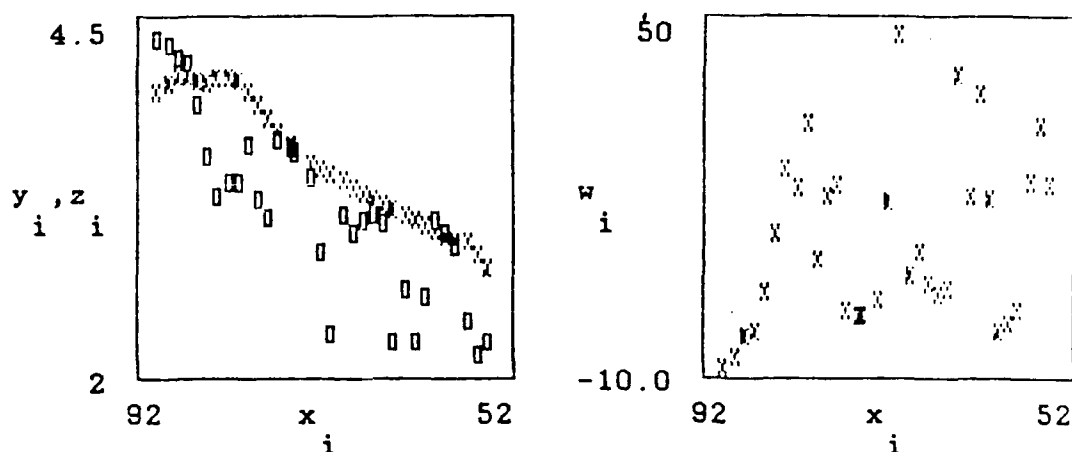
Figure 7.4 Overcast sky radiance vs zenith angle (4NOV 87)
x_i=zenith angle (°)
y_i=AGA radiance (mW/cm^2-sr) (rectangle points)
z_i=LOWTRAN 6 radiance (mW/cm^2-sr) (x points)
w_i=error=(z_i/y_i-1)%
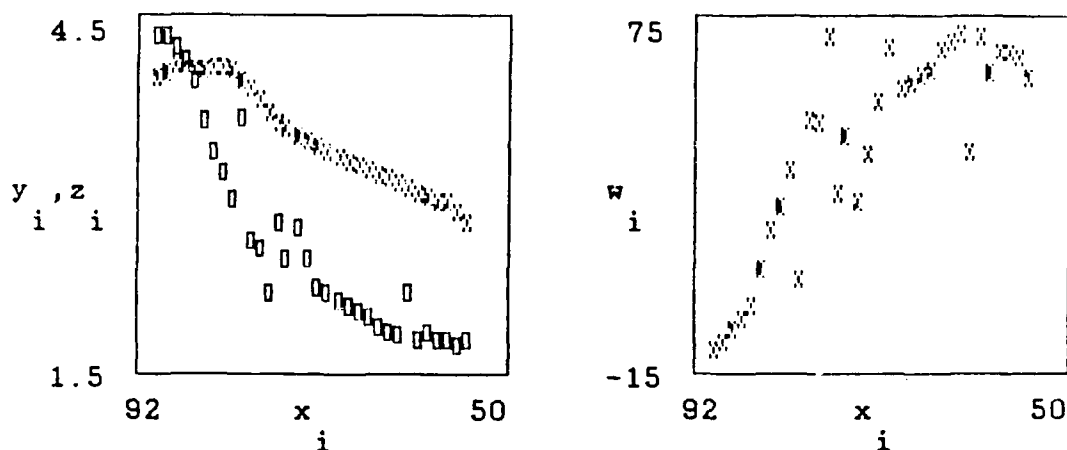
Figure 7.5 Fair sky radiance vs zenith angle (4NOV 87)
x_i=zenith angle (°)
y_i=AGA radiance (mW/cm^2-sr) (rectangle points)
z_i=LOWTRAN 6 radiance (mW/cm^2-sr) (x points)
w_i=error=(z_i/y_i-1)%
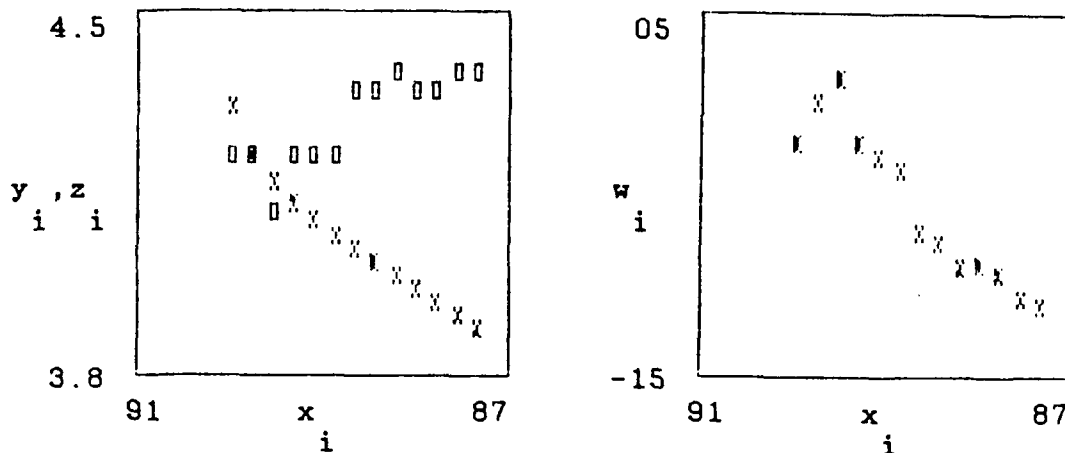
Figure 7.6 Fair sky radiance vs zenith angle (14JUL88)
     x_i=zenith angle (°)
     y_i=AGA radiance (mW/cm^2-sr) (rectangle points)
     z_i=LOWTRAN 6 radiance (mW/cm^2-sr) (x points)
     w_i=error=(z_i/y_i-1)%
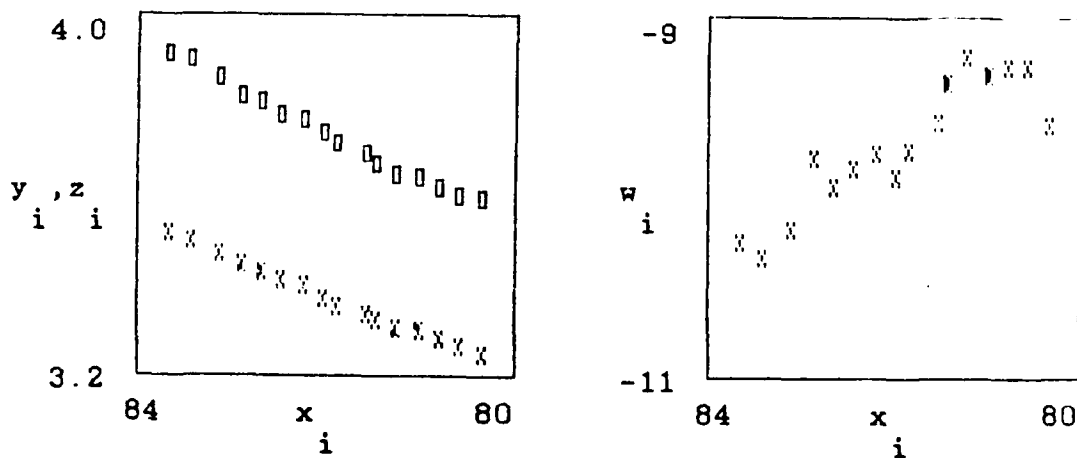
Figure 7.7 Fair sky radiance vs zenith angle (14JUL88)
     x_i=zenith angle (°)
     y_i=AGA radiance (mW/cm^2-sr) (rectangle points)
     z_i=LOWTRAN 6 radiance (mW/cm^2-sr) (x points)
     w_i=error=(z_i/y_i-1)%

83
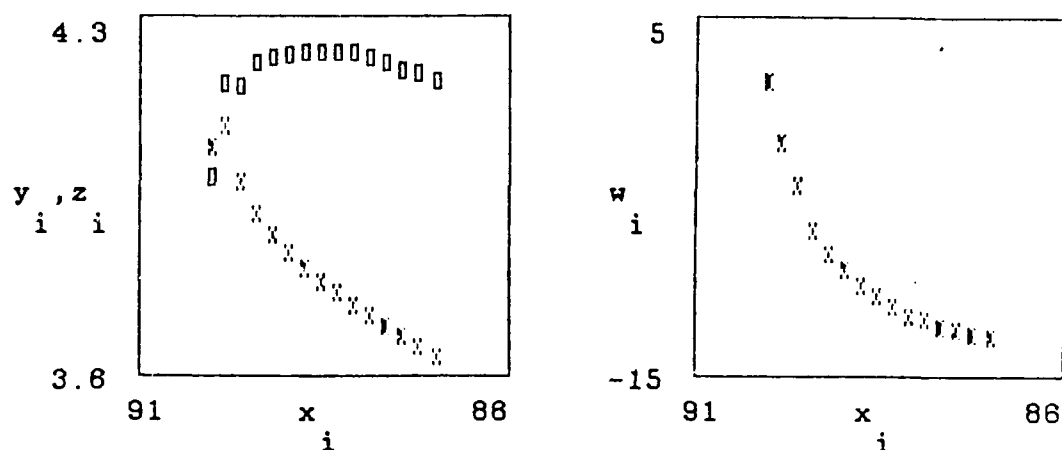
Figure 7.8   Fair sky radiance vs zenith angle (15JUL88 A)
    x_i=zenith angle (°)
    y_i=AGA radiance (mW/cm^2-sr) (rectangle points)
    z_i=LOWTRAN 6 radiance (mW/cm^2-sr) (x points)
    w_i=error=(z_i/y_i-1)%
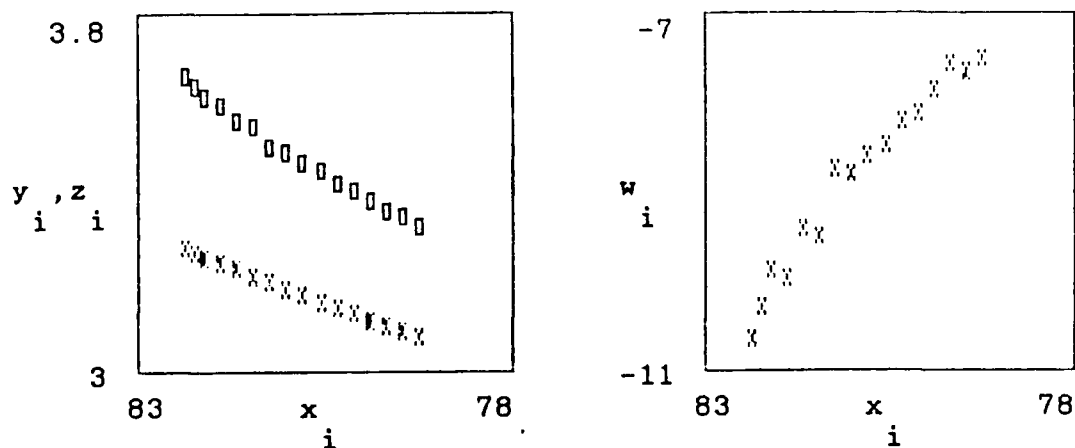
Figure 7.9   Fair sky radiance vs zenith angle (15JUL88 A)
    x_i=zenith angle (°)
    y_i=AGA radiance (mW/cm^2-sr) (rectangle points)
    z_i=LOWTRAN 6 radiance (mW/cm^2-sr) (x points)
    w_i=error=(z_i/y_i-1)%

84
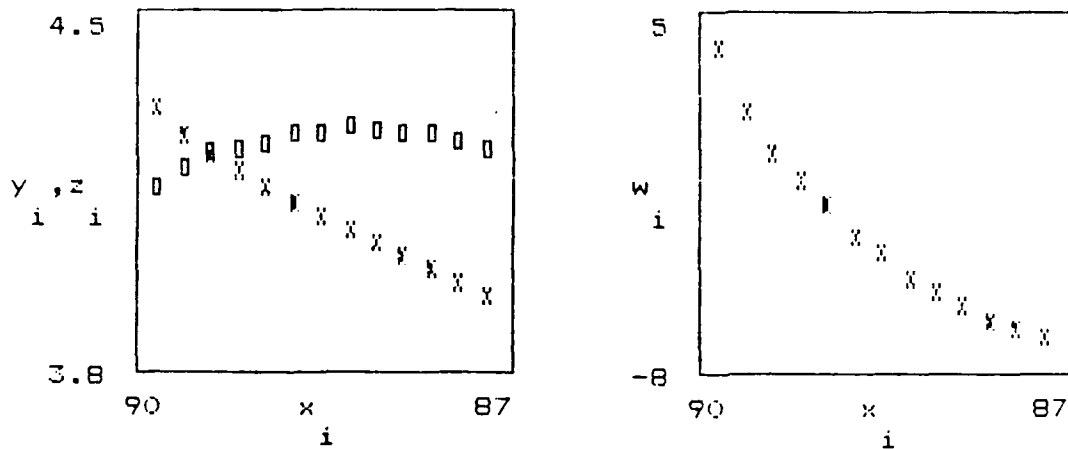
Figure 7.10 Fair sky radiance vs zenith angle (15JUL88 B)
   x_i=zenith angle (˚)
   y_i=AGA radiance (mW/cm^2-sr) (rectangle points)
   z_i=LOWTRAN 6 radiance (mW/cm^2-sr) (x points)
   w_i=error=(z_i/y_i-1)%
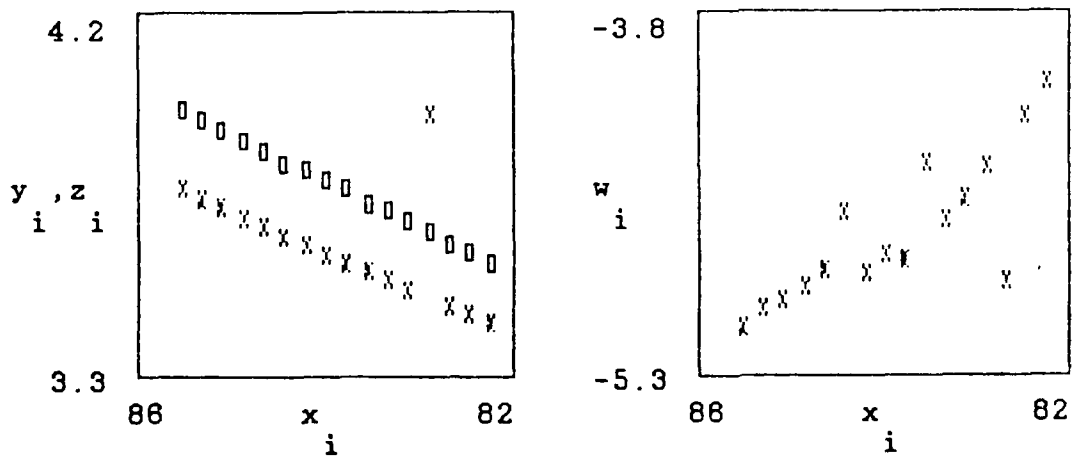
Figure 7.11 Fair sky radiance vs zenith angle (15JUL88 B)
   x_i=zenith angle (˚)
   y_i=AGA radiance (mW/cm^2-sr) (rectangle points)
   z_i=LOWTRAN 6 radiance (mW/cm^2-sr) (x points)
   w_i=error=(z_i/y_i-1)%
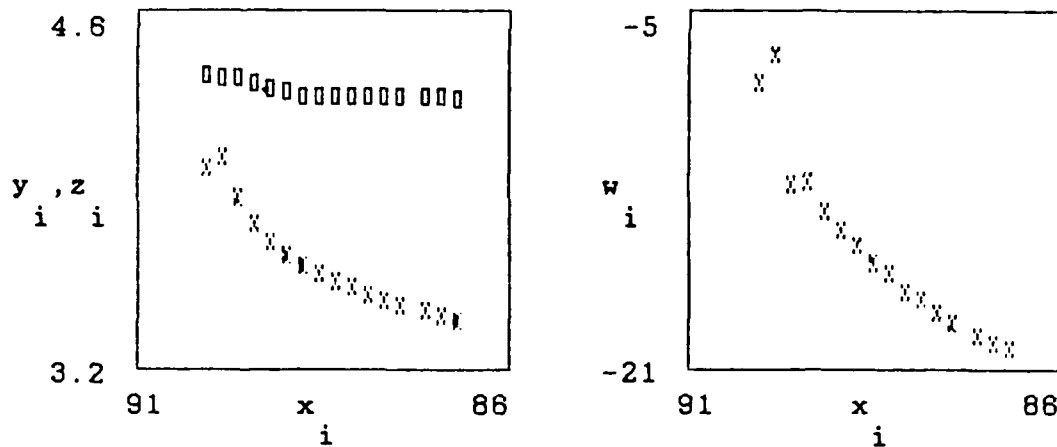
Figure 7.12 Overcast sky radiance vs zenith angle (25JUL88)
x_i=zenith angle (°)
y_i=AGA radiance (mW/cm^2-sr) (rectangle points)
z_i=LOWTRAN 6 radiance (mW/cm^2-sr) (x points)
w_i=error=(z_i/y_i-1)%
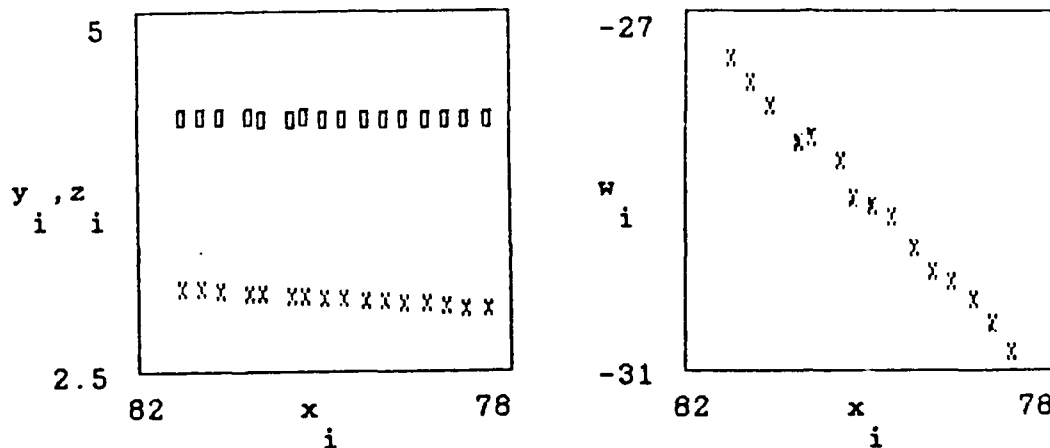
Figure 7.13 Overcast sky radiance vs zenith angle (25JUL88)
x_i=zenith angle (°)
y_i=AGA radiance (mW/cm^2-sr) (rectangle points)
z_i=LOWTRAN 6 radiance (mW/cm^2-sr) (x points)
w_i=error=(z_i/y_i-1)%

86
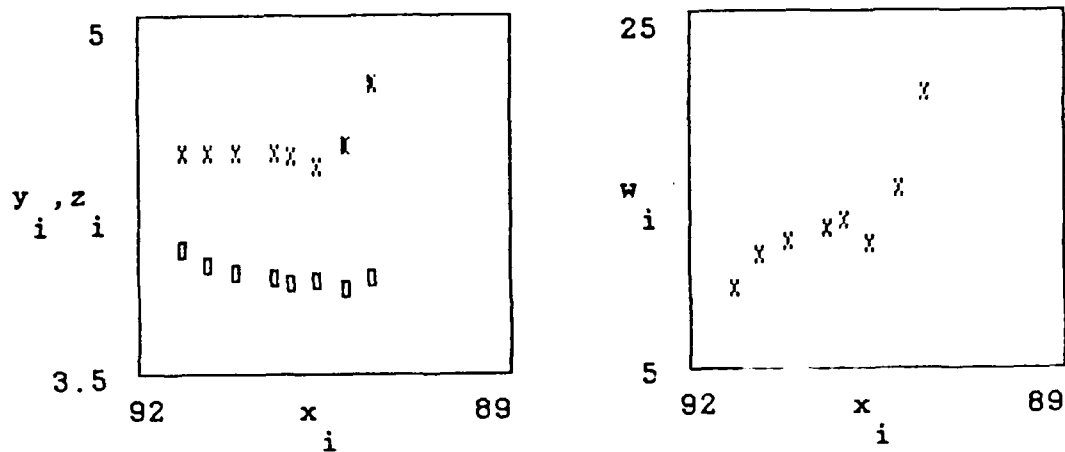
Figure 7.14 Sea surface SH radiance vs zenith angle (4NOV87)
Overcast sky, x_i=zenith angle (°)
y_i=AGA radiance (mW/cm^2-sr) (rectangle points)
z_i=LOWTRAN 6 radiance (mW/cm^2-sr) (x points)
w_i=error=(z_i/y_i-1)%
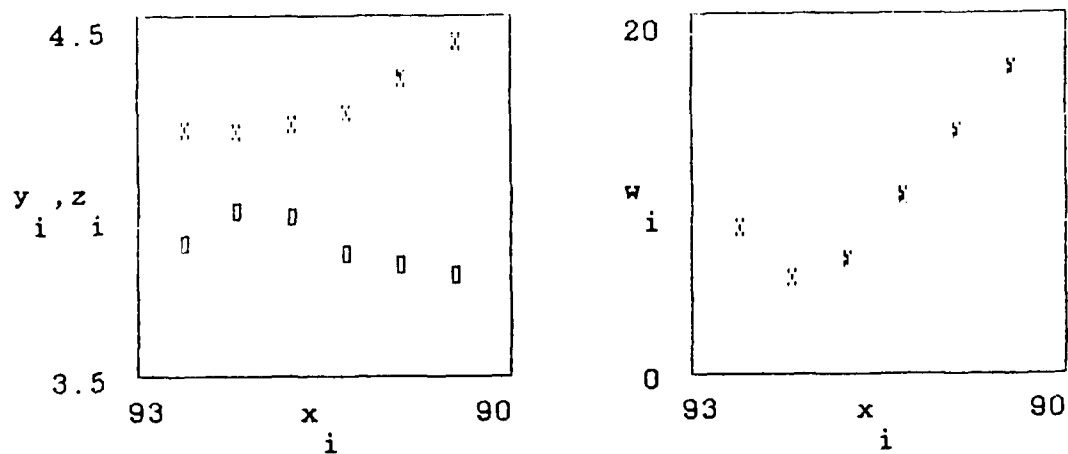
Figure 7.15 'Sea surface SH radiance vs zenith angle (4NOV87)
Fair sky, x_i=zenith angle (°)
y_i=AGA radiance (mW/cm^2-sr) (rectangle points)
z_i=LOWTRAN 6 radiance (mW/cm^2-sr) (x points)
w_i=error=(z_i/y_i-1)%

87
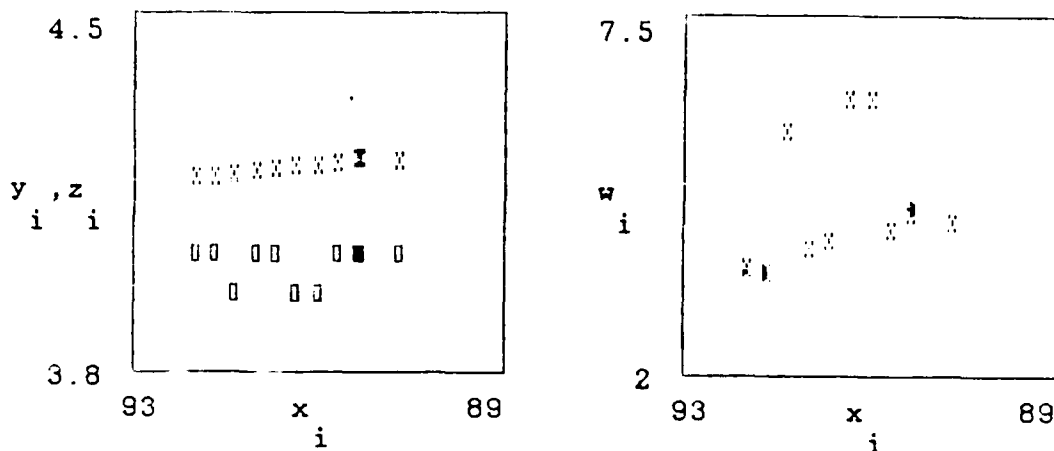
Figure 7.16 Sea surface SH radiance vs zenith angle (14JUL88)
Fair sky, x_i=zenith angle ($^\circ$)
y_i=AGA radiance (mW/cm^2-sr) (rectangle points)
z_i=LOWTRAN 6 radiance (mW/cm^2-sr) (x points)
w_i=error=(z_i/y_i-1)%
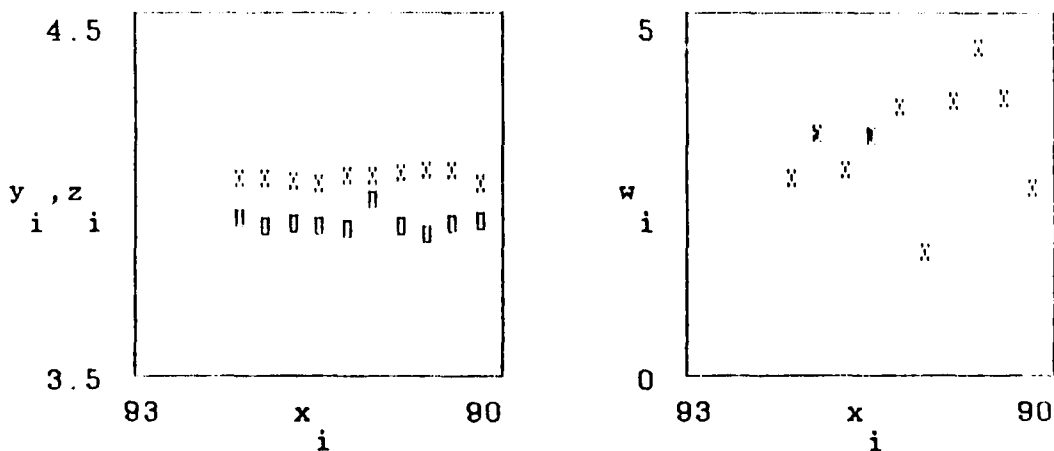
Figure 7.17 Sea surface SH radiance vs zenith angle (15JUL88)
Fair sky, x_i=zenith angle ($^\circ$)
y_i=AGA radiance (mW/cm^2-sr) (rectangle points)
z_i=LOWTRAN 6 radiance (mW/cm^2-sr) (x points)
w_i=error=(z_i/y_i-1)%
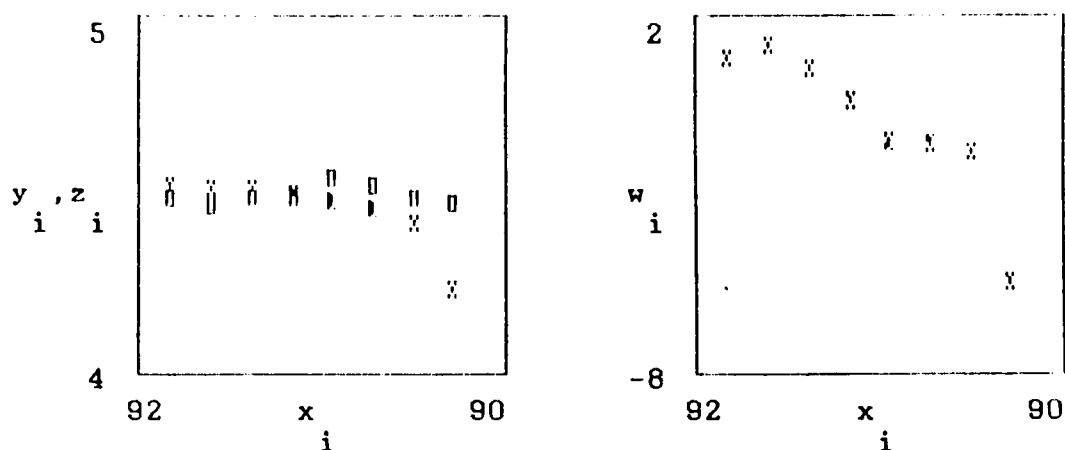
Figure 7.18 Sea surface SH radiance vs zenith angle (25JUL88)
    Overcast sky, x_i=zenith angle ($^\circ$)
    y_i=AGA radiance (mW/cm^2-sr) (rectangle points)
    z_i=LOWTRAN 6 radiance (mW/cm^2-sr) (x points)
    w_i=error=(z_i/y_i-1)%

(a)   (b)
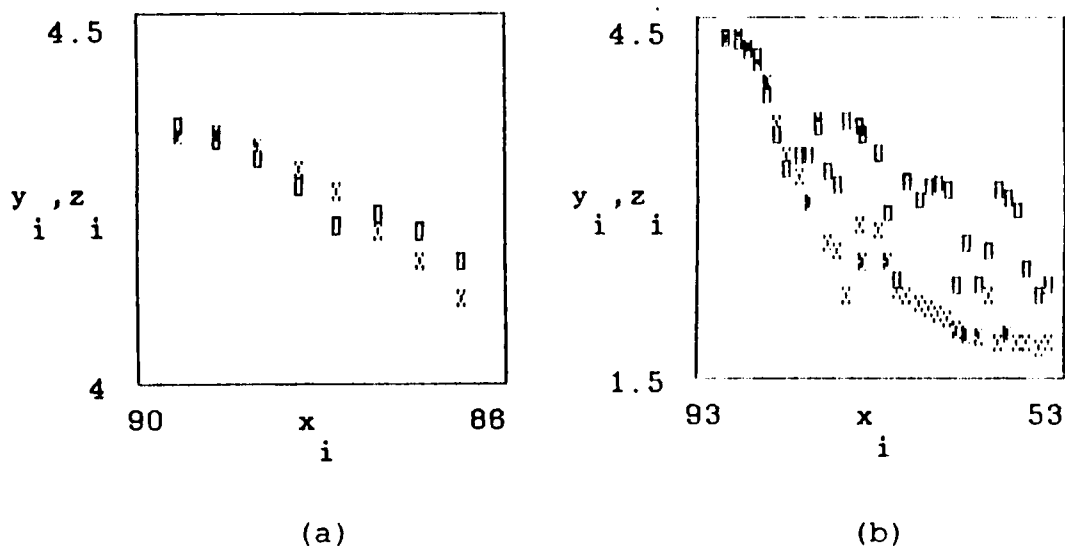
Figure 7.19   AGA sky radiance vs zenith angle (4NOV87)
    x_i=zenith angle ($^\circ$)
    y_i=overcast radiance (mW/cm^2-sr, rect.points)
    z_i=fair radiance (mW/cm^2-sr) (x points)
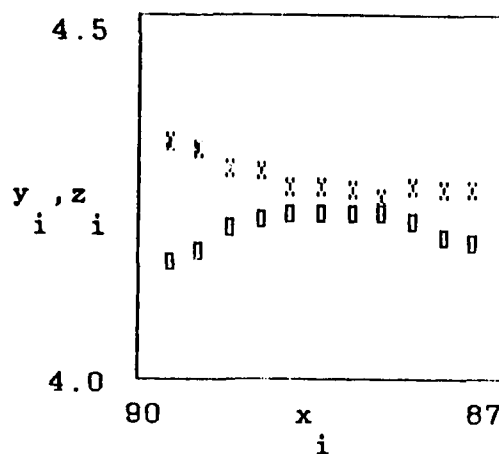
Figure 7.20   AGA sky radiance vs zenith angle (15, 25JUL88)
x_i=zenith angle $(\degree)$
y_i=fair rad. (mW/cm^2-sr,rect.points) at 4.02 m/s
z_i=overcast rad.(mW/cm^2-sr, x points) at 4.9 m/s
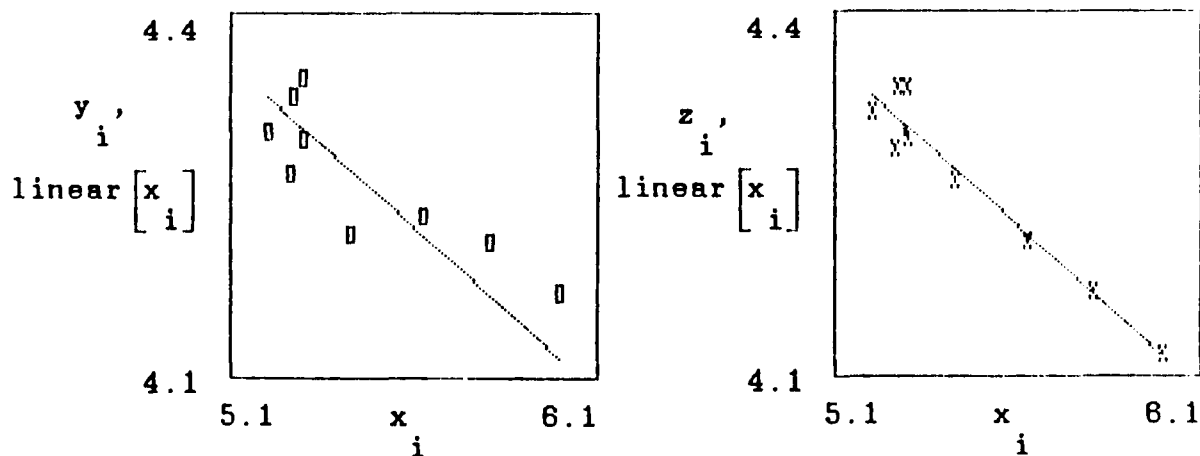
Figure 7.21   AGA sky radiance vs wind speed (4NOV87)
x_i=wind speed m/s
y_i=overcast radiance (mW/cm^2-sr) (rect.points)
z_i=fair radiance (mW/cm^2-sr) (x points)
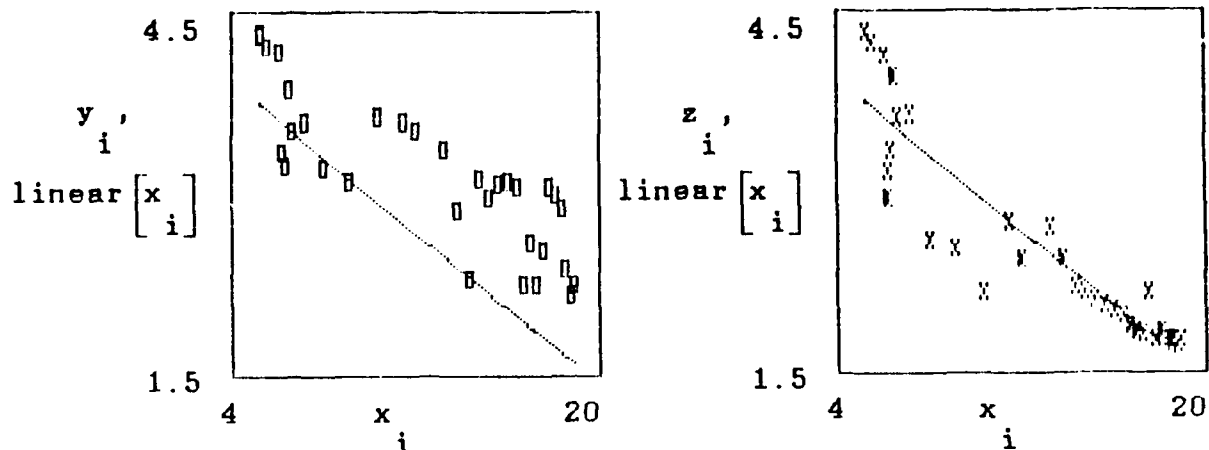
Figure 7.22   AGA sky radiance vs wind speed (4NOV87)
x_i=wind speed (m/s)
y_i=overcast radiance (mW/cm^2-sr) (rect.points)
z_i=fair radiance (mW/cm^2-sr) (x points)
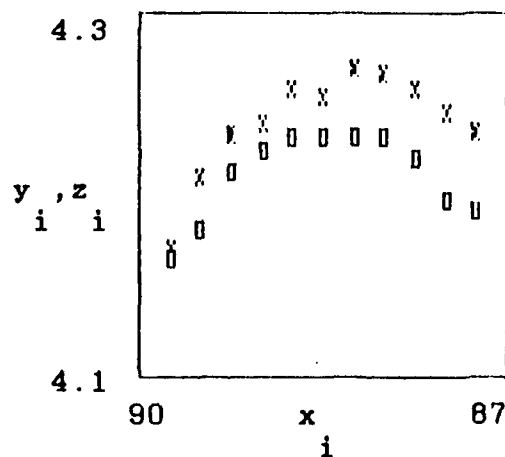
Figure 7.23   AGA fair sky radiance vs zenith angle (15JUL88)
xi=zenith angle (°)
y_i=radiance (mW/cm^2-sr) at 4.02 m/s
z_i=radiance (mW/cm^2-sr) at 2.50 m/s
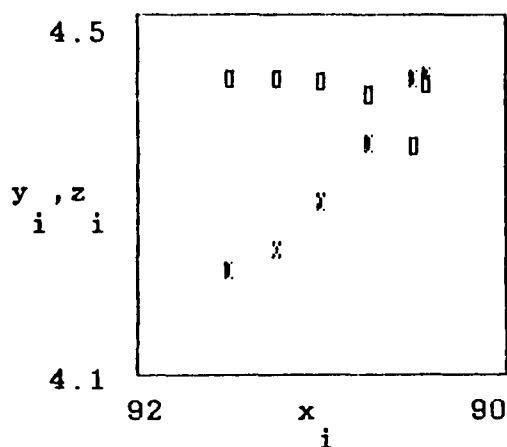
x_i=zenith angle ($^\circ$)
y_i=overcast rad. at 2.057 m/s
   (rectangle points)
z_i=fair radiance at 2.057 m/s
   (x points)

(a)
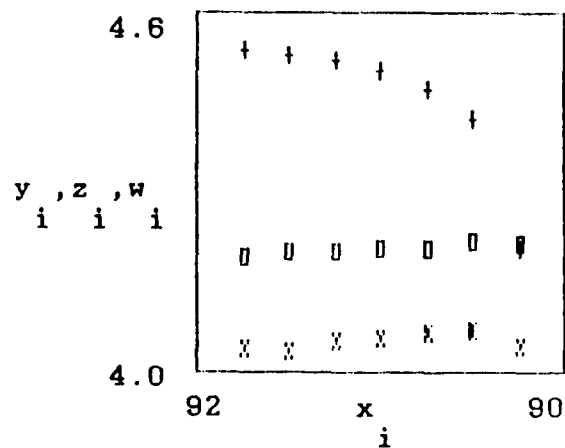
x_i=zenith angle ($^\circ$)
y_i=fair radiance at 3.55 m/s
   (rectangle points)
z_i=fair radiance at 4.51 m/s
   (x points)
w_i=overcast rad. at 4.9 m/s

(b)

Figure 7.24   SH sea surface radiance (mW/cm^2-sr) vs
zenith angle ($^\circ$), [(a) NOV87,(b) JUL88]

TABLE 2.1 SELECTED VALUES OF THE SPECTRAL INTEGRAL OF THE THERMAL DERIVATIVE OF PLANCK LAW [REF. 1:P. 28]

$$\frac{\partial W}{\partial T} = \int_{\lambda_1}^{\lambda_2} \frac{\partial W_\lambda (T_B)}{\partial T} \, d\lambda \quad \left[\frac{w}{cm^2 {}^\circ K}\right] \text{ for}$$

$\lambda_1 [\mu m]$	$\lambda_2 [\mu m]$	$T_B = 280^\circ K$	$T_B = 290^\circ K$	$T_B = 300^\circ K$	$T_B = 310^\circ K$
3	5	1.1×10^{-5}	1.54×10^{-5}	2.1×10^{-5}	2.81×10^{-5}
3	5.5	2.01×10^{-5}	2.73×10^{-5}	3.62×10^{-5}	4.72×10^{-5}
3.5	5	1.06×10^{-5}	1.47×10^{-5}	2×10^{-5}	2.65×10^{-5}
3.5	5.5	1.97×10^{-5}	2.66×10^{-5}	3.52×10^{-5}	4.57×10^{-5}
4	5	9.18×10^{-6}	1.26×10^{-5}	1.69×10^{-5}	2.23×10^{-5}
4	5.5	1.83×10^{-5}	2.45×10^{-5}	3.22×10^{-5}	4.14×10^{-5}
8	10	8.47×10^{-5}	9.65×10^{-5}	1.09×10^{-4}	1.21×10^{-4}
8	12	1.58×10^{-4}	1.77×10^{-4}	1.97×10^{-4}	2.17×10^{-4}
8	14	2.15×10^{-4}	2.38×10^{-4}	2.62×10^{-4}	2.86×10^{-4}
10	12	7.34×10^{-5}	8.08×10^{-5}	8.81×10^{-5}	9.55×10^{-5}
10	14	1.3×10^{-4}	1.42×10^{-4}	1.53×10^{-4}	1.65×10^{-5}
12	14	5.67×10^{-5}	6.10×10^{-5}	6.52×10^{-5}	6.92×10^{-5}

TABLE 4.1 PARTICLES RESPONSIBLE FOR ATMOSPHERIC SCATTERING [REF. 6:P. 20]

TYPE	RADIUS (μm)	CONCETRATION (cm^{-3})
Air molecule	10^{-4}	10^{19}
Aitken nucleus	$10^{-3}-10^{-4}$	10^4-10^2
Haze particle	$10^{-2}-1$	10^3-10
Fog droplet	$1-10$	$100-10$
Cloud droplet	$1-10$	$300-10$
Raindrop	10^2-10^4	$10^{-2}-10^{-4}$

TABLE 5.1 TECHNICAL CHARACTERISTICS OF AGA THERMOVISION 780 [REF. 7, 13]

PERFORMANCE
Spectral Range   : 3-5.6 μm and/or 8-14 μm
Frame Rate   : 6.25/sec
Field Rate   : 25/sec
Interlace   : 4:1

REPLACEABLE FORE OPTICS
FOV Azimuth   : 3.5°, 7°, 12°, 20°, 40°
FOV Elevation   : 3.5°, 7°, 12°, 20°, 40°
IFOV Azimuth   : 1.1 mrad
IFOV Elevation   : 1.1 mrad
NEΔT   : 0.12 °C at 22 °C
MDT   : <0.1 °C
Dynamic Range   : -20 to 900 °C

OPTICAL DATA
Effective aperture area   : 24 cm^2
Aperture diameter   : 5.5 cm
Effective focal length   : 9.9 cm
f/number   : 1.8

DETECTOR
Type SW   : Photovoltaic InSb
Type LW   : Photoconductive HgCdTe
Number of Elements   : 1
Peak Wavelength SW   : 5 μm
Peak Wavelength LW   : 10 μm

COOLING SYSTEM
Liquid Nitrogen   : -196 °C

OTHER CHARACTERISTICS
Size (cm)   : 19.0 L x 12.5 H x 8.0 W
Weight (kg)   : 1.6 (head only)
Power (W)   : 21 (8-15 V ac) head
                                : 35 (100-240 V ac, 40-450 Hz)
                                           electronics
Calibration   :   Up   to   850   °C   (higher
                                : with filter)

TABLE 5.2 LW CALIBRATION CONSTANTS OF AGA THERMOVISION 780 [REF. 2]

INDIVIDUAL CALIBRATION OF 780 DUAL BBAR

SERIAL NUMBERS
```
  SCANNER                    : LWDR 4011
  DETECTOR                   : G 1739
  FILTER                     : NOF
  LENS                       : 7 3105
```

CALIBRATION CONDITIONS
```
  AMBIENT TEMPERATURE        : 24 °C
  RELATIVE HUMIDITY          : 55%
  OBJECT DISTANCE            : 1.0 m
  CALIBRATION DATE           : 82-09-27
```

CALIBRATION CURVE CONSTANTS

APERTURE	A	B	C
1.8	-3581	1506.49	-0.436
2.5	-4060	1569.49	-0.759
3.6	-6514	1629.70	-1.824
5.1	5420	1610.70	2.796
7.2	1123	1606.54	1.098
10.0	584	1604.29	0.885
14.0	306	1610.60	0.773
20.0	195	1650.51	0.767

TABLE 6.1 : TEMPERATURE AND RADIANCE OF SKY IMAGE

DATE:4NOV87 TIME:09:24 ELEV.ANGLE:0.0° SKY:Overcast

R.V. POINT SUR DATA   **MOSS LANDING DATA**   **AGA DATA**

DISTANCE	:0.35 NM			
TIME	:10.23	TIME	:10.23	SCANNER TYPE:780
AIR TEMP	:14.4°C	AIR TEMP	:17°C	SCANNER VERS:LWB
SS TEMP	:14.1°C	SS TEMP	:15°C	SERIAL # :4011
WIND SPEED:3-5 KTS				F O V :3.5°
WIND DIR	:130°			FILTER CODE :N O F
DEW POINT	:6.7°C			APERTURE :1.8
REL HUMID	:59.1			THERMALRANGE:20
PRESSURE	:1016 mb			EMISSIVITY :0.97

# OF LINES	ZENITH ANGLE (°)	SPOT TEMP (°C)	RADIANCE (W/cm^2-sr)	REMARKS
1	88.251	12.9	(4.266)E-3	
3	88.359	13.0	(4.273)E-3	
5	88.469	13.0	(4.273)E-3	
7	88.578	13.1	(4.280)E-3	
9	88.688	13.4	(4.302)E-3	
11	88.797	13.6	(4.316)E-3	
13	88.906	13.7	(4.323)E-3	
15	89.016	13.7	(4.323)E-3	
17	89.125	13.8	(4.330)E-3	
19	89.234	13.8	(4.330)E-3	
21	89.344	13.8	(4.330)E-3	
23	89.453	13.8	(4.330)E-3	
25	89.563	14.0	(4.345)E-3	
27	89.672	13.8	(4.330)E-3	
29	89.781	13.8	(4.330)E-3	
31	89.891	9.1	(4.001)E-3	
33	90.0	8.2	(3.940)E-3	
35	90.109	7.8	(3.913)E-3	
37	90.219	7.5	(3.893)E-3	
39	90.328	7.2	(3.873)E-3	
41	90.438	7.5	(3.893)E-3	
43	90.547	7.6	(3.900)E-3	
45	90.656	7.2	(3.873)E-3	
47	90.766	7.5	(3.893)E-3	
49	90.875	7.6	(3.900)E-3	
51	90.984	7.8	(3.913)E-3	
53	91.094	8.5	(3.960)E-3	
55	91.203	8.2	(3.940)E-3	
57	91.311	8.8	(3.981)E-3	
59	91.422	8.6	(3.967)E-3	
61	91.531	8.5	(3.960)E-3	
63	91.641	9.6	(4.036)E-3	
30	89.945	13.3	(4.294)E-3	Horizon

TABLE 6.2 : TEMPERATURE AND RADIANCE OF SKY IMAGE

```
------------------------------------------------------------
DATE:4NOV87 TIME:09:25 ELEV.ANGLE:3.5° SKY:Overcast
------------------------------------------------------------
```

R.V. POINT SUR DATA   MOSS LANDING DATA   AGA DATA

DISTANCE :0.35 NM		
TIME :10.23	TIME :10.23	SCANNER TYPE:780
AIR TEMP :14.4°C	AIR TEMP :17°C	SCANNER VERS:LWB
SS TEMP :14.1°C	SS TEMP :15°C	SERIAL # :4011
WIND SPEED:3-5 KTS		F O V :3.5°
WIND DIR :130°		FILTER CODE :N O F
DEW POINT :6.7°C		APERTURE :1.8
REL HUMID :59.1		THERMALRANGE:20
PRESSURE 1016 mb		EMISSIVITY :0.97

```
------------------------------------------------------------
```

# OF LINES	ZENITH ANGLE(°)	SPOT TEMP(°C)	RADIANCE (W/cm²-sr)	R E M A R K S
1	84.75	10.0	(4.063)E-3	
3	84.859	10.1	(4.070)E-3	
5	84.969	10.0	(4.063)E-3	
7	85.078	9.7	(4.042)E-3	
9	85.188	8.8	(3.981)E-3	
11	85.297	6.2	(3.806)E-3	
13	85.406	7.2	(3.873)E-3	
15	85.516	7.2	(3.873)E-3	
17	85.625	6.6	(3.833)E-3	
19	85.734	6.8	(3.846)E-3	
21	85.844	6.8	(3.846)E-3	
23	85.953	6.9	(3.853)E-3	
25	86.063	8.8	(3.981)E-3	
27	86.172	9.3	(4.015)E-3	
29	86.281	10.7	(4.111)E-3	
31	86.391	11.5	(4.167)E-3	
33	86.5	11.5	(4.167)E-3	
35	86.609	11.7	(4.181)E-3	
37	86.719	12.0	(4.202)E-3	
39	86.828	11.8	(4.188)E-3	
41	86.938	12.1	(4.209)E-3	
43	87.047	12.1	(4.209)E-3	
45	87.156	12.1	(4.209)E-3	
47	87.266	12.4	(4.231)E-3	
49	87.375	12.4	(4.231)E-3	
51	87.484	11.7	(4.181)E-3	
53	87.594	12.1	(4.209)E-3	
55	87.703	12.1	(4.209)E-3	
57	87.813	12.2	(4.216)E-3	
59	87.922	12.5	(4.238)E-3	
61	88.031	12.6	(4.245)E-3	
63	88.141	12.9	(4.266)E-3	

TABLE 6.3 : TEMPERATURE AND RADIANCE OF SKY IMAGE

DATE:4NOV87 TIME:09:26 ELEV.ANGLE:7.0° SKY:Overcast

R.V. POINT SUR DATA   MOSS LANDING DATA   AGA DATA

DISTANCE :0.35 NM			
TIME :10.23	TIME :10.23	SCANNER TYPE:780	
AIR TEMP :14.4°C	AIR TEMP :17°C	SCANNER VERS:LWB	
SS TEMP :14.1°C	SS TEMP :15°C	SERIAL # :4011	
WIND SPEED:3-5 KTS		F O V :3.5°	
WIND DIR :130°		FILTER CODE :N O F	
DEW POINT :6.7°C		APERTURE :1.8	
REL HUMID :59.1		THERMALRANGE:20	
PRESSURE :1016 mb		EMISSIVITY :0.97	

# OF LINES	ZENITH ANGLE(°)	SPOT TEMP(°C)	RADIANCE (W/cm^2-sr)	R E M A R K S
1	81.25	-4.6	(3.132)E-3	
3	81.359	-5.6	(3.074)E-3	
5	81.469	-5.6	(3.074)E-3	
7	81.578	-5.6	(3.074)E-3	
9	81.688	-4.6	(3.132)E-3	
11	81.797	-2.5	(3.257)E-3	
13	81.906	-1.2	(3.336)E-3	
15	82.016	-0.6	(3.372)E-3	
17	82.125	-0.9	(3.354)E-3	
19	82.234	-1.5	(3.317)E-3	
21	82.344	-2.9	(3.233)E-3	
23	82.453	-3.5	(3.197)E-3	
25	82.563	-3.5	(3.197)E-3	
27	82.672	-3.2	(3.215)E-3	
29	82.781	-2.9	(3.233)E-3	
31	82.891	-2.9	(3.233)E-3	
33	83.0	-2.9	(3.233)E-3	
35	83.109	-2.5	(3.257)E-3	
37	83.219	-2.5	(3.257)E-3	
39	83.328	-2.2	(3.275)E-3	
41	83.438	-2.2	(3.275)E-3	
43	83.547	-1.5	(3.317)E-3	
45	83.656	-0.6	(3.372)E-3	
47	83.766	1.4	(3.497)E-3	
49	83.875	2.0	(3.534)E-3	
51	83.984	2.6	(3.573)E-3	
53	84.094	2.3	(3.553)E-3	
55	84.203	2.0	(3.534)E-3	
57	84.313	2.0	(3.534)E-3	
59	84.422	5.7	(3.773)E-3	
61	84.531	6.6	(3.833)E-3	
63	84.641	7.4	(3.886)E-3	

TABLE 6.4 : TEMPERATURE AND RADIANCE OF SKY IMAGE

DATE:4NOV87 TIME:09:27 ELEV.ANGLE:10.5°SKY:Overcast

R.V. POINT SUR DATA   MOSS LANDING DATA   AGA DATA

DISTANCE :0.35 NM
TIME   :10.23   TIME   :10.23   SCANNER TYPE:780
AIR TEMP :14.4°C   AIR TEMP :17°C   SCANNER VERS:LWB
SS TEMP :14.1°C   SS TEMP :15°C   SERIAL # :4011
WIND SPEED:3-5 KTS   F O V   :3.5°
WIND DIR :130°   FILTER CODE :N O F
DEW POINT :6.7°C   APERTURE   :1.8
REL HUMID :59.1   THERMALRANGE:20
PRESSURE :1016 mb   EMISSIVITY :0.97

# OF LINES	ZENITH ANGLE (°)	SPOT TEMP (°C)	RADIANCE (W/cm^2-sr)	R E M A R K S
1	77.75	-4.9	(3.115)E-3	
3	77.859	-4.6	(3.132)E-3	
5	77.969	-4.2	(3.156)E-3	
7	78.078	-3.9	(3.174)E-3	
9	78.188	-3.9	(3.174)E-3	
11	78.297	-3.9	(3.174)E-3	
13	78.406	-3.2	(3.215)E-3	
15	78.516	-2.9	(3.233)E-3	
17	78.625	-3.2	(3.215)E-3	
19	78.374	-3.2	(3.215)E-3	
21	78.844	-2.9	(3.233)E-3	
23	78.953	-2.9	(3.233)E-3	
25	79.063	-2.2	(3.275)E-3	
27	79.112	-1.5	(3.317)E-3	
29	79.281	-1.9	(3.293)E-3	
31	79.391	-2.2	(3.275)E-3	
33	79.5	-1.9	(3.293)E-3	
35	79.609	-1.2	(3.336)E-3	
37	79.719	-1.5	(3.317)E-3	
39	79.828	-1.9	(3.293)E-3	
41	79.938	-3.2	(3.611)E-3	
43	80.047	-4.6	(3.132)E-3	
45	80.156	-5.6	(3.074)E-3	
47	80.266	-5.6	(3.074)E-3	
49	80.375	-6.3	(3.034)E-3	
51	80.484	-6.6	(3.017)E-3	
53	80.594	-7.0	(2.994)E-3	
55	80.703	-7.3	(2.977)E-3	
57	80.813	-7.3	(2.977)E-3	
59	80.922	-6.6	(3.017)E-3	
61	81.031	-5.9	(3.057)E-3	
63	81.141	-5.2	(3.097)E-3	

TABLE 6.5 : TEMPERATURE AND RADIANCE OF SKY IMAGE

DATE:4NOV87 TIME:09:27 ELEV.ANGLE:14.0°SKY:Overcast

R.V. POINT SUR DATA		MOSS LANDING DATA		AGA DATA	
DISTANCE	:0.35 NM				
TIME	:10.23	TIME	:10.23	SCANNER TYPE	:780
AIR TEMP	:14.4°C	AIR TEMP	:17°C	SCANNER VERS	:LWB
SS TEMP	:14.1°C	SS TEMP	:15°C	SERIAL #	:4011
WIND PEED	:3-5 KTS			F O V	:3.5°
WIND DIR	:130°			FILTER CODE	:N O F
DEW POINT	:6.7°C			APERTURE	:1.8
REL HUMID	:59.1			THERMALRANGE	:20
PRESSURE	:1016 mb			EMISSIVITY	:0.97

# OF LINES	ZENITH ANGLE(°)	SPOT TEMP(°C)	RADIANCE (W/cm^2-sr)	R E M A R K S
1	74.25	1.9	(3.528)E-3	
3	74.359	2.2	(3.547)E-3	
5	74.469	2.2	(3.547)E-3	
7	74.578	2.2	(3.547)E-3	
9	74.688	2.6	(3.573)E-3	
11	74.797	2.6	(3.573)E-3	
13	74.906	2.9	(3.592)E-3	
15	75.016	2.9	(3.592)E-3	
17	75.125	2.9	(3.592)E-3	
19	75.234	2.6	(3.573)E-3	
21	75.344	2.6	(3.573)E-3	
23	75.353	2.9	(3.592)E-3	
25	75.563	2.9	(3.592)E-3	
27	75.672	2.9	(3.592)E-3	
29	75.781	2.9	(3.592)E-3	
31	75.891	3.2	(3.611)E-3	
33	76.0	3.2	(3.611)E-3	
35	76.109	3.2	(3.611)E-3	
37	76.219	3.8	(3.649)E-3	
39	76.328	3.5	(3.630)E-3	
41	76.438	3.5	(3.630)E-3	
43	76.547	3.5	(3.630)E-3	
45	76.656	3.8	(3.649)E-3	
47	76.766	4.4	(3.688)E-3	
49	76.875	4.4	(3.688)E-3	
51	76.984	4.1	(3.669)E-3	
53	77.094	3.8	(3.649)E-3	
55	77.203	3.8	(3.649)E-3	
57	77.313	3.8	(3.649)E-3	
59	77.422	4.1	(3.669)E-3	
61	77.531	3.8	(3.649)E-3	
63	77.641	3.5	(3.630)E-3	

TABLE 6.6 : TEMPERATURE AND RADIANCE OF SKY IMAGE

DATE:4NOV87 TIME:09:28 ELEV.ANGLE:17.5°SKY:Overcast

R.V. POINT SUR DATA   MOSS LANDING DATA   AGA DATA

DISTANCE	:0.35 NM		
TIME	:10.23	TIME :10.23	SCANNER TYPE:780
AIR TEMP	:14.4°C	AIR TEMP :17°C	SCANNER VERS:LWB
SS TEMP	:14.1°C	SS TEMP :15°C	SERIAL # :4011
WIND SPEED:3-5 KTS			F O V :3.5°
WIND DIR	:130°		FILTER CODE :N O F
DEW POINT	:6.7°C		APERTURE :1.8
REL HUMID	:59.1		THERMALRANGE:20
PRESSURE	:1016 mb		EMISSIVITY :0.97

# OF LINES	ZENITH ANGLE (°)	SPOT TEMP (°C)	RADIANCE (W/cm^2-sr)	R E M A R K S
1	70.75	-11	(2.771)E-3	
3	70.859	-14	(2.612)E-3	
5	70.969	-19	(2.359)E-3	
7	71.078	-20	(2.311)E-3	
9	71.188	-20	(2.311)E-3	
11	71.297	-20	(2.311)E-3	
13	71.406	-21	(2.263)E-3	
15	71.516	-20	(2.311)E-3	
17	71.625	-20	(2.311)E-3	
19	71.734	-20	(2.311)E-3	
21	71.844	-18	(2.408)E-3	
23	71.953	-16	(2.509)E-3	
25	72.063	-13	(2.664)E-3	
27	72.172	-13	(2.664)E-3	
29	72.281	-9.1	(2.876)E-3	
31	72.391	-6.2	(3.040)E-3	
33	72.5	-5.2	(3.097)E-3	
35	72.609	-4.2	(3.156)E-3	
37	72.719	-5.2	(3.097)E-3	
39	72.828	-4.2	(3.156)E-3	
41	72.938	-2.1	(3.281)E-3	
43	73.047	-2.1	(3.281)E-3	
45	73.156	-1.2	(3.336)E-3	
47	73.266	-0.8	(3.360)E-3	
49	73.375	-0.5	(3.379)E-3	
51	73.484	-0.2	(3.397)E-3	
53	73.594	-0.2	(3.397)E-3	
55	73 703	0.1	(3.416)E-3	
57	73.`13	0.1	(3.416)E-3	
59	73.922	0.1	(3.416)E-3	
61	74.031	0.1	(3.416)E-3	
63	74.141	0.1	(3.416)E-3	

TABLE 6.7 : TEMPERATURE AND RADIANCE OF SKY IMAGE

```
DATE:4NOV87 TIME:09:29 ELEV.ANGLE:21.0°SKY:Overcast
```

R.V. POINT SUR DATA   MOSS LANDING DATA   AGA DATA

DISTANCE	:0.35 NM		
TIME	:10.23	TIME :10.23	SCANNER TYPE:780
AIR TEMP	:14.4°C	AIR TEMP :17°C	SCANNER VERS:LWB
SS TEMP	:14.1°C	SS TEMP :15°C	SERIAL # :4011
WIND SPEED:3-5 KTS			F O V :3.5°
WIND DIR	:130°		FILTER CODE :N O F
DEW POINT	:6.7°C		APERTURE :1.8
REL HUMID	:59.1		THERMALRANGE:20
PRESSURE	:1016 mb		EMISSIVITY :0.97

# OF LINES	ZENITH ANGLE(°)	SPOT TEMP(°C)	RADIANCE (W/cm^2-sr)	R E M A R K S
1	67.25	-3.8	(3.180)E-3	
3	67.359	-4.5	(3.138)E-3	
5	67.469	-4.5	(3.138)E-3	
7	67.578	-4.8	(3.121)E-3	
9	67.688	-5.2	(3.097)E-3	
11	67.797	-5.9	(3.057)E-3	
13	67.906	-5.2	(3.097)E-3	
15	68.016	-4.2	(3.156)E-3	
17	68.125	-4.8	(3.121)E-3	
19	68.234	-6.2	(3.040)E-3	
21	68.344	-5.9	(3.057)E-3	
23	68.453	-5.5	(3.080)E-3	
25	68.563	-5.2	(3.097)E-3	
27	68.672	-5.2	(3.097)E-3	
29	68.781	-6.6	(3.017)E-3	
31	68.891	-6.2	(3.040)E-3	
33	69.0	-6.9	(2.999)E-3	
35	69.109	-6.6	(3.017)E-3	
37	69.219	-7.3	(2.977)E-3	
39	69.238	-7.3	(2.977)E-3	
41	69.438	-5.9	(3.057)E-3	
43	69.547	-5.9	(3.057)E-3	
45	69.656	-5.9	(3.057)E-3	
47	69.766	-5.2	(3.097)E-3	
49	69.875	-5.2	(3.097)E-3	
51	69.984	-5.2	(3.097)E-3	
53	70.094	-4.5	(3.138)E-3	
55	70.203	-4.8	(3.121)E-3	
57	70.313	-3.8	(3.180)E-3	
59	70.422	-3.5	(3.197)E-3	
61	70.531	-3.1	(3.221)E-3	
63	70.641	-3.1	(3.221)E-3	

TABLE 6.8 : TEMPERATURE AND RADIANCE OF SKY IMAGE

DATE:4NOV87 TIME:09:29 ELEV.ANGLE:24.5˚SKY:Overcast

R.V. POINT SUR DATA   **MOSS LANDING DATA** **AGA DATA**

R.V. POINT SUR DATA	MOSS LANDING DATA	AGA DATA
DISTANCE :0.35 NM		
TIME :10.23	TIME :10.23	SCANNER TYPE:780
AIR TEMP :14.4˚C	AIR TEMP :17˚C	SCANNER VERS:LWB
SS TEMP :14.1˚C	SS TEMP :15˚C	SERIAL # :4011
WIND SPEED:3-5 KTS		F O V :3.5˚
WIND DIR :130˚		FILTER CODE :N O F
DEW POINT :6.7˚C		APERTURE :1.8
REL HUMID :59.1		THERMALRANGE:20
PRESSURE :1016 mb		EMISSIVITY :0.97

# OF LINES	ZENITH ANGLE(˚)	SPOT TEMP(˚C)	RADIANCE (W/cm^2-sr)	R E M A R K S
1	63.75	-21	(2.263)E-3	
3	63.859	-21	(2.263)E-3	
5	63.969	-22	(2.219)E-3	
7	64.078	-23	(2.169)E-3	
9	64.188	-21	(2.263)E-3	
11	64.297	-23	(2.169)E-3	
13	64.406	-23	(2.169)E-3	
15	64.516	-25	(2.078)E-3	
17	64.625	-21	(2.263)E-3	
19	64.734	-15	(2.560)E-3	
21	64.844	-12	(2.718)E-3	
23	64.953	-10	(2.826)E-3	
25	65.063	-10	(2.826)E-3	
27	65.172	-09.6	(2.848)E-3	
29	65.281	-09.3	(2.865)E-3	
31	65.391	-10	(2.826)E-3	
33	65.5	-12	(2.718)E-3	
35	65.609	-07.5	(2.965)E-3	
37	65.719	-05.7	(3.068)E-3	
39	65.828	-05.0	(3.109)E-3	
41	65.938	-04.3	(3.150)E-3	
43	66.047	-03.6	(3.191)E-3	
45	66.156	-03.6	(3.191)E-3	
47	66.266	-04.0	(3.168)E-3	
49	66.375	-04.3	(3.150)E-3	
51	66.484	-05.0	(3.109)E-3	
53	66.594	-04.7	(3.127)E-3	
55	66.703	-05.0	(3.109)E-3	
57	66.813	-04.7	(3.127)E-3	
59	66.922	-04.7	(3.127)E-3	
61	67.031	-05.0	(3.109)E-3	
63	67.141	-04.3	(3.150)E-3	

TABLE 6.9 : TEMPERATURE AND RADIANCE OF SKY IMAGE

DATE:4NOV87 TIME:09:29 ELEV.ANGLE:28˚ SKY:Overcast

R.V. POINT SUR DATA   MOSS LANDING DATA   AGA DATA

DISTANCE	:0.35 NM				
TIME	:10.23	TIME	:10.23	SCANNER TYPE	:780
AIR TEMP	:14.4˚C	AIR TEMP	:17˚C	SCANNER VERS	:LWB
SS TEMP	:14.1˚C	SS TEMP	:15˚C	SERIAL #	:4011
WIND SPEED	:3-5 KTS			F O V	:3.5˚
WIND DIR	:130˚			FILTER CODE	:N O F
DEW POINT	:6.7˚C			APERTURE	:1.8
REL HUMID	:59.1			THERMALRANGE	:20
PRESSURE	:1016 mb			EMISSIVITY	:0.97

# OF LINES	ZENITH ANGLE (˚)	SPOT TEMP (˚C)	RADIANCE (W/cm^2-sr)	R E M A R K S
1	60.25	-05.4	(3.086)E-3	
3	60.359	-06.0	(3.051)E-3	
5	60.469	-06.4	(3.028)E-3	
7	60.578	-06.7	(3.011)E-3	
9	60.688	-07.1	(2.988)E-3	
11	60.797	-07.8	(2.948)E-3	
13	60.906	-09.3	(2.865)E-3	
15	61.016	-11	(2.771)E-3	
17	61.125	-13	(2.644)E-3	
19	61.234	-15	(2.560)E-3	
21	61.344	-15	(2.560)E-3	
23	61.453	-14	(2.614)E-3	
25	61.563	-14	(2.614)E-3	
27	61.672	-15	(2.560)E-3	
29	61.781	-15	(2.560)E-3	
31	61.891	-15	(2.560)E-3	
33	62.0	-15	(2.560)E-3	
35	62.109	-17	(2.612)E-3	
37	62.219	-20	(2.311)E-3	
39	62.328	-21	(2.263)E-3	
41	62.438	-21	(2.263)E-3	
43	62.547	-23	(2.169)E-3	
45	62.656	-23	(2.169)E-3	
47	62.766	-20	(2.311)E-3	
49	62.875	-18	(2.408)E-3	
51	62.984	-20	(2.311)E-3	
53	63.094	-19	(2.359)E-3	
55	63.203	-19	(2.359)E-3	
57	63.313	-17	(2.612)E-3	
59	63.422	-17	(2.612)E-3	
61	63.531	-17	(2.612)E-3	
63	63.641	-15	(2.560)E-3	

TABLE 6.10 : TEMPERATURE AND RADIANCE OF SKY IMAGE

DATE:4NOV87 TIME:09:30 ELEV.ANGLE:31.5°SKY:Overcast

R.V. POINT SUR DATA   **MOSS LANDING DATA**   **AGA DATA**

R.V. POINT SUR DATA	MOSS LANDING DATA	AGA DATA
DISTANCE :0.35 NM		
TIME :10.23	TIME :10.23	SCANNER TYPE:780
AIR TEMP :14.4°C	AIR TEMP :17°C	SCANNER VERS:LWB
SS TEMP :14.1°C	SS TEMP :15°C	SERIAL # :4011
WIND SPEED:3-5 KTS		F O V :3.5°
WIND DIR :130°		FILTER CODE :N O F
DEW POINT :6.7°C		APERTURE :1.8
REL HUMID :59.1		THERMALRANGE:20
PRESSURE :1016 mb		EMISSIVITY :0.97

# OF LINES	ZENITH ANGLE (°)	SPOT TEMP (°C)	RADIANCE (W/cm²-sr)	R E M A R K S
1	56.75	-18	(2.408)E-3	
3	56.859	-19	(2.359)E-3	
5	56.969	-18	(2.408)E-3	
7	57.078	-17	(2.612)E-3	
9	57.188	-16	(2.509)E-3	
11	57.297	-16	(2.509)E-3	
13	57.406	-15	(2.560)E-3	
15	57.516	-16	(2.509)E-3	
17	57.625	-14	(2.162)E-3	
19	57.734	-10	(2.826)E-3	
21	57.844	-09.3	(2.865)E-3	
23	57.953	-08.9	(2.887)E-3	
25	58.063	-08.5	(2.909)E-3	
27	58.172	-08.5	(2.909)E-3	
29	58.281	-07.8	(2.948)E-3	
31	58.391	-07.5	(2.965)E-3	
33	58.5	-08.2	(2.926)E-3	
35	58.609	-08.9	(2.8870E-3	
37	58.719	-09.3	(2.865)E-3	
39	58.828	-08.2	(2.926)E-3	
41	58.938	-07.8	(2.948)E-3	
43	59.047	-07.5	(2.965)E-3	
45	59.156	-06.7	(3.011)E-3	
47	59.266	-06.7	(3.011)E-3	
49	59.375	-07.1	(2.988)E-3	
51	59.484	-07.1	(2.988)E-3	
53	59.594	-07.8	(2.948)E-3	
55	59.703	-08.2	(2.926)E-3	
57	59.813	-07.8	(2.948)E-3	
59	59.922	-06.7	(3.011)E-3	
61	60.031	-07.1	(2.988)E-3	
63	60.141	-07.1	(2.988)E-3	

TABLE 6.11 : TEMPERATURE AND RADIANCE OF SKY IMAGE

DATE:4NOV87 TIME:09:30 ELEV.ANGLE:35.0°SKY:Overcast

R.V. POINT SUR DATA		**MOSS LANDING DATA**		**AGA DATA**
DISTANCE	:0.35 NM			
TIME	:10.23	TIME	:10.23	SCANNER TYPE:780
AIR TEMP	:14.4°C	AIR TEMP	:17°C	SCANNER VERS:LWB
SS TEMP	:14.1°C	SS TEMP	:15°C	SERIAL # :4011
WIND SPEED:3-5 KTS				F O V :3.5°
WIND DIR	:130°			FILTER CODE :N O F
DEW POINT	:6.7°C			APERTURE :1.8
REL HUMID	:59.1			THERMALRANGE:20
PRESSURE	:1016 mb			EMISSIVITY :0.97

# OF LINES	ZENITH ANGLE(°)	SPOT TEMP(°C)	RADIANCE (W/cm^2-sr)	R E M A R K S
1	53.25	-13	(2.664)E-3	
3	53.359	-13	(2.664)E-3	
5	53.469	-14	(2.612)E-3	
7	53.578	-14	(2.612)E-3	
9	53.678	-15	(2.560)E-3	
11	53.797	-17	(2.612)E-3	
13	53.906	-18	(2.408)E-3	
15	54.016	-20	(2.311)E-3	
17	54.125	-20	(2.311)E-3	
19	54.234	-18	(2.408)E-3	
21	54.344	-19	(2.359)E-3	
23	54.453	-21	(2.263)E-3	
25	54.563	-22	(2.216)E-3	
27	54.672	-23	(2.169)E-3	
29	54.781	-21	(2.263)E-3	
31	54.891	-22	(2.216)E-3	
33	55.0	-25	(2.078)E-3	
35	55.109	-27	(1.989)E-3	
37	55.219	-26	(2.033)E-3	
39	55.328	-21	(2.263)E-3	
41	55.438	-20	(2.311)E-3	
43	55.547	-19	(2.359)E-3	
45	55.656	-19	(2.359)E-3	
47	55.766	-23	(2.169)E-3	
49	55.875	-23	(2.169)E-3	
51	56.984	-23	(2.169)E-3	
53	56.094	-23	(2.169)E-3	
55	56.203	-23	(2.169)E-3	
57	56.313	-23	(2.169)E-3	
59	56.422	-22	(2.216)E-3	
61	56.531	-21	(2.263)E-3	
63	56.641	-23	(2.169)E-3	

TABLE 6.12 : TEMPERATURE AND RADIANCE OF SKY IMAGE

```
--------------------------------------------------------
DATE:4NOV87 TIME:10:32 ELEV.ANGLE:0.0°  SKY:
--------------------------------------------------------
```

R.V. POINT SUR DATA MOSS LANDING DATA AGA DATA

```
DISTANCE   :0.35 NM
TIME       :10.23    TIME       :10.23    SCANNER  TYPE:780
AIR TEMP   :14.4°C   AIR TEMP   :17°C     SCANNER VERS:LWB
SS  TEMP   :14.1°C   SS  TEMP   :15°C     SERIAL   #  :4011
WIND SPEED:3-5 KTS                        F O V       :7°
WIND DIR  :130°                           FILTER CODE :N O F
DEW POINT :6.7°C                          APERTURE    :1.8
REL HUMID :59.1                           THERMALRANGE:20
PRESSURE  :1016 mb                        EMISSIVITY  :0.97
```

# OF LINES	ZENITH ANGLE (°)	SPOT TEMP (°C)	RADIANCE (W/cm²-sr)	REMARKS
1	86.5	10.8	(4.118)E-3	
3	86.719	11.4	(4.160)E-3	
5	86.938	11.5	(4.167)E-3	
7	87.156	12.0	(4.202)E-3	
9	87.375	12.1	(4.2090E-3	
11	87.594	12.5	(4.238)E-3	
13	87.813	12.8	(4.259)E-3	
15	88.031	13.1	(4.280)E-3	
17	88.25	13.2	(4.287)E-3	
19	88.469	13.3	(4.294)E-3	
21	88.688	13.6	(4.316)E-3	
23	88.906	13.7	(4.323)E-3	
25	89.125	13.9	(4.337)E-3	
27	89.344	13.9	(4.337)E-3	
29	89.563	13.9	(4.337)E-3	
31	89.781	13.7	(4.323)E-3	
33	90.0	7.4	(3.886)E-3	
35	90.219	6.3	(3.813)E-3	
37	90.438	5.9	(3.786)E-3	
39	90.656	5.9	(3.786)E-3	
41	90.875	6.3	(3.813)E-3	
43	91.094	6.9	(3.853)E-3	
45	91.313	6.8	(3.846)E-3	
47	91.531	7.2	(3.873)E-3	
49	91.75	8.3	(3.947)E-3	
51	91.969	7.5	(3.893)E-3	
53	92.188	8.5	(3.960)E-3	
55	92.406	6.3	(3.813)E-3	
57	92.625	7.2	(3.873)E-3	
59	92.844	9.1	(4.001)E-3	
61	93.063	13.6	←.(Wall)	
63	93.281	>13.6	←.(Wall)	
32	89.890	13.3	(4.294)E-3	Horizon

TABLE 6.13 : TEMPERATURE AND RADIANCE OF SKY IMAGE

DATE:4NOV87 TIME:10:33 ELEV.ANGLE:7.0° SKY:Mostly cloudy

R.V. POINT SUR DATA   **MOSS LANDING DATA**   **AGA DATA**

DISTANCE	:0.35 NM				
TIME	:10.23	TIME	:10.23	SCANNER TYPE:	780
AIR TEMP	:14.4°C	AIR TEMP	:17°C	SCANNER VERS:	LWB
SS TEMP	:14.1°C	SS TEMP	:15°C	SERIAL #	:4011
WIND SPEED:	3-5 KTS			F O V	:7°
WIND DIR	:130°			FILTER CODE	:N O F
DEW POINT	:6.7°C			APERTURE	:1.8
REL HUMID	:59.1			THERMALRANGE:	20
PRESSURE	:1016 mb			EMISSIVITY	:0.97

# OF LINES	ZENITH ANGLE (°)	SPOT TEMP (°C)	RADIANCE (W/cm^2-sr)	R E M A R K S
1	79.5	3.6	(3.637)E-3	
3	79.719	4.2	(3.675)E-3	
5	79.938	3.6	(3.637)E-3	
7	80.156	-8.0*	(2.937)E-3	
9	80.375	-8.0*	(2.937)E-3	
11	80.594	-7.3*	(2.977)E-3	
13	80.813	-6.6*	(3.017)E-3	
15	81.031	-7.6*	(2.960)E-3	
17	81.25	-6.2*	(3.040)E-3	
19	81.469	-6.6*	(3.017)E-3	
21	81.688	-6.2*	(3.040)E-3	
23	81.906	-5.2*	(3.097)E-3	
25	82.125	-3.5*	(3.197)E-3	
27	82.344	4.2	(3.675)E-3	
29	82.563	5.4	(3.753)E-3	
31	82.781	-1.2*	(3.336)E-3	
33	83.0	-1.5*	(3.317)E-3	
35	83.219	-0.8*	(3.360)E-3	
37	83.438	-1.2*	(3.336)E-3	
39	83.656	2.7	(3.579)E-3	
41	83.875	2.7	(3.579)E-3	
43	84.094	2.7	(3.579)E-3	
45	84.313	3.3	(3.617)E-3	
47	84.531	3.0	(3.598)E-3	
49	84.75	3.9	(3.656)E-3	
51	84.969	4.5	(3.695)E-3	
53	85.188	7.2	(3.873)E-3	
55	85.406	8.4	(3.954)E-3	
57	85.625	6.6	(3.833)E-3	
59	85.844	8.4	(3.954)E-3	
61	86.063	8.7	(3.974)E-3	
63	86.281	7.5	(3.893)E-3	

(*) Cloudy areas

108

TABLE 6.14 : TEMPERATURE AND RADIANCE OF SKY IMAGE

DATE:4NOV87 TIME:10:34 ELEV.ANGLE:14.0°SKY:Mostly blue sky

R.V. POINT SUR DATA   **MOSS LANDING DATA**   **AGA DATA**

R.V. POINT SUR DATA	MOSS LANDING DATA	AGA DATA
DISTANCE :0.35 NM		
TIME :10.23	TIME :10.23	SCANNER TYPE:780
AIR TEMP :14.4°C	AIR TEMP :17°C	SCANNER VERS:LWB
SS TEMP :14.1°C	SS TEMP :15°C	SERIAL # :4011
WIND SPEED:3-5 KTS		F O V :7°
WIND DIR :130°		FILTER CODE :N O F
DEW POINT :6.7°C		APERTURE :1.8
REL HUMID :59.1		THERMALRANGE:20
PRESSURE :1016 mb		EMISSIVITY :0.97

# OF LINES	ZENITH ANGLE (°)	SPOT TEMP (°C)	RADIANCE (W/cm^2-sr)	R E M A R K S
1	72.5	-19	(2.359)E-3	
3	72.719	-17	(2.458)E-3	
5	72.938	-10	(2.826)E-3	
7	73.156	-10	(2.826)E-3	
9	73.375	-12	(2.718)E-3	
11	73.594	-11	(2.771)E-3	
13	73.813	-14	(2.612)E-3	
15	74.031	-19	(2.359)E-3	
17	74.25	-16	(2.509)E-3	
19	74.469	-17	(2.458)E-3	
21	74.688	-16	(2.509)E-3	
23	74.906	-17	(2.458)E-3	
25	75.125	-17	(2.458)E-3	
27	75.344	-15	(2.560)E-3	
29	75.563	-11.0*	(2.771)E-3	
31	75.781	-14.0*	(2.612)E-3	
33	76.0	-09.7*	(2.843)E-3	
35	76.219	-05.1*	(3.103)E-3	
37	76.438	-08.6*	(2.904)E-3	
39	76.656	-12	(2.178)E-3	
41	76.875	-17	(2.458)E-3	
43	77.094	-16	(2.509)E-3	
45	77.313	-16	(2.509)E-3	
47	77.531	-16	(2.509)E-3	
49	77.75	-15	(2.560)E-3	
51	77.969	-15	(2.560)E-3	
53	78.188	-15	(2.560)E-3	
55	78.406	-15	(2.560)E-3	
57	78.625	-14	(2.612)E-3	
59	78.844	-14	(2.612)E-3	
61	79.063	-12	(2.718)E-3	
63	79.281	-13	(2.664)E-3	

(*) Cloudy area.

TABLE 6.15 : TEMPERATURE AND RADIANCE OF SKY IMAGE

DATE:4NOV87 TIME:10:35 ELEV.ANGLE:21.0°SKY:Scattered clouds

R.V. POINT SUR DATA   MOSS LANDING DATA   AGA DATA

DISTANCE :0.35 NM		
TIME :10.23	TIME :10.23	SCANNER TYPE:780
AIR TEMP :14.4°C	AIR TEMP :17°C	SCANNER VERS:LWB
SS TEMP :14.1°C	SS TEMP :15°C	SERIAL # :4011
WIND SPEED:3-5 KTS		F O V :7°
WIND DIR :130°		FILTER CODE :N O F
DEW POINT :6.7°C		APERTURE :1.8
REL HUMID :59.1		THERMALRANGE:20
PRESSURE :1016 mb		EMISSIVITY :0.97

# OF LINES	ZENITH ANGLE (°)	SPOT TEMP (°C)	RADIANCE (W/cm^2-sr)	R E M A R K S
1	65.5	-27	(1.989)E-3	
3	65.719	-27	(1.989)E-3	
5	65.938	-27	(1.989)E-3	
7	66.156	-27	(1.989)E-3	
9	66.375	-27	(1.989)E-3	
11	66.594	-26	(2.033)E-3	
13	66.813	-26	(2.033)E-3	
15	67.031	-26	(2.033)E-3	
17	67.25	-26	(2.033)E-3	
19	67.469	-26	(2.033)E-3	
21	67.688	-25	(2.078)E-3	
23	67.906	-25	(2.078)E-3	
25	68.125	-25	(2.078)E-3	
27	68.344	-25	(2.078)E-3	
29	68.563	-25	(2.0780E-3	
31	68.781	-24	(2.123)E-3	
33	69.0	-24	(2.123)E-3	
35	69.219	-24	(2.123)E-3	
37	69.438	-24	(2.123)E-3	
39	69.656	-23	(2.169)E-3	
41	69.875	-23	(2.169)E-3	
43	70.094	-23	(2.169)E-3	
45	70.313	-23	(2.169)E-3	
47	70.531	-23	(2.169)E-3	
49	70.25	-22	(2.216)E-3	
51	70.969	-22	(2.216)E-3	
53	71.188	-22	(2.216)E-3	
55	71.406	-22	(2.216)E-3	
57	71.625	-21	(2.263)E-3	
59	71.844	-21	(2.263)E-3	
61	72.063	-20	(2.311)E-3	
63	72.281	-17	(2.458)E-3	

110

TABLE 6.16 : TEMPERATURE AND RADIANCE OF SKY IMAGE

DATE:4NOV87 TIME:10:37 ELEV.ANGLE:28.0°SKY:Mostly blue sky

R.V. POINT SUR DATA   **MOSS LANDING DATA** **AGA DATA**

DISTANCE   :0.35 NM
TIME   :10.23   TIME   :10.23   SCANNER TYPE:780
AIR TEMP   :14.4°C   AIR TEMP   :17°C   SCANNER VERS:LWB
SS TEMP   :14.1°C   SS TEMP   :15°C   SERIAL   # :4011
WIND SPEED:3-5 KTS   F O V   :7°
WIND DIR   :130°   FILTER CODE :N O F
DEW POINT :6.7°C   APERTURE   :1.8
REL HUMID :59.1   THERMALRANGE:20
PRESSURE   :1016 mb   EMISSIVITY :0.97

# OF LINES	ZENITH ANGLE(°)	SPOT TEMP(°C)	RADIANCE $(W/cm^2\text{-}sr)$	R E M A R K S
1	58.5	-24.0*	(2.123)E-3	
3	58.719	-29.0*	(1.903)E-3	
5	58.938	-29.0*	(1.903)E-3	
7	59.156	-30.0*	(1.861)E-3	
9	59.375	-32.0	(1.778)E-3	
11	59.594	-32.0	(1.778)E-3	
13	59.813	-32.0	(1.778)E-3	
15	60.031	-32.0	(1.778)E-3	
17	60.25	-32.0	(1.778)E-3	
19	60.469	-18.0*	(2.408)E-3	
21	60.688	-12.0*	(2.718)E-3	
23	60.906	-11.0*	(2.771)E-3	
25	61.125	-15.0*	(2.560)E-3	
27	61.344	-23.0*	(2.169)E-3	
29	61.563	-28.0*	(1.946)E-3	
31	61.781	-30.0*	(1.861)E-3	
33	62.0	-31.0*	(1.819)E-3	
35	62.219	-29.0*	(1.903)E-3	
37	62.438	-31.0	(1.819)E-3	
39	62.656	-31.0	(1.819)E-3	
41	62.875	-31.0	(1.819)E-3	
43	63.094	-31.0	(1.819)E-3	
45	63.313	-31.0	(1.819)E-3	
47	63.531	-30.0	(1.861)E-3	
49	63.575	-31.0	(1.819)E-3	
51	63.969	-30.0	(1.861)E-3	
53	64.188	-30.0	(1.861)E-3	
55	64.406	-30.0	(1.861)E-3	
57	64.625	-29.0	(1.903)E-3	
59	64.844	-29.0	(1.903)E-3	
61	65.063	-30.0	(1.861)E-3	
63	65.281	-29.0	(1.903)E-3	

(*) Cloudy areas.

TABLE 6.17 : TEMPERATURE AND RADIANCE OF SKY IMAGE

DATE:4NOV87 TIME:10:38 ELEV.ANGLE:35.0°SKY:Mostly blue sky

R.V. POINT SUR DATA   MOSS LANDING DATA   AGA DATA

DISTANCE	:0.35 NM			
TIME	:10.23	TIME	:10.23	SCANNER TYPE:780
AIR TEMP	:14.4°C	AIR TEMP	:17°C	SCANNER VERS:LWB
SS TEMP	:14.1°C	SS TEMP	:15°C	SERIAL # :4011
WIND SPEED:3-5 KTS				F O V :7°
WIND DIR	:130°			FILTER CODE :N O F
DEW POINT :6.7°C				APERTURE :1.8
REL HUMID :59.1				THERMALRANGE:20
PRESSURE :1016 mb				EMISSIVITY :0.97

# OF LINES	ZENITH ANGLE(°)	SPOT TEMP(°C)	RADIANCE (W/cm^2-sr)	R E M A R K S
1	51.5	-35.0	(1.659)E-3	
3	51.719	-35.0	(1.659)E-3	
5	51.938	-35.0	(1.659)E-3	
7	52.156	-35.0	(1.659)E-3	
9	52.375	-34.0	(1.699)E-3	
11	52.594	-34.0	(1.699)E-3	
13	52.813	-34.0	(1.699)E-3	
15	53.031	-34.0	(1.699)E-3	
17	53.25	-34.0	(1.699)E-3	
19	53.469	-34.0	(1.699)E-3	
21	53.688	-34.0	(1.699)E-3	
23	53.906	-34.0	(1.699)E-3	
25	54.125	-34.0	(1.699)E-3	
27	54.344	-34.0	(1.699)E-3	
29	54.563	-34.0	(1.699)E-3	
31	54.781	-33.0	(1.738)E-3	
33	55.0	-33.0	(1.738)E-3	
35	55.219	-33.0	(1.738)E-3	
37	55.438	-33.0	(1.738)E-3	
39	55.656	-33.0	(1.738)E-3	
41	55.875	-33.0	(1.738)E-3	
43	56.094	-33.0	(1.738)E-3	
45	56.313	-33.0	(1.738)E-3	
47	56.531	-32.0	(1.778)E-3	
49	56.75	-32.0	(1.778)E-3	
51	56.969	-32.0	(1.778)E-3	
53	57.188	-32.0	(1.778)E-3	
55	57.406	-31.0	(1.778)E-3	
57	57.625	-31.0	(1.778)E-3	
59	57.844	-31.0	(1.778)E-3	
61	58.063	-31.0	(1.778)E-3	
63	58.281	-31.0	(1.778)E-3	

TABLE 6.18 : TEMPERATURE AND RADIANCE OF SKY IMAGE

DATE:14JUL88 TIME:13:18 ELEV.ANGLE:0.0°SKY:Fair

MONTEREYBAY BOUY DATA   MOSS LANDING DATA   AGA DATA

LOCATION:3648N/12224W LOCATION:364802N/1214717W

TIME	:11:00	TIME	:12:50	SCANNER TYPE:780
AIR TEMP	:12.9°C	AIR TEMP	:14.9°C	SCANNER VERS:LWB
SS TEMP	:12.8°C	REL HUMID	:77 %	SERIAL # :4011
WIND SPEED	:4 m/s	WIND SP	:3.1 m/s	F O V :7°
WIND DIR	:320°	WIND DIR	:256°	FILTER CODE :N O F
PRESSURE	:1017 mb	PRESSURE	:1012.6mb	APERTURE :1.8
				RANGE/LEVEL : 5 / 4 3
TIDE HEIGHT :1.1 m		DEW POINT:12.8°C		EMISSIVITY :0.97

# OF LINES	ZENITH ANGLE(°)	SPOT TEMP(°C)	RADIANCE (W/cm^2-sr)	R E M A R K S
1	89.478	11.3	(4.153)E-3	
3	89.587	11.3	(4.153)E-3	
5	89.697	11.3	(4.153)E-3	
7	89.806	11.3	(4.153)E-3	
9	89.915	11.3	(4.153)E-3	
10	89.97	11.9	(4.153)E-3	Horizon
11	90.134	9.6	(4.036)E-3	
13	90.243	9.6	(4.036)E-3	
15	90.353	9.6	(4.036)E-3	
17	90.462	8.5	(3.960)E-3	
19	90.572	9.6	(4.036)E-3	
21	90.681	8.5	(3.960)E-3	
23	90.79	9.6	(4.036)E-3	
25	90.90	8.5	(3.960)E-3	
27	91.009	8.5	(3.960)E-3	
29	91.118	9.6	(4.036)E-3	
31	91.228	8.5	(3.960)E-3	
33	91.337	9.6	(4.036)E-3	
35	91.447	9.6	(4.036)E-3	
37	91.556	8.5	(3.960)E-3	
39	91.665	9.6	(4.036)E-3	
41	91.775	8.5	(3.960)E-3	
43	91.884	8.5	(3.960)E-3	
45	91.993	8.5	(3.960)E-3	
47	92.103	9.6	(4.036)E-3	
49	92.212	8.5	(3.960)E-3	
51	92.322	9.6	(4.036)E-3	
53	92.431	11.3	(4.153)E-3	
55	92.54	>11.3	-	
57	92.65	-	-	
59	92.759	-	-	
61	92.868	-	-	
63	92.978	-	-	

TABLE 6.19 : TEMPERATURE AND RADIANCE OF SKY IMAGE

DATE:14JUL88 TIME:13:20 ELEV.ANGLE:0.0°SKY:Fair

MONTEREYBAY BOUY DATA MOSS LANDING DATA   AGA DATA

MONTEREYBAY BOUY DATA		MOSS LANDING DATA		AGA DATA	
LOCATION:3648N/12224W		LOCATION:364802N/1214717W			
TIME	:11:00	TIME	:12:50	SCANNER TYPE:780	
AIR TEMP	:12.9°C	AIR TEMP	:14.9°C	SCANNER VERS:LWB	
SS TEMP	:12.8°C	REL HUMID:77 %		SERIAL # :4011	
WIND SPEED	:4 m/s	WIND SP	:3.1 m/s	F O V :7°	
WIND DIR	:320°	WIND DIR :256°		FILTER CODE :N O F	
PRESSURE	:1017 mb	PRESSURE :1012.6mb		APERTURE :1.8	
				RANGE/LEVEL : 5 / 4 3	
TIDE HEIGHT :1.1 m		DEW POINT:12.8°C		EMISSIVITY :0.97	

# OF LINES	ZENITH ANGLE(°)	SPOT TEMP(°C)	RADIANCE (W/cm^2-sr)	R E M A R K S
1	87.236	14.5	(4.381)E-3	
3	87.345	14.5	(4.381)E-3	
5	87.454	14.0	(4.345)E-3	
7	87.564	14.5	(4.381)E-3	
9	87.673	14.0	(4.381)E-3	
11	87.783	14.0	(4.345)E-3	
13	87.892	14.5	(4.381)E-3	
15	88.001	14.0	(4.345)E-3	
17	88.111	14.0	(4.345)E-3	
19	88.22	14.5	(4.381)E-3	
21	88.329	14.0	(4.345)E-3	
23	88.439	14.0	(4.345)E-3	
25	88.548	14.0	(4.345)E-3	
27	88.658	14.0	(4.345)E-3	
29	88.767	14.0	(4.345)E-3	
31	88.876	12.3	(4.224)E-3	
33	88.986	12.3	(4.224)E-3	
35	89.095	12.3	(4.224)E-3	
37	89.204	12.3	(4.224)E-3	
39	89.314	12.3	(4.224)E-3	
41	89.423	12.3	(4.224)E-3	
43	89.533	11.8	(4.118)E-3	
45	89.642	12.3	(4.224)E-3	
47	89.751	12.3	(4.224)E-3	
49	89.861	11.8	(4.118)E-3	
51	89.97	12.3	(4.224)E-3	Horizon
53	-	-	-	
55	-	-	-	
57	-	-	-	
59	-	-	-	
61	-	-	-	
63	-	-	-	

TABLE 6.20 : TEMPERATURE AND RADIANCE OF SKY IMAGE

DATE:14JUL88 TIME:13:30 ELEV.ANGLE:82.0°SKY:Fair

MONTEREYBAY BOUY DATA MOSS LANDING DATA AGA DATA

LOCATION:3648N/12224W LOCATION:364802N/1214717W

TIME	:11:00	TIME	:12:50	SCANNER TYPE:780
AIR TEMP	:12.9°C	AIR TEMP :14.9°C		SCANNER VERS:LWB
SS TEMP	:12.8°C	REL HUMID:77 %		SERIAL # :4011
WIND SPEED	:4 m/s	WIND SP :3.1 m/s		F O V :7°
WIND DIR	:320°	WIND DIR :256°		FILTER CODE :N O F
PRESSURE	:1017 mb	PRESSURE :1012.6mb		APERTURE :1.8

RANGE/LEVEL : 5 / 4 3

TIDE HEIGHT :1.1 m   DEW POINT:12.8°C   EMISSIVITY :0.97

# OF LINES	ZENITH ANGLE (°)	SPOT TEMP (°C)	RADIANCE (W/cm^2-sr)	R E M A R K S
1	80.469	2.9	(3.592)E-3	
3	80.351	2.8	(3.585)E-3	
5	80.468	3.0	(3.598)E-3	
7	80.579	3.1	(3.604)E-3	
9	80.688	3.3	(3.617)E-3	
11	80.797	3.5	(3.630)E-3	
13	80.906	3.6	(3.637)E-3	
15	81.016	3.8	(3.649)E-3	
17	81.125	3.7	(3.643)E-3	
19	81.234	4.0	(3.662)E-3	
21	81.343	4.1	(3.669)E-3	
23	81.453	4.3	(3.682)E-3	
25	81.563	4.4	(3.688)E-3	
27	81.672	4.6	(3.701)E-3	
29	81.781	4.8	(3.714)E-3	
31	81.891	5.0	(3.727)E-3	
33	82.0	5.2	(3.740)E-3	
35	82.109	5.4	(3.754)E-3	
37	82.219	5.6	(3.767)E-3	
39	82.328	5.7	(3.773)E-3	
41	82.438	5.8	(3.780)E-3	
43	82.547	6.1	(3.800)E-3	
45	82.656	6.2	(3.806)E-3	
47	82.766	6.4	(3.820)E-3	
49	82.875	6.4	(3.820)E-3	
51	82.984	6.7	(3.839)E-3	
53	83.094	7.0	(3.859)E-3	
55	83.202	7.3	(3.880)E-3	
57	83.313	7.5	(3.900)E-3	
59	83.422	7.6	(3.900)E-3	
61	83.531	7.8	(3.913)E-3	
63	83.641	8.0	(3.927)E-3	

TABLE 6.21 : TEMPERATURE AND RADIANCE OF SKY IMAGE

DATE:15JUL88 TIME:11:22 ELEV.ANGLE:0.0°SKY:Fair

MONTEREYBAY BOUY DATA MOSS LANDING DATA AGA DATA

LOCATION:3648N/12224W	LOCATION:364802N/1214717W	
TIME :09:00	TIME :10:29	SCANNER TYPE:780
AIR TEMP :13.6°C	AIR TEMP :14.5°C	SCANNER VERS:LWB
SS TEMP :11.7°C	REL HUMID:81.5 %	SERIAL # :4011
WIND SPEED :5 m/s	WIND SP :4.02 m/s	F O V :7°
WIND DIR :320°	WIND DIR :226°	FILTER CODE :N O F
PRESSURE :1018 mb	PRESSURE :1013.4mb	APERTURE :1.8
		RANGE/LEVEL : 5 / 4 0
TIDE HEIGHT :0.6 m	DEW POINT:11.7°C	EMISSIVITY :0.97

# OF LINES	ZENITH ANGLE(°)	SPOT TEMP(°C)	RADIANCE (W/cm^2-sr)	R E M A R K S
1	88.981	12.2	(4.216)E-3	
3	89.09	12.1	(4.209)E-3	
5	89.20	12.0	(4.202)E-3	
7	89.309	12.0	(4.202)E-3	
9	89.418	11.8	(4.188)E-3	
11	89.528	11.6	(4.174)E-3	
13	89.637	11.6	(4.174)E-3	
15	89.747	11.4	(4.174)E-3	
17	89.856	11.5	(4.167)E-3	
19	89.965	11.4	(4.174)E-3	
20	90.02	10.9	(4.125)E-3	Horizon
21	90.074	9.5	(4.029)E-3	
23	90.184	8.1	(3.933)E-3	
25	90.293	8.0	(3.927)E-3	
27	90.403	7.9	(3.920)E-3	
29	90.512	7.9	(3.920)E-3	
31	90.622	7.5	(3.893)E-3	
33	90.731	8.3	(3.947)E-3	
35	90.84	7.8	(3.913)E-3	
37	90.95	7.4	(3.886)E-3	
39	91.059	8.9	(3.988)E-3	
41	91.168	7.7	(3.906)E-3	
43	91.278	7.7	(3.906)E-3	
45	91.387	7.7	(3.906)E-3	
47	91.497	7.8	(3.913)E-3	
49	91.606	8.1	(3.933)E-3	
51	91.715	8.0	(3.927)E-3	
53	91.825	8.2	(3.940)E-3	
55	91.934	7.8	(3.913)E-3	
57	92.043	7.6	(3.900)E-3	
59	92.153	8.2	(3.940)E-3	
61	92.262	9.0	(3.995)E-3	
63	92.372	-	-	

TABLE 6.22 : TEMPERATURE AND RADIANCE OF SKY IMAGE

DATE:15JUL88 TIME:11:51 ELEV.ANGLE:0.0°SKY:Fair

MONTEREYBAY BOUY DATA   MOSS LANDING DATA   AGA DATA

LOCATION:3648N/12224W	LOCATION:364802N/1214717W		
TIME :09:00	TIME :10:29	SCANNER TYPE:780
AIR TEMP :13.6°C	AIR TEMP :14.5°C	SCANNER VERS:LWB
SS TEMP :11.7°C	REL HUMID:81.5 %	SERIAL # :4011
WIND SPEED :5.0 m/s	WIND SP :4.02 m/s	F O V :7°
WIND DIR :320°	WIND DIR :226°	FILTER CODE :N O F
PRESSURE :1018 mb	PRESSURE :1013.4mb	APERTURE :1.8
		RANGE/LEVEL : 5 / 4 0
TIDE HEIGHT :0.6 m	DEW POINT:11.7°C	EMISSIVITY :0.97

# OF LINES	ZENITH ANGLE(°)	SPOT TEMP(°C)	RADIANCE (W/cm²-sr)	R E M A R K S
1	86.903	11.6	(4.174)E-3	
3	87.012	11.6	(4.174)E-3	
5	87.122	11.8	(4.188)E-3	
7	87.231	11.8	(4.188)E-3	
9	87.34	11.9	(4.195)E-3	
11	87.45	11.9	(4.195)E-3	
13	87.559	12.0	(4.202)E-3	
15	87.668	12.1	(4.209)E-3	
17	87.778	12.3	(4.224)E-3	
19	87.887	12.2	(4.216)E-3	
21	87.997	12.4	(4.231)E-3	
23	88.106	12.4	(4.231)E-3	
25	88.215	12.4	(4.231)E-3	
27	88.325	12.4	(4.231)E-3	
29	88.434	12.4	(4.231)E-3	
31	88.543	12.4	(4.231)E-3	
33	88.653	12.4	(4.231)E-3	
35	88.762	12.4	(4.231)E-3	
37	88.872	12.3	(4.224)E-3	
39	88.981	12.3	(4.224)E-3	
41	89.09	12.3	(4.224)E-3	
43	89.2	12.2	(4.216)E-3	
45	89.309	12.1	(4.209)E-3	
47	89.418	12.1	(4.209)E-3	
49	89.528	11.6	(4.174)E-3	
51	89.637	11.4	(4.160)E-3	
53	89.747	11.5	(4.167)E-3	
55	89.856	11.5	(4.167)E-3	
57	89.965	11.4	(4.160)E-3	
58	90.02	8.9	(3.988)E-3	Horizon
59	90.074	10.7	(4.111)E-3	
61	-	-	-	
63	-	-	-	

TABLE 6.23 : TEMPERATURE AND RADIANCE OF SKY IMAGE

DATE:15JUL88 TIME:12:02 ELEV.ANGLE:81.0°SKY:Fair

MONTEREYBAY BOUY DATA MOSS LANDING DATA AGA DATA

MONTEREYBAY BOUY DATA		MOSS LANDING DATA		AGA DATA	
LOCATION:3648N/12224W		LOCATION:364802N/1214717W			
TIME	:09:00	TIME	:10:29	SCANNER TYPE:780	
AIR TEMP	:13.6°C	AIR TEMP	:14.5°C	SCANNER VERS:LWB	
SS TEMP	:11.7°C	REL HUMID:81.5 %		SERIAL #	:4011
WIND SPEED	:5 m/s	WIND SP	:4.02 m/s	F O V	:7°
WIND DIR	:320°	WIND DIR	:226°	FILTER CODE	:N O F
PRESSURE	:1018 mb	PRESSURE	:1013.4mb	APERTURE	:1.8
				RANGE/LEVEL	: 5 / 4 0
TIDE HEIGHT	:0.6 m	DEW POINT:11.7°C		EMISSIVITY	:0.97

# OF LINES	ZENITH ANGLE(°)	SPOT TEMP(°C)	RADIANCE (W/cm^2-sr)	R E M A R K S
1	79.25	-1.4	(3.324)E-3	
3	79.359	-1.3	(3.330)E-3	
5	79.469	-1.1	(3.342)E-3	
7	79.578	-0.9	(3.354)E-3	
9	79.688	-0.9	(3.354)E-3	
11	79.797	-0.7	(3.336)E-3	
13	79.906	-0.5	(3.379)E-3	
15	80.016	-0.4	(3.385)E-3	
17	80.125	-0.1	(3.403)E-3	
19	80.234	0.1	(3.416)E-3	
21	80.344	0.2	(3.422)E-3	
23	80.453	0.4	(3.434)E-3	
25	80.563	0.6	(3.447)E-3	
27	80.672	0.8	(3.459)E-3	
29	80.781	0.9	(3.465)E-3	
31	80.891	1.1	(3.478)E-3	
33	81.0	1.3	(3.490)E-3	
35	81.109	1.5	(3.503)E-3	
37	81.219	1.5	(3.503)E-3	
39	81.328	1.9	(3.528)E-3	
41	81.438	2.0	(3.547)E-3	
43	81.547	2.2	(3.547)E-3	
45	81.656	2.4	(3.560)E-3	
47	81.766	2.6	(3.573)E-3	
49	81.875	3.0	(3.598)E-3	
51	81.984	3.0	(3.598)E-3	
53	82.094	3.2	(3.611)E-3	
55	82.203	3.4	(3.624)E-3	
57	82.213	3.6	(3.637)E-3	
59	82.422	3.7	(3.643)E-3	
61	82.351	4.0	(3.662)E-3	
63	82.641	4.2	(3.675)E-3	

TABLE 6.24 : TEMPERATURE AND RADIANCE OF SKY IMAGE

DATE:15JUL88 TIME:12:43 ELEV.ANGLE:0.0°SKY:Fair

MONTEREYBAY BOUY DATA MOSS LANDING DATA AGA DATA

LOCATION:3648N/12224W LOCATION:364802N/1214717W

TIME	:18:00	TIME	:12:39	SCANNER TYPE:780
AIR TEMP	:13.7°C	AIR TEMP	:15.5°C	SCANNER VERS:LWB
SS TEMP	:11.8°C	REL HUMID	:73.5 %	SERIAL # :4011
WIND SPEED	:5 m/s	WIND SP	:2.5 m/s	F O V :7°
WIND DIR	:320°	WIND DIR	:235°	FILTER CODE :N O F
PRESSURE	:1018 mb	PRESSURE	:1013.1mb	APERTURE :1.8
				RANGE/LEVEL : 5 / 4 2
TIDE HEIGHT :1.1 m		DEW POINT:11.8°C		EMISSIVITY :0.97

# OF LINES	ZENITH ANGLE(°)	SPOT TEMP(°C)	RADIANCE (W/cm^2-sr)	R E M A R K S
1	89.508	12.7	(4.252)E-3	
3	89.617	12.6	(4.245)E-3	
5	89.727	12.5	(4.238)E-3	
7	89.836	12.4	(4.231)E-3	
9	89.945	12.2	(4.216)E-3	
10	90.0	10.9	(4.125)E-3	Horizon
11	90.054	9.2	(4.008)E-3	
13	90.164	8.9	(3.988)E-3	
15	90.273	8.7	(3.974)E-3	
17	90.383	8.8	(3.981)E-3	
19	90.492	8.6	(3.967)E-3	
21	90.602	10.4	(4.091)E-3	
23	90.711	10.0	(4.063)E-3	
25	90.82	9.6	(4.036)E-3	
27	90.93	10.0	(4.063)E-3	
29	91.039	10.7	(4.111)E-3	
31	91.148	9.9	(4.056)E-3	
33	91.258	9.6	(4.036)E-3	
35	91.367	10.1	(4.070)E-3	
37	91.477	10.3	(4.084)E-3	
39	91.586	9.9	(4.056)E-3	
41	91.805	9.3	(4.015)E-3	
43	91.914	8.9	(3.988)E-3	
45	92.023	9.1	(4.001)E-3	
47	92.133	11.5	(4.167)E-3	
49	92.242	10.8	(4.118)E-3	
51	92.352	9.6	(4.036)E-3	
53	92.461	9.5	(4.029)E-3	
55	92.57	9.4	(4.022)E-3	
57	92.68	9.1	(4.001)E-3	
59	92.789	9.5	(4.029)E-3	
61	92.898	9.5	(4.029)E-3	
63	93.008	9.4	(4.022)E-3	

TABLE 6.25 : TEMPERATURE AND RADIANCE OF SKY IMAGE

DATE:15JUL88 TIME:12:43 ELEV.ANGLE:0.0˚SKY:Fair

MONTEREYBAY BOUY DATA MOSS LANDING DATA AGA DATA

MONTEREYBAY BOUY DATA	MOSS LANDING DATA	AGA DATA
LOCATION:3648N/12224W	LOCATION:364802N/1214717W	
TIME :18:00	TIME :12:39	SCANNER TYPE:780
AIR TEMP :13.7˚C	AIR TEMP :15.5˚C	SCANNER VERS:LWB
SS TEMP :11.8˚C	REL HUMID:73.5 %	SERIAL # :4011
WIND SPEED :5 m/s	WIND SP :2.5 m/s	F O V :7˚
WIND DIR :320˚	WIND DIR :235˚	FILTER CODE :N O F
PRESSURE :1018 mb	PRESSURE :1013.1mb	APERTURE :1.8
		RANGE/LEVEL : 5 / 4 2
TIDE HEIGHT :1.1 m	DEW POINT:11.8˚C	EMISSIVITY :0.97

# OF LINES	ZENITH ANGLE(˚)	SPOT TEMP(˚C)	RADIANCE (W/cm^2-sr)	R E M A R K S
1	87.102	12.3	(4.223)E-3	
3	87.211	12.4	(4.231)E-3	
5	87.32	12.5	(4.238)E-3	
7	87.43	12.6	(4.245)E-3	
9	87.539	12.6	(4.245)E-3	
11	87.648	12.8	(4.259)E-3	
13	87.758	12.8	(4.258)E-3	
15	87.867	12.8	(4.258)E-3	
17	87.977	12.9	(4.266)E-3	
19	88.086	12.9	(4.266)E-3	
21	88.195	12.9	(4.266)E-3	
23	88.305	13.0	(4.273)E-3	
25	88.414	12.9	(4.266)E-3	
27	88.523	12.8	(4.258)E-3	
29	88.633	12.8	(4.258)E-3	
31	88.742	12.8	(4.258)E-3	
33	88.852	12.7	(4.251)E-3	
35	88.961	12.5	(4.238)E-3	
37	89.07	12.5	(4.238)E-3	
39	89.18	12.4	(4.231)E-3	
41	89.289	12.3	(4.224)E-3	
43	89.398	12.3	(4.224)E-3	
45	89.508	12.1	(4.2090E-3	
47	89.617	11.9	(4.195)E-3	
49	89.727	11.6	(4.174)E-3	
51	89.836	11.4	(4.160)E-3	
53	89.945	11.4	(4.160)E-3	
55	90.0	10.9	(4.125)E-3	Horizon
57	90.054	8.2	(3.940)E-3	
59	90.164	8.1	(3.934)E-3	
61	90.273	8.2	(3.940)E-3	
63	90.383	8.8	(3.981)E-3	

TABLE 6.26 : TEMPERATURE AND RADIANCE OF SKY IMAGE

DATE:15JUL88 TIME:13:15 ELEV.ANGLE:84.0°SKY:Fair

MONTEREYBAY BOUY DATA   MOSS LANDING DATA   AGA DATA

MONTEREYBAY BOUY DATA		MOSS LANDING DATA		AGA DATA	
LOCATION:3648N/12224W		LOCATION:364802N/1214717W			
TIME	:18:00	TIME	:12:39	SCANNER TYPE	:780
AIR TEMP	:13.7°C	AIR TEMP	:15.5°C	SCANNER VERS	:LWB
SS TEMP	:11.8°C	REL HUMID	:73.5 %	SERIAL #	:4011
WIND SPEED	:5 m/s	WIND SP	:2.5 m/s	F O V	:7°
WIND DIR	:320°	WIND DIR	:235°	FILTER CODE	:N O F
PRESSURE	:1018 mb	PRESSURE	:1013.1mb	APERTURE	:1.8
				RANGE/LEVEL	: 5 / 4 2
TIDE HEIGHT	:1.1 m	DEW POINT	:11.8°C	EMISSIVITY	: 0 . 9 7

# OF LINES	ZENITH ANGLE(°)	SPOT TEMP(°C)	RADIANCE (W/cm^2-sr)	REMARKS
1	82.25	2.7	(3.578)E-3	
3	82.359	2.9	(3.592)E-3	
5	82.469	3.1	(3.604)E-3	
7	82.578	3.3	(3.617)E-3	
9	82.688	3.4	(3.624)E-3	
11	82.797	3.6	(3.637)E-3	
13	82.906	3.9	(3.655)E-3	
15	83.016	4.2	(3.675)E-3	
17	83.125	4.3	(3.682)E-3	
19	83.234	4.5	(3.695)E-3	
21	83.344	4.7	(3.707)E-3	
23	83.453	4.9	(3.720)E-3	
25	83.563	4.9	(3.720)E-3	
27	83.672	5.2	(3.740)E-3	
29	83.781	5.5	(3.760)E-3	
31	83.891	5.6	(3.767)E-3	
33	84.0	5.8	(3.780)E-3	
35	84.109	6.0	(3.794)E-3	
37	84.219	6.2	(3.806)E-3	
39	84.328	6.4	(3.820)E-3	
41	84.438	6.4	(3.820)E-3	
43	84.547	6.7	(3.839)E-3	
45	84.656	6.9	(3.853)E-3	
47	84.766	7.2	(3.873)E-3	
49	84.875	7.3	(3.880)E-3	
51	84.984	7.5	(3.893)E-3	
53	85.094	7.7	(3.906)E-3	
55	85.203	7.8	(3.913)E-3	
57	85.313	8.1	(3.933)E-3	
59	85.422	8.3	(3.947)E-3	
61	85.531	8.5	(3.960)E-3	
63	85.641	8.7	(3.974)E-3	

TABLE 6.27 : TEMPERATURE AND RADIANCE OF SKY IMAGE

DATE:25JUL88 TIME:13:44 ELEV.ANGLE:0.0°SKY:Overcast

MONTEREYBAY BOUY DATA MOSS LANDING DATA AGA DATA

MONTEREYBAY BOUY DATA	MOSS LANDING DATA	AGA DATA
LOCATION:3648N/12224W	LOCATION:364802N/1214717W	
TIME :13:00	TIME :13:44	SCANNER TYPE:780
AIR TEMP :17.8°C	AIR TEMP :16.1°C	SCANNER VERS:LWB
SS TEMP :15.4°C	REL HUMID:94.0 %	SERIAL # :4011
WIND SPEED :4.9 m/s	WIND SP :4.9 m/s	F O V :3.5°
WIND DIR :274°	WIND DIR :274°	FILTER CODE :N O F
PRESSURE :1013.6mb	PRESSURE :1013.6mb	APERTURE :1.8
		RANGE/LEVEL : 5 / 4 4
TIDE HEIGHT :0.9 m	DEW POINT:15.3°C	EMISSIVITY :0.97

# OF LINES	ZENITH ANGLE(°)	SPOT TEMP(°C)	RADIANCE (W/cm^2-sr)	REMARKS
1	88.429	13.6	(4.316)E-3	
3	88.538	13.6	(4.316)E-3	
5	88.648	13.6	(4.316)E-3	
7	88.757	13.7	(4.323)E-3	
9	88.866	13.7	(4.323)E-3	
11	88.976	13.7	(4.323)E-3	
13	89.085	13.7	(4.323)E-3	
15	89.195	13.9	(4.337)E-3	
17	89.304	13.8	(4.330)E-3	
19	89.413	14.0	(4.345)E-3	
21	89.523	14.1	(4.353)E-3	
23	89.632	14.2	(4.361)E-3	
25	89.741	14.1	(4.353)E-3	
27	89.851	14.1	(4.353)E-3	
29	89.960	14.4	(4.373)E-3	
31	90.070	14.9	(4.410)E-3	Horizon
33	90.179	15.6	(4.460)E-3	
35	90.288	15.9	(4.482)E-3	
37	90.398	16.2	(4.504)E-3	
39	90.507	16.1	(4.497)E-3	
41	90.616	16.3	(4.512)E-3	
43	90.726	16.6	(4.534)E-3	
45	90.835	16.5	(4.526)E-3	
47	90.945	16.9	(4.556)E-3	
49	91.054	16.7	(4.541)E-3	
51	91.163	16.5	(4.526)E-3	
53	91.273	16.6	(4.534)E-3	
55	91.382	16.1	(4.497)E-3	
57	91.491	16.0	(4.449)E-3	
59	91.601	15.8	(4.475)E-3	
61	91.710	16.1	(4.497)E-3	
63	91.82	16.1	(4.497)E-3	

TABLE 6.28 : TEMPERATURE AND RADIANCE OF SKY IMAGE

DATE:25JUL88 TIME:14:20 ELEV.ANGLE:0.0°SKY:Overcast

MONTEREYBAY BOUY DATA   MOSS LANDING DATA   AGA DATA

MONTEREYBAY BOUY DATA	MOSS LANDING DATA	AGA DATA
LOCATION:3648N/12224W	LOCATION:364802N/1214717W	
TIME :13:00	TIME :13:44	SCANNER TYPE:780
AIR TEMP :17.8°C	AIR TEMP :16.1°C	SCANNER VERS:LWB
SS TEMP :15.4°C	REL HUMID:94.0 %	SERIAL # :4011
WIND SPEED :4.9 m/s	WIND SP :4.9 m/s	F O V :3.5°
WIND DIR :274°	WIND DIR :274°	FILTER CODE :N O F
PRESSURE :1013.6mb	PRESSURE :1013.6mb	APERTURE :1.8
		RANGE/LEVEL : 5 / 4 4
TIDE HEIGHT :0.9 m	DEW POINT:15.3°C	EMISSIVITY :0.97

# OF LINES	ZENITH ANGLE (°)	SPOT TEMP (°C)	RADIANCE (W/cm^2-sr)	R E M A R K S
1	86.570	12.8	(4.258)E-3	
3	86.679	12.7	(4.251)E-3	
5	86.788	12.8	(4.258)E-3	
7	86.898	12.8	(4.258)E-3	
9	87.007	12.7	(4.251)E-3	
11	87.116	12.9	(4.266)E-3	
13	87.335	12.8	(4.258)E-3	
15	87.445	12.9	(4.266)E-3	
17	87.554	12.8	(4.258)E-3	
19	87.663	12.9	(4.266)E-3	
21	87.773	12.9	(4.2660E-3	
23	87.882	12.8	(4.258)E-3	
25	87.991	12.7	(4.251)E-3	
27	88.101	12.9	(4.266)E-3	
29	88.210	12.9	(4.2660E-3	
31	88.320	12.8	(4.258)E-3	
33	88.429	12.9	(4.266)E-3	
35	88.538	12.9	(4.266)E-3	
37	88.648	13.0	(4.273)E-3	
39	88.757	12.9	(4.266)E-3	
41	88.866	13.0	(4.273)E-3	
43	88.976	13.1	(4.280)E-3	
45	89.085	13.2	(4.287)E-3	
47	89.195	13.3	(4.294)E-3	
49	89.304	13.2	(4.287)E-3	
51	89.413	13.5	(4.309)E-3	
53	89.523	13.7	(4.323)E-3	
55	89.632	13.8	(4.330)E-3	
57	89.741	13.8	(4.330)E-3	
59	89.851	13.8	(4.330)E-3	
61	89.960	13.8	(4.3300E-3	
63	90.070	14.0	(4.345)E-3	Horizon

TABLE 6.29 : TEMPERATURE AND RADIANCE OF SKY IMAGE

DATE:25JUL88 TIME:15:05 ELEV.ANGLE:80.0°SKY:Overcast

MONTEREYBAY BOUY DATA MOSS LANDING DATA AGA DATA

LOCATION:3648N/12224W		LOCATION:364802N/1214717W			
TIME	:13:00	TIME	:13:44	SCANNER TYPE:780	
AIR TEMP	:17.8°C	AIR TEMP	:16.1°C	SCANNER VERS:LWB	
SS TEMP	:15.4°C	REL HUMID:94.0 %		SERIAL #	:4011
WIND SPEED	:4.9 m/s	WIND SP	:4.9 m/s	F O V	:3.5°
WIND DIR	:274°	WIND DIR :274°		FILTER CODE	:N O F
PRESSURE	:1013.6mb	PRESSURE :1013.6mb		APERTURE	:1.8
				RANGE/LEVEL : 5 / 4 4	
TIDE HEIGHT :0.9 m		DEW POINT:15.3°C		EMISSIVITY	:0.97

# OF LINES	ZENITH ANGLE(°)	SPOT TEMP(°C)	RADIANCE (W/cm^2-sr)	R E M A R K S
1	78.250	12.8	(4.258)E-3	
3	78.359	12.8	(4.258)E-3	
5	78.468	12.8	(4.258)E-3	
7	78.578	12.8	(4.258)E-3	
9	78.687	12.7	(4.251)E-3	
11	78.796	12.7	(4.251)E-3	
13	78.906	12.7	(4.251)E-3	
15	79.015	12.7	(4.251)E-3	
17	79.125	12.7	(4.251)E-3	
19	79.234	12.8	(4.258)E-3	
21	79.343	12.8	(4.258)E-3	
23	79.453	12.7	(4.251)E-3	
25	79.565	12.8	(4.258)E-3	
27	79.671	12.8	(4.258)E-3	
29	79.781	12.7	(4.251)E-3	
31	79.890	12.8	(4.258)E-3	
33	80.000	12.8	(4.258)E-3	
35	80.109	12.9	(4.266)E-3	
37	80.218	12.9	(4.266)E-3	
39	80.328	12.8	(4.258)E-3	
41	80.437	12.8	(4.258)E-3	
43	80.546	12.9	(4.266)E-3	
45	80.655	12.8	(4.258)E-3	
47	80.764	12.9	(4.266)E-3	
49	80.784	12.9	(4.266)E-3	
51	80.983	12.9	(4.266)E-3	
53	81.092	12.9	(4.2660E-3	
55	81.202	12.8	(4.258)E-3	
57	81.311	12.9	(4.266)E-3	
59	81.420	12.9	(4.266)E-3	
61	81.530	12.9	(4.266)E-3	
63	81.639	12.9	(4.266)E-3	

TABLE 6.30 : VALIDATION OF AGA SPOT TEMPERATURES

STANDARD PARAMETERS

SCANNER	TYPE	:780	FILTER CODE	:NOF
SCANNER	VERSION	:LWB	EMISSIVITY	:00.97
SERIAL	NUMBER	:4011	TRANSMISSIVITY	:01.00
LENS	FOV	:7	ISOTHERM MARKER	:0.0

7NOV88
Distance = 2 m
$T_{bb} = 20\ °C$ $\qquad\qquad T_{bb} = 22\ °C$
$T_{amb}/T_{atm} = 17.5\ °C$
f/1.8

THERM ERROR RANGE TEMP(°C)	THERM LEVEL TEMP%	SPOT TEMP(°C)	ERROR TEMP%	RANGE	LEVEL%	THERM RANGE	THERM SPOT LEVEL
2	49	20.5	02.5	2	50	21.7	-01.3
5	49	20.2	01.0	5	49	22.2	00.9
10	49	18.6	-07.0	10	49	21.8	00.9
20	48	17.6	-12.0	20	49	20.9	-05.0
50	49	16.1		50	49	18.0	
100	49	11.2		100	48	12.6	
200	48	-00.9		200	49	3.7	
500	49	-47.0		500	49	-32.0	
1000	49	-212.0		1000	49	-212.2	

14NOV88
Distance = 2 m
$T_{bb} = 20\ °C$
$T_{amb}/T_{atm} = 16.8\ °C$ $\qquad\qquad T_{amb}/T_{atm} = 16.9\ °C$
f/1.8

THERM ERROR RANGE TEMP(°C)	THERM LEVEL TEMP%	SPOT TEMP(°C)	ERROR TEMP%	RANGE	LEVEL%	THERM RANGE	THERM SPOT LEVEL
2	50	22.9	14.5	2	49	21.7	8.5
5	49	21.6	-07.5	5	49	21.5	7.5
10	49	21.3	06.5	10	49	21.3	6.5
20	48	20.1	00.5	20	48	19.6	-2.0
50	47	17.5		50	47	17.8	
100	43	12.4		100	45	12.3	
200	40	00.1		200	40	0.1	
500	21	-46.0		500	27	-52.0	
1000	24	-213.0		1000	05	-213.0	

(Continued)

14NOV88
Distance = 2 m
T_{bb} = 22 °C
T_{amb}/T_{atm} = 17 °C
f/1.8

16NOV88
Distance = 1 m
T_{bb} = 20 °C
T_{amb}/T_{atm} = 16.9 °C

THERM ERROR RANGE TEMP(°C)	THERM LEVEL TEMP%	SPOT TEMP(°C)	ERROR	THERM RANGE TEMP(°C)	THERM TEMP%	RANGE	THERM SPOT LEVEL
2	51	24.3	10.45	2	48	19.3	-3.5
5	51	23.9	08.60	5	48	19.3	-3.5
10	50	23.0	04.54	10	48	19.1	-4.5
20	50	21.9	00.45	20	48	18.2	-9.0
50	48	19.1		50	47	15.5	
100	45	15.0		100	44	08.7	
200	40	-06.3		200	41	-02.1	
500	22	-51.0		500	29	-117.0	
1000	15	-213.0		1000	10	-212.0	

17NOV88
Distance = 1 m
T_{bb} = 100 °C
T_{amb}/T_{atm} = 21 °C
f/1.8   f/5.1

THERM ERROR RANGE TEMP(°C)	THERM LEVEL TEMP%	SPOT TEMP(°C)	ERROR	THERM RANGE TEMP(°C)	THERM TEMP%	RANGE	THERM SPOT LEVEL
2	141	> 99.9	---	2	26	98.6	4.25
5	142	100.0	00.00	5	26	98.2	0.71
10	142	99.9	-0.70	10	26	99.2	0.68
20	139	99.0	-1.00	20	25	96.0	-4.00
50	138	97.8		50	23	87.9	
100	136	95.7		100	20	71.9	
200	131	90.6		200	15	43.0	
500	114	79.1		500	07	-207.0	
1000	088	37.9		1000	00	-207.0	

AVERAGE ERROR IN SPOT/BLACKBODY TEMPERATURE VS THERMAL RANGE (THERMAL LEVEL IGNORED)

THERM RANGE	AVER. ERROR %
2	4.25
5	0.71
10	0.68
20	-4.00

(Thermal Range and Thermal Level in isothermal units IU).

TABLE 7.1 : RADIOSONDE DATA FOR NOV 87

```
-------------------------------------------------------------
FLIGHT NAME                            : SC8701
STATION IDENTIFIER                     : 11-87 STUDENT CRUISE FL1
STATION LATITUDE    (in DD.MM.SS)      : 036.20.00 N
STATION LONGITUDE (in DDD.MM.SS)       : 122.01.30 W
LOCAL LAUNCH DATE (YYMMDD)             : 871104
GREENWICH   LAUNCH TIME    (HHMM) : 2302
LOCAL       LAUNCH TIME    (HHMM) : 1502
-------------------------------------------------------------
```

ALTITUDE (meters)	PRESSURE (mbar)	TEMPER. (° C)	DEWPOINT (° C)	REL.HUM. (%)	WSPEED (m/sec)
0	1013.3	17.1	11.3	68.1	(5.3)
492	956.6	15.9	8.5	61.1	5.6
1003	900.3	12.3	5.8	64.3	7.0
1492	849.1	9.2	3.0	64.9	7.2
2040	794.6	6.0	0.9	69.7	3.2
2512	749.9	3.8	-3.0	61.1	11.0
3010	705.1	0.0	-4.5	71.3	17.1
3529	600.0	-3.4	-5.6	84.6	26.3
4055	617.8	-8.1	-8.6	96.4	26.8
4504	583.0	-10.1	-10.2	99.2	23.0
5003	546.3	-13.6	-13.8	98.5	21.5
5515	510.6	-16.4	-17.8	88.8	20.6
6022	477.1	-20.0	-26.3	57.2	22.5
6494	447.5	-23.1	-30.6	50.5	22.6
7009	416.9	-27.1	-32.8	58.2	24.1
7488	389.9	-31.2	-41.2	36.6	23.7
8044	360.2	-35.8	-45.4	36.3	24.6
8509	336.7	-40.0	-48.4	39.7	25.4
9048	310.9	-44.4	-52.5	39.4	25.5
9523	289.4	-49.1	-55.5	46.0	25.7
10007	268.8	-50.0	-60.8	25.7	28.3
10522	248.5	-48.5	-61.5	19.5	29.3
11030	230.0	-50.3	-63.8	17.6	26.2

TABLE 7.2 : RADIOSONDE DATA FOR JULY 88

----

14 JULY 1988   (TIME 13:18)

ALTITUDE (km)	PRESS (mbar)	TEMP (°C)	DP (°C)	RH (%)	WSPEED (m / s)
00.000	1017.0	12.9	12.8	78	4.0
00.019	1012.6	14.9	12.7	77	3.1
00.024	1011.6	14.9	12.6	76	-
16.000	103.5	-56.5	-	2.1	-

15 JULY 1988 A   (TIME 11:22)

ALTITUDE (km)	PRESS (mbar)	TEMP (°C)	DP (°C)	RH (%)	WSPEED (m/s)
00.000	1018	13.6	11.7	89	5.0
00.019	1013.4	14.5	11.6	88	4.02
00.024	1012.4	14.5	11.5	87	-
16.000	103.5	-56.5	-	2.1	-

15 JULY 1988 B   (TIME 12:43)

ALTITUDE (km)	PRESS (mbar)	TEMP (°C)	DP (°C)	RH (%)	WSPEED (m/s)
00.000	1018	13.7	11.8	78	5.0
00.019	1013.1	15.5	11.7	77	2.5
00.024	1012.1	15.5	11.6	76	-
16.000	103.5	-56.5	-	2.1	-

25 JULY 1988   (TIME 13:44)

ALTITUDE (km)	PRESS (mbar)	TEMP (°C)	DP (°C)	RH (%)	WSPEED (m/s)
00.000	1014.6	17.8	15.4	95	4.9
00.019	1013.6	16.1	15.3	94	4.9
00.024	1012.6	16.1	15.2	93	-
16.000	103.5	-56.5	-	2.1	-

TABLE 7.3 : INPUT DATA FOR LOWTRAN 6

Atmospheric model	:New model (for radiosonde data), 7
Atmospheric path	:Vertical path to space, 2
Mode	:Radiance mode, 1
Temp/Pressure profile	:Normal operation, 0
Water vapor profile	:Midlatitude winter (summer), 3 (2)
Ozone profile	: " " " " "
Radiosonde data	:Yes, 1
Supress prinding	:No, 0
Temperature of earth	:Temp. of 1rst atmospheric layer
Surface albedo	:Left blank=Blackbody
Extinction type	:Navy maritime extinction, 3
Seasonal dependence	:Fall/Winter, 2 (Spring/Summer, 3)
Aerosol profile	:Stratospheric background, 1
Air mass character	:3
Cirrus cloud attenuat.	:No, 0
Vert. structure algor.	:No, 0
Meteor. range(km)	:Default value
Wind speed (m/s)	:As required
Average wind speed (m/s)	:Default value
Precipitation rate(mm/h)	:Default value
# of atmospheric levels	:23 for November 87, 4 for July 88

Data of atmospheric layers:

Altitude of layer	(km)	:Radiosonde data
Pressure of layer	(mbar)	: " "
Temperature	($^{\circ}$ C)	: " "
Dew point	($^{\circ}$ C)	: " "
Rel. humid.	(%)	: " "
Water vapor density	(gr/cubic meter)	:Default value
Ozone density	(gr/cubic meter)	: " "
Aerosol Number density		: " "
Meteorological range	(km)	: " "
Aerosol extinction		: " "
Aerosol season control		: " "
Aerosol profile		: " "

New model of atmosphere	:Blank
Initial altitude km	:0.014
Final altitude	:Blank
Initial zenith angle ($^{\circ}$)	:As required
Radius of the earth	:Default value (6371.23 km)
Normal program operation	:Yes, 0
Initial frequency (cm^{-1})	:710
Final frequency (cm^{-1})	:1250
Frequ.increment (cm^{-1})	:40

**TABLE 7.4 : VALIDATION OF RADIANCE FOR 4 NOV 87
OVERCAST SKY - ZENITH RANGE 90°-86.5°**

ZENITH ANGLE (°)	ALTITUDE (m)	BOUND TEMP (°K)	AVERAGE WSPEED (m/s)	AGA RADIANCE (W/cm²-sr)	LOWTRAN RADIANCEL (W/cm²-sr)	%ERROR LOWTRAN -AGA
89.945	029.35	290.25	5.30	4.294E-3	3.950E-3	-8.01
89.563	136.03	290.25	5.30	4.345E-3	3.984E-3	-8.30
89.125	258.33	290.40	5.27	4.330E-3	4.002E-3	-7.57
88.688	380.34	289.95	5.20	4.302E-3	4.021E-3	-6.53
88.251	502.33	288.95	5.26	4.266E-3	4.036E-3	-5.39
87.813	624.57	287.79	5.43	4.216E-3	4.077E-3	-3.29
87.375	746.48	286.65	5.63	4.231E-3	4.088E-3	-3.37
86.938	868.66	285.65	5.81	4.209E-3	4.088E-3	-2.87
86.500	990.77	285.52	6.00	4.167E-3	4.081E-3	-2.06

**TABLE 7.5 : VALIDATION OF RADIANCE FOR 4 NOV 87
FAIR SKY - ZENITH RANGE 90°-86.5°**

ZENITH ANGLE (°)	ALTITUDE (m)	BOUND TEMP (°K)	AVERAGE WSPEED (m/s)	AGA RADIANCE (W/cm²-sr)	LOWTRAN RADIANCE (W/cm²-sr)	%ERROR LOWTRAN -AGA
89.890	044.71	290.25	5.30	4.294E-3	3.960E-3	-7.77
89.563	136.03	290.25	5.30	4.337E-3	3.984E-3	-8.13
89.125	258.33	290.40	5.27	4.337E-3	4.002E-3	-7.72
88.688	380.34	289.90	5.20	4.316E-3	4.021E-3	-6.80
88.250	502.61	288.85	5.26	4.287E-3	4.035E-3	-5.80
87.813	624.57	287.95	5.43	4.259E-3	4.077E-3	-4.20
87.375	746.78	286.55	5.63	4.209E-3	4.088E-3	-2.87
86.938	868.66	285.70	5.81	4.167E-3	4.088E-3	-1.89
86.500	990.77	285.50	6.00	4.118E-3	4.081E-3	-0.89

TABLE 7.6 : VALIDATION OF RADIANCE FOR 4 NOV 87
OVERCAST SKY - ZENITH RANGE 90˚-55˚

ZENITH ANGLE (˚)	ALTITUDE (m)	BOUND TEMP (˚K)	AVERAGE WSPEED (m/s)	AGA RADIANCE (W/cm²-sr)	LOWTRAN RADIANCE (W/cm²-sr)	%ERROR LOWTRAN -AGA
89.781	0075.15	290.25	05.30	4.330E-3	3.972E-3	-8.26
88.688	0380.34	289.90	05.20	4.302E-3	4.021E-3	-6.53
87.594	0685.68	287.25	05.52	4.209E-3	4.086E-3	-2.92
86.500	0990.77	285.51	06.03	4.167E-3	4.078E-3	-2.13
85.406	1295.50	283.85	06.49	3.873E-3	4.046E-3	4.46
84.313	1595.50	281.60	06.65	3.534E-3	4.030E-3	14.03
83.219	1903.19	280.70	06.38	3.257E-3	4.064E-3	24.77
82.125	2206.19	277.95	06.16	3.354E-3	4.071E-3	21.37
81.031	2508.40	277.05	06.16	3.354E-3	4.040E-3	32.15
79.938	2809.42	274.55	07.15	3.611E-3	3.962E-3	9.72
78.844	3109.69	272.40	07.94	3.233E-3	3.886E-3	20.19
77.750	3408.84	270.55	09.05	3.115E-3	3.797E-3	21.89
76.656	3706.75	268.00	10.30	3.649E-3	3.697E-3	1.31
75.563	4003.04	265.55	11.45	3.592E-3	3.606E-3	0.38
74.969	4163.46	264.30	12.00	3.547E-3	3.564E-3	0.47
73.375	4591.70	262.40	13.20	3.379E-3	3.485E-3	3.13
72.281	4883.58	260.45	13.80	2.876E-3	3.438E-3	19.54
71.188	5173.42	258.95	14.30	2.311E-3	3.400E-3	47.12
70.094	5461.64	256.95	14.71	3.138E-3	3.362E-3	7.13
69.000	5747.88	254.85	15.13	2.999E-3	3.322E-3	10.95
67.906	6032.03	252.95	15.62	3.097E-3	3.282E-3	5.97
66.813	6313.73	251.25	16.00	3.127E-3	3.247E-3	3.83
65.719	6593.39	249.45	16.37	3.068E-3	3.212E-3	4.69
64.625	6870.65	246.90	16.70	2.263E-3	3.170E-3	40.07
63.531	7145.41	245.05	17.00	2.612E-3	3.136E-3	20.06
62.438	7417.33	242.65	17.24	2.263E-3	3.098E-3	36.89
61.344	7686.79	240.55	17.52	2.560E-3	3.061E-3	19.57
60.250	7953.46	238.05	17.82	3.086E-3	3.021E-3	-2.10
59.156	8217.23	235.75	18.08	3.011E-3	2.983E-3	-0.90
58.063	8477.78	233.50	18.30	2.909E-3	2.947E-3	1.30
56.969	8735.48	230.95	18.53	2.408E-3	2.946E-3	22.34
55.875	8990.00	226.75	18.75	2.169E-3	2.857E-3	31.71
54.781	9241.25	277.05	18.87	2.263E-3	2.765E-3	22.18

TABLE 7.7 : VALIDATION OF RADIANCE FOR 4 NOV 87
FAIR SKY - ZENITH RANGE 90°-55°

ZENITH ANGLE (°)	ALTI TUDE (m)	BOUND TEMP (°K)	AVERAGE WSPEED (m/s)	AGA RADIANCE (W/cm²-sr)	LOWTRAN RADIANCE (W/cm²-sr)	%ERROR LOWTRAN -AGA
89.781	0075.15	290.25	05.30	4.323E-3	3.972E-3	-8.80
88.688	0380.34	289.90	05.20	4.316E-3	4.021E-3	-6.83
87.594	0685.68	287.25	05.52	4.238E-3	4.086E-3	-3.58
86.500	0990.77	285.51	06.03	4.118E-3	4.078E-3	-0.97
85.406	1295.50	283.85	06.49	3.954E-3	4.046E-3	2.32
84.313	1595.50	281.60	06.65	3.617E-3	4.030E-3	11.40
83.219	1903.19	280.70	06.38	3.360E-3	4.064E-3	20.95
82.125	2206.19	277.95	06.16	3.197E-3	4.071E-3	27.33
81.031	2508.40	277.05	06.16	2.960E-3	4.040E-3	36.48
79.938	2809.42	274.55	07.15	3.637E-3	3.962E-3	8.93
78.844	3109.69	272.40	07.94	2.612E-3	3.886E-3	48.77
77.750	3408.84	270.55	09.05	2.560E-3	3.797E-3	48.32
76.656	3706.75	268.00	10.30	2.178E-3	3.697E-3	69.74
75.563	4003.04	265.55	11.45	2.771E-3	3.606E-3	30.13
74.969	4163.46	264.30	12.00	2.458E-3	3.564E-3	44.99
73.375	4591.70	262.40	13.20	2.718E-3	3.485E-3	28.21
72.281	4883.58	260.45	13.80	2.458E-3	3.438E-3	39.86
71.188	5173.42	258.95	14.30	2.216E-3	3.400E-3	53.42
70.094	5461.64	256.95	14.71	2.169E-3	3.362E-3	66.89
69.000	5747.88	254.85	15.13	2.123E-3	3.322E-3	56.47
67.906	6032.03	252.95	15.62	2.078E-3	3.282E-3	57.94
66.813	6313.73	251.25	16.00	2.033E-3	3.247E-3	59.71
65.719	6593.39	249.45	16.37	1.989E-3	3.212E-3	61.48
64.625	6870.65	246.90	16.70	1.903E-3	3.170E-3	66.57
63.531	7145.41	245.05	17.00	1.861E-3	3.136E-3	68.51
62.438	7417.33	242.65	17.24	1.819E-3	3.098E-3	70.31
61.344	7686.79	240.55	17.52	2.169E-3	3.061E-3	41.12
60.250	7953.46	238.05	17.82	1.778E-3	3.021E-3	69.91
59.156	8217.23	235.75	18.08	1.861E-3	2.983E-3	60.29
58.063	8477.78	233.50	18.30	1.778E-3	2.947E-3	65.74
56.969	8735.48	230.95	18.53	1.778E-3	2.946E-3	65.69
55.875	8990.00	226.75	18.75	1.738E-3	2.857E-3	64.38
54.781	9241.25	277.05	18.87	1.738E-3	2.765E-3	59.09

TABLE 7.8 : VALIDATION OF RADIANCE FOR 14 JULY 88
FAIR SKY - ZENITH RANGE HORIZON-87.345°

ZENITH ANGLE (°)	ALTI TUDE (m)	BOUND TEMP (°K)	WIND WSPEED (m/s)	AGA RADIANCE (W/cm²-sr)	LOWTRAN RADIANCE (W/cm²-sr)	%ERROR LOWTRAN -AGA
89.970	0022.37	216.65	03.10	4.224E-3	4.315E-3	-2.10
89.751	0083.53	"	"	4.224E-3	4.225E-3	0.00
89.533	0144.40	"	"	4.118E-3	4.171E-3	1.28
89.314	0205.56	"	"	4.224E-3	4.133E-3	-2.15
89.095	0266.71	"	"	4.224E-3	4.101E-3	-2.91
88.876	0327.85	"	"	4.224E-3	4.072E-3	-3.59
88.658	0388.72	"	"	4.345E-3	4.044E-3	6.92
88.439	0449.85	"	"	4.345E-3	4.018E-3	-7.52
88.220	0510.98	"	"	4.381E-3	3.993E-3	-8.85
88.001	0572.11	"	"	4.345E-3	3.967E-3	-8.69
87.783	0623.94	"	"	4.345E-3	3.942E-3	-9.27
87.564	0694.05	"	"	4.381E-3	3.918E-3	-10.56
87.345	0755.15	"	"	4.381E-3	3.894E-3	-11.11

TABLE 7.9 : VALIDATION OF RADIANCE FOR 14 JULY 88
FAIR SKY - ZENITH RANGE 83.641°-80.361°

ZENITH ANGLE (°)	ALTI TUDE (m)	BOUND TEMP (°K)	AVERAGE WSPEED (m/s)	AGA RADIANCE (W/cm²-sr)	LOWTRAN RADIANCE (W/cm²-sr)	%ERROR LOWTRAN -AGA
83.641	1786.12	216.65	3.1	3.193E-3	3.517E-3	-10.12
83.422	1846.89	"	"	3.900E-3	3.496E-3	-10.35
83.094	1937.85	"	"	3.859E-3	3.466E-3	-10.18
82.875	1948.55	"	"	3.820E-3	3.446E-3	-9.79
82.656	2059.22	"	"	3.806E-3	3.427E-3	-9.95
82.438	2119.58	"	"	3.780E-3	3.408E-3	-9.84
82.219	2180.19	"	"	3.767E-3	3.399E-3	-9.76
82.000	2240.76	"	"	3.740E-3	3.370E-3	-9.89
81.781	2301.31	"	"	3.714E-3	3.352E-3	-9.74
81.563	2361.54	"	"	3.688E-3	3.334E-3	-9.59
81.453	2391.93	"	"	3.669E-3	3.325E-3	-9.37
81.234	2452.39	"	"	3.643E-3	3.307E-3	-9.22
81.016	2512.53	"	"	3.637E-3	3.298E-3	-9.32
80.797	2572.92	"	"	3.617E-3	3.281E-3	-9.28
80.579	2633.00	"	"	3.598E-3	3.264E-3	-9.28
80.361	2693.03	"	"	3.592E-3	3.247E-3	-9.60

TABLE 7.10 : VALIDATION OF RADIANCE FOR 15 JULY 88 A
FAIR SKY - ZENITH RANGE HORIZON-87.012˚

ZENITH ANGLE (˚)	ALTI TUDE (m)	BOUND TEMP (˚K)	WIND WSPEED (m/s)	AGA RADIANCE (W/cm^2-sr)	LOWTRAN RADIANCE (W/cm^2-sr)	%ERROR LOWTRAN -AGA
90.020	0008.41	216.65	04.02	3.988E-3	4.042E-3	1.35
89.856	0054.21	"	"	4.167E-3	4.083E-3	-2.01
89.637	0115.36	"	"	4.160E-3	3.980E-3	-4.32
89.418	0176.52	"	"	4.209E-3	3.919E-3	-6.86
89.200	0237.39	"	"	4.216E-3	3.875E-3	-8.08
88.981	0298.54	"	"	4.224E-3	3.841E-3	-9.06
88.762	0359.68	"	"	4.231E-3	3.811E-3	-9.92
88.543	0420.82	"	"	4.231E-3	3.785E-3	-10.54
88.325	0481.68	"	"	4.231E-3	3.761E-3	-11.10
88.106	0542.80	"	"	4.231E-3	3.738E-3	-11.65
87.887	0603.92	"	"	4.216E-3	3.716E-3	-11.85
87.668	0665.03	"	"	4.209E-3	3.695E-3	-12.21
87.450	0725.85	"	"	4.195E-3	3.675E-3	-12.39
87.231	0786.94	"	"	4.188E-3	3.655E-3	-12.72
87.012	0848.02	"	"	4.174E-3	3.636E-3	-12.88

TABLE 7.11 : VALIDATION OF RADIANCE FOR 15 JULY 88 A
FAIR SKY - ZENITH RANGE 82.351˚-79.250˚

ZENITH ANGLE (˚)	ALTI TUDE (m)	BOUND TEMP (˚K)	AVERAGE WSPEED (m/s)	AGA RADIANCE (W/cm^2-sr)	LOWTRAN RADIANCE (W/cm^2-sr)	%ERROR LOWTRAN -AGA
82.531	2143.66	216.65	4.02	3.662E-3	3.272E-3	-10.64
82.312	2181.85	"	"	3.637E-3	3.262E-3	-10.31
82.094	2214.77	"	"	3.611E-3	3.254E-3	-9.88
81.875	2275.33	"	"	3.598E-3	3.239E-3	-9.97
81.656	2335.85	"	"	3.560E-3	3.225E-3	-9.41
81.438	2396.07	"	"	3.547E-3	3.210E-3	-9.50
81.219	2456.52	"	"	3.503E-3	3.196E-3	-8.76
81.000	2516.95	"	"	3.490E-3	3.182E-3	-8.82
80.781	2577.33	"	"	3.465E-3	3.167E-3	-8.60
80.563	2637.40	"	"	3.447E-3	3.154E-3	-8.50
80.344	2677.71	"	"	3.422E-3	3.140E-3	-8.24
80.125	2757.98	"	"	3.403E-3	3.126E-3	-8.13
79.906	2818.21	"	"	3.379E-3	3.113E-3	-7.87
79.688	2878.13	"	"	3.354E-3	3.100E-3	-7.57
79.469	2938.27	"	"	3.342E-3	3.086E-3	-7.66
79.250	2998.38	"	"	3.324E-3	3.074E-3	-7.52

134

TABLE 7.12 : VALIDATION OF RADIANCE FOR 15 JULY 88 B FAIR SKY - ZENITH RANGE HORIZON-87.211°

ZENITH ANGLE (°)	ALTI TUDE (m)	BOUND TEMP (°K)	WIND WSPEED (m/s)	AGA RADIANCE (W/cm^2-sr)	LOWTRAN RADIANCE (W/cm^2-sr)	%ERROR LOWTRAN -AGA
90.000	0014.00	216.65	02.50	4.125E-3	–	–
89.836	0059.79	"	"	4.160E-3	4.313E-3	3.67
89.617	0120.95	"	"	4.195E-3	4.255E-3	1.43
89.398	0182.10	"	"	4.224E-3	4.218E-3	-0.14
89.180	0242.97	"	"	4.231E-3	4.186E-3	-1.06
88.961	0304.12	"	"	4.238E-3	4.157E-3	-1.91
88.742	0365.27	"	"	4.258E-3	4.129E-3	-3.02
88.523	0426.41	"	"	4.258E-3	4.102E-3	-3.66
88.305	0487.26	"	"	4.273E-3	4.076E-3	-4.61
88.086	0548.39	"	"	4.266E-3	4.049E-3	-5.08
87.867	0609.50	"	"	4.258E-3	4.023E-3	-5.51
87.648	0670.61	"	"	4.259E-3	3.998E-3	-6.12
87.430	0731.43	"	"	4.245E-3	3.972E-3	-6.43
87.211	0792.52	"	"	4.231E-3	3.947E-3	-6.71

TABLE 7.13 : VALIDATION OF RADIANCE FOR 15 JULY 88 B FAIR SKY - ZENITH RANGE 85.531°-82.250°

ZENITH ANGLE (°)	ALTI TUDE (m)	BOUND TEMP (°K)	AVERAGE WSPEED (m/s)	AGA RADIANCE (W/cm^2-sr)	LOWTRAN RADIANCE (W/cm^2-sr)	%ERROR LOWTRAN -AGA
85.531	1260.71	216.65	2.5	3.960E-3	3.758E-3	-5.10
85.313	1321.39	"	"	3.933E-3	3.735E-3	-5.03
85.094	1382.34	"	"	3.906E-3	3.711E-3	-4.99
84.875	1443.26	"	"	3.880E-3	3.688E-3	-4.94
84.656	1504.16	"	"	3.853E-3	3.665E-3	-4.87
84.438	1564.76	"	"	3.820E-3	3.643E-3	-4.63
84.219	1625.62	"	"	3.806E-3	3.620E-3	-4.88
84.000	1686.45	"	"	3.780E-3	3.598E-3	-4.81
83.781	1747.26	"	"	3.760E-3	3.576E-3	-4.83
83.563	1807.77	"	"	3.720E-3	3.555E-3	-4.43
83.344	1868.52	"	"	3.707E-3	3.534E-3	-4.66
83.125	1929.98	"	"	3.682E-3	3.513E-3	-4.58
83.906	1989.96	"	"	3.655E-3	3.942E-3	-4.45
82.688	2050.35	"	"	3.624E-3	3.471E-3	-4.92
82.469	2111.00	"	"	3.604E-3	3.451E-3	-4.24
82.250	2171.61	"	"	3.578E-3	3.431E-3	-4.10

TABLE 7.14 : VALIDATION OF RADIANCE FOR 25 JULY 88
OVERCAST SKY - ZENITH RANGE HORIZON-86.679°

ZENITH ANGLE (°)	ALTITUDE (m)	BOUND TEMP (°K)	WIND WSPEED (m/s)	AGA RADIANCE (W/cm^2-sr)	LOWTRAN RADIANCE (W/cm^2-sr)	%ERROR LOWTRAN -AGA
90.070	0000.00	216.65	04.9	4.345E-3	3.985E-3	-8.28
89.851	0055.60	"	"	4.330E-3	4.026E-3	-7.02
89.632	0116.76	"	"	4.330E-3	3.871E-3	-12.67
89.413	0177.91	"	"	4.309E-3	3.768E-3	-12.55
89.195	0238.79	"	"	4.294E-3	3.700E-3	-13.83
88.976	0244.93	"	"	4.280E-3	3.649E-3	-14.74
88.757	0361.08	"	"	4.266E-3	3.609E-3	-15.40
88.538	0422.22	"	"	4.266E-3	3.576E-3	-16.17
88.320	0483.07	"	"	4.258E-3	3.548E-3	-16.67
88.101	0544.20	"	"	4.266E-3	3.522E-3	-17.44
87.882	0605.32	"	"	4.258E-3	3.499E-3	-17.82
87.663	0664.43	"	"	4.266E-3	3.479E-3	-18.44
87.445	0727.25	"	"	4.266E-3	3.459E-3	-18.91
87.116	0819.02	"	"	4.266E-3	3.432E-3	-19.54
86.898	0879.81	"	"	4.258E-3	3.415E-3	-19.79
86.679	0940.87	"	"	4.251E-3	3.398E-3	-20.06

TABLE 7.15 : VALIDATION OF RADIANCE FOR 25 JULY 88
OVERCAST SKY - ZENITH RANGE 81.530°-78.250°

ZENITH ANGLE (°)	ALTITUDE (m)	BOUND TEMP (°K)	AVERAGE WSPEED (m/s)	AGA RADIANCE (W/cm^2-sr)	LOWTRAN RADIANCE (W/cm^2-sr)	%ERROR LOWTRAN -AGA
81.530	2370.66	216.65	4.9	4.266E-3	3.091E-3	-27.54
81.311	2431.85	"	"	4.266E-3	3.080E-3	-27.80
81.092	2491.50	"	"	4.266E-3	3.069E-3	-28.05
80.874	2576.50	"	"	4.266E-3	3.052E-3	-28.45
80.655	2612.06	"	"	4.258E-3	3.048E-3	-28.41
80.437	2672.11	"	"	4.258E-3	3.037E-3	-28.67
80.218	2732.39	"	"	4.266E-3	3.026E-3	-29.06
80.000	2792.37	"	"	4.258E-3	3.016E-3	-29.16
79.781	2852.57	"	"	4.251E-3	3.006E-3	-29.28
79.565	2911.90	"	"	4.258E-3	2.996E-3	-29.63
79.343	2972.86	"	"	4.258E-3	2.985E-3	-29.89
79.125	3032.67	"	"	4.251E-3	2.975E-3	-30.01
78.906	3092.70	"	"	4.251E-3	2.966E-3	-30.22
78.687	3152.69	"	"	4.251E-3	2.956E-3	-30.46
78.468	3212.64	"	"	4.258E-3	2.946E-3	-30.81
78.250	3272.26	"	"	4.258E-3	2.937E-3	-31.02

TABLE 7.16 : VALIDATION OF SCHWARTZ-HON MODEL FOR 4 NOV 87
OVERCAST SKY - WSPEED 2.057m/s - SST 14.1°C

θ_v / θ_i	ϵ_s / θ_r	L_i / L_s	T_{bb}	L_{SH} / L_{AGA}	% ERROR	RANGE
90.109	00.215	3.873E-3		4.715E-3		
			280.71		20.49	13.30
89.891	85.475	4.005E-3		3.913E-3		
90.328	00.229	3.856E-3		4.460E-3		
			280.64		15.15	2.516
89.672	85.739	4.000E-3		3.873E-3		
90.547	00.244	3.828E-3		4.374E-3		
			280 48		12.15	1.481
89.453	85.283	3.988E-3		3.900E-3		
90.766	00.259	3.982E-3		4.416E-3		
			282.16		13.43	1.053
89.234	85.187	4.112E-3		3.893E-3		
90.984	00.273	4.034E-3		4.426E-3		
			282.77		13.10	0.818
89.016	85.091	4.157E-3		3.913E-3		
91.203	00.288	4.057E-3		4.426E-3		
			283.08		12.33	0.668
88.797	84.955	4.180E-3		3.940E-3		
91.422	00.302	4.068E-3		4.429E-3		
			283.27		11.64	0.565
88.578	84.899	4.194E-3		3.967E-3		
91.641	00.317	4.067E-3		4.426E-3		
			283.35		09.66	0.484
88.359	84.803	4.200E-3		4.036E-3		

θ_v = zenith angle, θ_i =180°-θ_v angle of incident ray, (°)
ϵ_s = sea surface emissivity, in Schwartz-Hon (SH) model
θ_r = reflection angle of sky radiance in SH model, (°)
L_i = sky radiance at θ_r, measured by AGA, (W/cm^2-sr)
L_{SST} = 4.487E-3 W/cm^2-sr = sea surface radiance at SST
L_s = ϵ_s(L_{SST}-Li)+L_i, (W/cm^2-sr)
T_{bb} = blackbody temperature of sea surface, (Eq. 8.1), (°K)
L_{AGA} = sea surface radiance, at θ_v, from AGA, (W/cm^2-sr)
L_{SH} = sea surface radiance, at θ_v, by LOWTRAN 6, (W/cm^2_sr)
RANGE = AGA-sea surface distance, by LOWTRAN 6, (km)

TABLE 7.17 : VALIDATION OF SCHWARTZ-HON MODEL FOR 4 NOV 87 FAIR SKY - WSPEED 2.057m/s - SST 14.1°C

θ_v / θ_i	ϵ_s / θ_r	L_i / L_s	T_{bb}	L_{SH} / L_{AGA}	% ERROR	RANGE
90.438	00.237	3.885E-3		4.429E-3		
------	------	--------	281.01	--------	16.98	1.86
89.562	85.531	4.027E-3		3.786E-3		
90.875	00.266	3.833E-3		4.328E-3		
------	------	--------	280.72	--------	13.50	0.920
89.125	85.139	4.006E-3		3.813E-3		
91.313	00.295	3.691E-3		4.227E-3		
------	------	--------	279.62	--------	09.90	0.612
88.617	84.947	3.925E-3		3.846E-3		
91.750	00.334	3.658E-3		4.202E-3		
------	------	--------	279.64	--------	06.46	0.459
88.250	84.755	3.926E-3		3.947E-3		
92.188	00.353	3.605E-3		4.177E-3		
------	------	--------	279.50	--------	05.479	0.367
87.812	84.563	3.916E-3		3.960E-3		
92.625	00.382	3.610E-3		4.189E-3		
------	------	--------	279.90	--------	08.15	0.306
87.375	84.371	3.945E-3		3.873E-3		

θ_v = zenith angle, θ_i =180°-θ_v angle of incident ray, (°)
ϵ_s = sea surface emissivity, in Schwartz-Hon (SH) model
θ_r = reflection angle of sky radiance in SH model, (°)
L_i = sky radiance at θ_r, measured by AGA, (W/cm^2-sr)
L_{SST} = 4.487E-3 W/cm^2-sr = sea surface radiance at SST
L_s = $\epsilon_s(L_{SST}$-Li)+L$_i$, (W/cm^2-sr)
T_{bb} = blackbody temperature of sea surface, (Eq. 8.1), (°K)
L_{AGA} = sea surface radiance, at θ_v, from AGA, (W/cm^2-sr)
L_{SH} = sea surface radiance, at θ_v, by LOWTRAN 6, (W/cm^2_sr)
RANGE = AGA-sea surface distance, by LOWTRAN 6, (km)

TABLE 7.18 : VALIDATION OF SCHWARTZ-HON MODEL FOR 14 JUL 88 FAIR SKY - AVER. WSPEED 3.55 m/s - SST 12.8 °C

θ_v / θ_i	ϵ_s / θ_r	L_i / L_s	T_{bb}	L_{SH} / L_{AGA}	% ERROR	RANGE
90.134	00.387	3.715E-3		4.213E-3		
			280.26		04.38	5.941
89.866	81.792	3.976E-3		4.036E-3		
90.538	00.396	3.716E-3		4.220E-3		
			280.35		04.55	2.269
89.647	81.800	3.983E-3		4.036E-3		
90.572	00.406	3.725E-3		4.217E-3		
			280.56		04.48	1.401
89.428	81.807	3.995E-3		4.036E-3		
90.790	00.416	3.718E-3		4.208E-3		
			280.55		04.26	1.015
89.210	81.815	3.997E-3		4.036E-3		
91.009	00.426	3.719E-3		4.206E-3		
			280.66		06.21	0.795
88.990	81.823	4.005E-3		3.960E-3		
91.228	00.436	3.720E-3		4.206E-3		
			280.75		06.21	0.653
88.770	81.831	4.012E-3		3.960E-3		
91.447	00.445	3.707E-3		4.201E-3		
			280.73		04.08	0.554
88.553	81.728	4.010E-3		4.036E-3		
91.665	00.445	3.687E-3		4.196E-3		
			280.70		03.96	0.482
88.335	81.564	4.008E-3		4.036E-3		
91.884	00.465	3.665E-3		4.188E-3		
			280.62		05.75	0.426
88.116	81.400	4.002E-3		3.960E-3		
92.103	00.475	3.644E-3		4.182E-3		
			280.56		03.61	0.381
87.897	81.235	3.998E-3		4.036E-3		
92.322	00.484	3.643E-3		4.185E-3		
			280.64		03.69	0.346
87.688	81.078	3.998E-3		4.036E-3		

139

θ_v = zenith angle, $\theta_i = 180° - \theta_v$ angle of incident ray, (°)

ϵ_s = sea surface emissivity, in Schwartz-Hon (SH) model, for sea surface wind speed 4 m/s

θ_r = reflection angle of sky radiance in SH model, for sea surface wind speed 4 m/s, (°)

L_i = sky radiance at θ_r, measured by AGA, (W/cm^2-sr)

L_{SST} = 4.390E-3 W/cm^2-sr = sea surface radiance at SST

L_s = $\epsilon_s(L_{SST}-Li)+L_i$, (W/cm^2-sr)

T_{bb} = blackbody temperature of sea surface, (Eq. 8.1), (°K)

L_{AGA} = sea surface radiance, at θ_v, from AGA, (W/cm^2-sr)

L_{SH} = sea surface radiance, at θ_v, by LOWTRAN 6, (W/cm^2_sr)

RANGE = AGA-sea surface distance, by LOWTRAN 6, (km)

TABLE 7.19 : VALIDATION OF SCHWARTZ-HON MODEL FOR 15 JUL 88 FAIR SKY - AVER. WSPEED 4.51m/s - SST 11.7°C

θ_v / θ_i	ϵ_s / θ_r	L_i / L_s	T_{bb}	L_{SH} / L_{AGA}	% ERROR	RANGE
90.184	00.446	3.438E-3		4.035E-3		
89.816	80.440	3.823E-3	278.08	3.933E-3	02.59	4.051
90.403	00.454	3.421E-3		4.071E-3		
89.597	80.343	3.824E-3	278.09	3.920E-3	03.85	2.003
90.622	00.462	3.416E-3		4.069E-3		
89.378	80.245	3.829E-3	278.16	3.893E-3	04.52	1.293
90.840	00.470	3.405E-3		4.062E-3		
89.160	80.149	3.830E-3	278.18	3.913E-3	03.80	0 . 9 5 6
91.059	00.478	3.393E-3		4.056E-3		
88.941	80.051	3.831E-3	278.19	3.988E-3	01.70	0.758
91.278	00.486	3.381E-3		4.052E-3		
88.722	79.954	3.832E-3	278.21	3.906E-3	03.73	0.628
91.497	00.494	3.359E-3		4.033E-3		
88.503	79.857	3.828E-3	278.15	3.913E-3	03.32	0.536
91.715	00.502	3.342E-3		4.039E-3		
88.285	79.760	3.827E-3	278.14	3.927E-3	02.85	0.468
91.934	00.510	3.354E-3		4.045E-3		
88.066	79.663	3.841E-3	278.33	3.913E-3	03.37	0.415
92.153	00.518	3.352E-3		4.048E-3		
87.847	79.565	3.848E-3	278.43	3.940E-3	02.74	0.373

θ_v = zenith angle, θ_i =180°-θ_v angle of incident ray, (°)
ϵ_s = sea surface emissivity, in Schwartz-Hon (SH) model, for sea surface wind speed 5m/s

θ_r = reflection angle of sky radiance in SH model, for sea surface wind speed 5m/s, (°)

L_i = sky radiance at θ_r, measured by AGA, (W/cm^2-sr)

L_{SST} = 4.390E-3 W/cm^2-sr = sea surface radiance at SST

L_s = $\epsilon_s(L_{SST}-Li)+L_i$, (W/cm^2-sr)

T_{bb} = blackbody temperature of sea surface, (Eq. 8.1), (°K)

L_{AGA} = sea surface radiance, at θ_v, from AGA, (W/cm^2-sr)

L_{SH} = sea surface radiance, at θ_v, by LOWTRAN 6, (W/cm^2-sr)

RANGE = AGA-sea surface distance, by LOWTRAN 6, (km)

TABLE 7.20 : VALIDATION OF SCHWARTZ-HON MODEL FOR 25 JUL 88 OVERCAST SKY - WSPEED 4.9 m/s - SST 15.4 °C

θ_v / θ_i	ϵ_s / θ_r	L_i / L_s	T_{bb}	L_{SH} / L_{AGA}	% ERROR	RANGE
90.288	00.444	4.261E-3		4.236E-3		
			282.35		-5.48	2.991
89.712	80.614	4.120E-3		4.482E-3		
90.507	00.452	4.263E-3		4.420E-3		
			286.19		-1.71	1.616
89.493	80.510	4.407E-3		4.497E-3		
90.726	00.461	4.258E-3		4.465E-3		
			286.19		-1.52	1.116
89.274	80.406	4.407E-3		4.534E-3		
90.945	00.469	4.260E-3		4.491E-3		
			286.24		-1.42	0.854
89.055	80.302	4.411E-3		4.556E-3		
91.163	00.477	4.266E-3		4.510E-3		
			286.32		-0.35	0.692
88.837	80.199	4.417E-3		4.497E-3		
91.382	00.485	4.264E-3		4.522E-3		
			286.34		00.55	0.582
88.618	80.095	4.418E-3		4.497E-3		
91.601	00.493	4.258E-3		4.529E-3		
			286.34		01.20	0.502
88.399	79.991	4.418E-3		4.475E-3		
91.820	00.493	4.258E-3		4.536E-3		
			286.34		00.86	0.442
88.180	79.991	4.418E-3		4.497E-3		

θ_v = zenith angle, θ_i =180°-θ_v angle of incident ray, (°)
ϵ_s = sea surface emissivity, for wind speed 5m/s
θ_r = reflection angle of sky radiance in SH model, for sea surface wind speed 5m/s, (°)
L_i = sky radiance at θ_r, measured by AGA, (W/cm^2-sr)
L_{SST} = 4.390E-3 W/cm^2-sr = sea surface radiance at SST
L_s = ϵ_s(L_{SST}-Li)+L_i, (W/cm^2-sr)
T_{bb} = blackbody temperature of sea surface, (Eq. 8.1), (°K)
L_{AGA} = sea surface radiance, at θ_v, from AGA, (W/cm^2-sr)
L_{SH} = sea surface radiance, at θ_v, by LOWTRAN 6, (W/cm^2_sr)
RANGE = AGA-sea surface distance, by LOWTRAN 6, (km)

143

LIST OF REFERENCES

1. Lloyd, J. M., Thermal Imaging Sustems, Plenum Press, NY, 1975.

2. AGA, Thermovision 780 Operating Manual, publication No 556 556 492/Ed II, AGA Infrared systems AB, NJ, 1980.

3. Pinson, L. J., Electro-Optics, John Wiley and Sons, NY, 1985.

4. Cooper, A. W., Electro-Optics, Sensors-Signals Systems, notes for studennts use in cources PH3252 and PH4253, Naval Postgraduate School, Monterey, CA, 1988.

5. Wolf, W. L. and Zissis, G. J., The Infrared Handbook, Office of Naval Research, Department of the Navy, VA, 1985.

6. McCartney, E. J., Optics of the Atmosphere, John Wiley and Sons, NY, 1976.

7. Dimitriadis, G., Thermal Image Measurements of Infrared Signatures, Naval Postgraduate School, Monterey, CA, 1986.

8. Feigelson, E. M., Radiatiom in a Cloudy Atmosphere, D. Reidel Publishing Company, Holland, 1984.

9. Schwartz, I. B. and Hon, D., Emissivity as a Function of Surface Roughness : ⁂ Computer Model, Naval Research Laboratory, D.C., 1986.

10. Skolnik, M. I., Introduction to Radar Systems, McGraw-Hill Book Company, NY, 1980.

11. Kneizvs, F. X., Atmospheric Transmittance/Radiance Computer Code LOWTRAN 6, Air Force Geophysics Laboratory, AFGL-TR-83-0187, 1983.

12. AGEMA Infrared Systems, DISCO 3.0 Operating Manual, Pharos Company, AGEMA, NJ, 1 July 1985.

13. Due, C. T., Optical-Mechanical, Active/Passive Imaging Systems - Volume II, Environmental Research Institute of Michigan, MI, May 1982.

14. NPGS/NACIT, <u>Infrared Measurements Notebook</u>, Naval Postgraduate School, Monterey, CA, 1987.

15. Ridgeway, M. G. and Psihogios, P. E., <u>Thermal Imaging Measurements Data</u>, Naval Postgraduate School, Monterey, CA, July 1988.

16. <u>MathCAD 2.0</u>, Mathsoft, Inc., Cambridge, MA 02139, 1987.

17. Ridgeway, M. G., <u>Calibration Experiment</u>, Naval Postgraduate School, Monterey, CA, 1988.

INITIAL DISTRIBUTION LIST

		No. Copies
1.	Defense Technical Information Center Cameron Station Alexandria, Virginia 22304-6145	2
2.	Library, Code 0142 Naval Postgraduate School Monterey, California 93943-5002	2
3.	Department Chairman, Code 61 Department of Physics Naval Postgraduate School Monterey, California 93943	1
4.	Prof. A. W. Cooper, Code 61Cr Department of Physics Naval Postgraduate School Monterey, California 93943	3
5.	Prof. D. D. Cleary, Code 61Cl Department of Physics Naval Posgraduate School Monterey, California 93943	1
6.	Department of the Navy Naval Environmental Prediction Research Facility Weapons Effects Assessment Division ATTN: John Cook Monterey, California 93943-5006	1
7.	Hellenic Army General Staff Technical Corps Division Mesogion Avenue-Holargos Athens GREECE	2
8.	Panagiotis Psihogios 67 Tsimiski St, 67 100 Xanthi GREECE	2